ABSTRACT

Title of Dissertation: DEVELOPMENT AND THE EARLY ANIMAL FOSSIL RECORD: EVOLUTION AND PHYLOGENETIC APPLICATIONS

Sarah Maureen Tweedt, Doctor of Philosophy, 2016

Dissertation directed by: Professor Charles F. Delwiche, Department of Cell Biology and Molecular Genetics
Dr. Douglas H. Erwin, Senior Scientist and Curator, Department of Paleobiology, National Museum of Natural History, Smithsonian Institution

Although evolutionary developmental biology and paleontology are linked by the study of morphology, the application of development to paleontological questions has only recently become more prominent. The growth of a robust developmental genetic framework for studying the origin and evolution of morphological features, however, holds great promise for understanding ancient animal life. As paleontology provides the historical record as well as the temporal and environmental context of past morphological evolution, uniting knowledge of developmental genetic systems with this historical record will form a key synthetic approach to understanding the early evolution of developmental processes.

Ultimately unraveling the sequence of ancient animal developmental evolution will require combining analysis of comparative developmental data, critical assessment of fossil morphology within a developmental framework, and the targeted exploration of specific geologic periods to fill in the missing record of key times in animal developmental evolution. This study addresses each of these three approaches.

First, I provide a new compilation and evaluation of recent comparative and experimental developmental biology data to review the nature of developmental 'toolkits' at the origin of the most basal animal clades. I reconstruct early animal developmental capacities and integrate these data within a temporal framework to better understand the context of earliest animal development. Second, I assess longstanding evolutionary hypotheses about the origin of the panarthropod clade and the phylogenetic position of Cambrian 'lobopod' fossils by examining signal present within current morphological datasets. I apply new methods to fossil panarthropod phylogeny estimation and suggest strategies for developmentally-informed phylogenetic coding of morphological data. Third, I present the discovery of the oldest spicule-bearing fossil sponges in the rock record, which co-occur in latest Ediacaran strata with classic enigmatic Ediacaran fauna. I provide a formal systematic description of fossil material from localities in both Nevada and southern Namibia.

The combined approaches presented herein are a first step towards a deeper integration of developmental principles in the study and discovery of ancient animal life, and contribute to our understanding of the evolution of ancient animal developmental processes.

DEVELOPMENT AND THE EARLY ANIMAL FOSSIL RECORD: EVOLUTION AND PHYLOGENETIC APPLICATIONS

by

Sarah Maureen Tweedt

Dissertation submitted to the Faculty of the Graduate School of the
University of Maryland, College Park, in partial fulfillment
of the requirements for the degree of
Doctor of Philosophy
2016

Advisory Committee:
Professor Charles F. Delwiche, Chair
Dr. Douglas H. Erwin, Co-chair
Associate Professor Alexandra E. Bely
Associate Professor Jeffrey W. Shultz (Dean's Representative)
Dr. Peter J. Wagner

Dedication

To my loving family and steadfast friends, for their constant encouragement and support.

Acknowledgements

I am grateful to Doug Erwin for his invaluable guidance, collaboration, and support through this academic journey, and I especially thank him for directing my intellectual growth in countless discussions and by giving me the opportunities to learn from colleagues and friends elsewhere. I thank all members of my committee for their patience and support for such an errant student, and for their help in getting me to the end. I thank the many past and present museum researchers who became my NMNH-based cohort of colleagues, collaborators, and friends: Marc Laflamme, Jocelynn Sessa, Graham Slater, Stephanie Bush, Simon Darroch, Rachel Racicot, and Emma Ransome. My fellow students Loren Petruny, Cheryl Ames and Jenna Moore have been an unending font of much needed academic and emotional camaraderie. A very special thanks goes out to Carl Simpson, Rachel Warnock and Emmy Smith, whose collaborations and discussions are constant learning experiences, and to Phoebe Cohen, who has supported me in the paleontological community as a mentor and compatriot. Allen Collins, Daphne Soares, Gal Haspel, Gene Hunt, Kevin Peterson, and Paul Myrow have all provided me with immeasurable advice. I thank staff in the Departments of Paleobiology and Invertebrate Zoology at the Smithsonian National Museum of Natural History, and the staff of the Biological Sciences Graduate Program at the University of Maryland. Additionally, I thank Han Zeng and Maoyan Zhu of the Nanjing Institute of Geology and Paleontology and Arne Nielsen of the Natural History Museum of Denmark for support and hospitality during my research travel. This work was funded by the NASA Astrobiology Institute Foundations of Complex Life MIT/Harvard Research Node, and a Cosmos Scholars Grant awarded by the Cosmos Club of Washington, DC. Chapter 2 has been published in

its entirety as chapter in the Springer volume *Evolutionary Transitions to Multicellular Life* (2015). Chapter 4 is under review for publication. Figure 1.1 was previously published in *Science* (334: 1091-1097).

Table of Contents

This Table of Contents is automatically generated by MS Word, linked to the Heading formats used within the Chapter text.

List of Tables

List of Figures

List of Abbreviations

Ma = Million years ago
LCA = Last common ancestor
PDA = Protostome-deuterostome ancestor
dGRNs / GRNs = (Developmental) gene regulatory networks
ELRC = Early Life Research Center; Nanjing Institute of Geology and Paleontology Collections, Chinese Academy of Sciences
USNM = United States National Museum; National Museum of Natural History, Smithsonian Institution Collections
MGUH = Museum Geologicum Universitatis Hauniensis; Geological Museum of the University of Copenhagen Collections, Natural History Museum of Denmark
EQ = Equal rates
LN = Lognormally-distributed rates
GM = Gamma-distributed rates
Exp = Exponential prior
Uni = Uniform prior
M = Ma et al. 2014 dataset
SC = Smith and Caron 2015 dataset
LP = Legg et al. 2013 dataset, reduced size
ACCTRAN = Accelerated transformation
DELTRAN = Delayed transformation
ASDSF = Average standard deviations of split frequencies
PSRFs = Potential scale reduction factors
ESS = Estimated sample size
HME = Harmonic mean estimator
SS = Stepping-stone
PP = Posterior probability
ChINs = Character identity networks
Fm = Formation
Mb = Member
Ediacaran = E
Cambrian = C

Chapter 1: Introduction

Development controls the generation of morphology and, by extension, changes in development control how morphological features change through time. While evolutionary developmental biology seeks to understand the biological mechanisms that generate living forms and how these mechanisms may create evolutionary change, paleontology utilizes the variation in extinct forms to understand past evolutionary pattern and process. Interaction between these disciplines has a long history predating their modern demarcation (Hall 2002), but the application of development to paleontology has only recently gained wider prominence. This is in large part due to the growth of a robust developmental genetic framework for studying the origin and evolution of morphological features, and the promise this holds for understanding ancient animal (metazoan) life.

Genetic Change and Morphological Evolution

The emergence of evolutionary developmental biology in the early to mid-1980s linked new discoveries of highly conserved developmental patterning genes shared by distant phyla (e.g. Lewis 1978; Duboule and Dollé 1989) with clear molecular mechanisms for genetic regulatory control (e.g. Jacob and Monad 1961; Britten and Davidson 1969, 1971). In just the last few decades the field has elucidated many of the genetic components governing aspects of embryonic development in numerous animal species and within an increasingly resolved phylogenetic framework. One of the most significant findings of evolutionary developmental research has been the importance of

genetic regulatory change in shaping animal morphology (e.g. Britten and Davidson 1969, 1971; True and Carroll 2000; Carroll 2008).

Regulatory variation and the contribution of few regulatory genes to morphological evolution is now viewed to be just as important, if not more so, than the additive contributions of genes of smaller effect. Perhaps the most striking example of this is the new appreciation for evolutionary questions presented by unexpected, phylogenetically "deep" genetic regulatory homology (Shubin et al. 2009). A wealth of comparative studies has revealed the presence of genes involved in the formation of complex morphological structures (e.g. genes specifying mesoderm or associated with sophisticated neurological functions) in the genomes of basal metazoans lacking these features, and although these molecular "tools" share evolutionary origins, they have been utilized in different ways by different lineages (e.g. Putnam et al. 2007; Srivastava et al. 2010b; Burkhardt et al. 2011). Importantly, this decoupling of gene presence from the presence of specific features makes it clear that morphology is not the product of individual genes, but rather the complex connections between multiple genes (e.g. Erwin and Davidson 2009). An understanding of how developmental genes are and were organized, regulated, and used is thus crucial to reconstructing the evolutionary history of development and the origin of morphological features As Waddington (1975) suggested, it may be most appropriate to view the evolution of organisms – or at least their morphology – as the evolution of developmental systems.

Development in Deep Time

Paleontology provides the historical record as well as the temporal and environmental context of past morphological evolution, and modern intersections

between developmental biology and paleontology initially focused on major patterns of morphological change through time. Recognition that changes in developmental timing could result in morphological novelty led to wide consideration and assessment of ontogenetic shifts within fossil lineages (e.g. Gould 1977). The rise of "morphospace" approaches from functional morphology also involved evolutionary development, albeit indirectly, by comparing the distribution of existing forms within some defined topological space. By measuring the occupation of actual morphologies with this space, paleontologists could assess temporal and evolutionary patterns of morphological change (reviewed in Erwin 2007). Morphospace studies also addressed whether the diversity of form is inherently constrained (e.g. Raup 1966; Foote 1990, 1992; reviewed in Erwin 2007) and how such constraints might reflect underlying developmental processes (e.g. Hughes et al. 1999). These developmental applications to the fossil record continue to be employed, and current paleontological studies often explore developmental evolution in deep time through morphospace-based methods or by analyzing ontogenetic stages within particular fossil lineages (e.g. Gerber 2014; Haug et al. 2012). Both approaches, however, primarily consider the phenotypic outcomes of unidentified, 'black box', developmental genetic mechanisms, and although they touch upon genetic organization, they do not explicitly accommodate comparative developmental genetic information.

Early Metazoan Life: Developmental and Paleontological Synthesis

Uniting knowledge of developmental genetic systems with the historical record of past form, and with the temporal and environmental context of the rock record, will form a key synthetic approach to understanding the evolution of developmental processes. This synthesis has been particularly successful in the study of vertebrate evolution (reviewed

in Wagner 2014) but has been more difficult to apply to the more ancient and elusive origins of the oldest invertebrate animals (e.g. Hall 2002), and indeed, to the origin of animal development itself. For example, the major genetic developmental differences between metazoan phyla are estimated to have evolved more than 600 million years ago (Ma), but the first fossil representatives of these groups appear almost 60 Ma later (Figure 1.1) (Erwin et al. 2011). This implies that the morphological complexity arising from divergent genetic developmental systems was only realized in ancient oceans after a substantial evolutionary lag, and likely required a particular ecological setting and additional genetic regulatory elaboration (Erwin et al. 2011). Ultimately unraveling the sequence of ancient animal developmental evolutionary change will require 1) continued investigations into comparative animal developmental and morphological history; 2) better informed, development-based partitioning of fossil form into a meaningful evolutionary context; and 3) targeted exploration of specific geologic periods to fill in the missing record of key times in animal developmental evolution.

This Study

The overall objective of this work is to develop a "macroevolution of development" research program through the integration of traditional field and specimen-based paleontology with comparative developmental biology and macroevolutionary theory. The three synthetic approaches to understanding developmental biology in deep time listed above are represented by three separate studies related to the macroevolution of development.

In chapter 2, I compile and evaluate recent comparative and experimental developmental biology data to review the nature of developmental 'toolkits' at the origin

of the most ancient animal clades. I outline the likely developmental capacities existing at the origin of Metazoa, the Placozoan-Eumetazoa last common ancestor (LCA), the Cnidarian-Bilaterian LCA, and the Protostome-Deuterostome LCA. I then integrate this data with the fossil record and within a phylogenetic framework to understand the temporal context of early developmental evolution.

In chapter 3, I assess longstanding evolutionary hypotheses about the origin of the Panarthropod clade and the position of Cambrian 'lobopod' fossil forms within a developmental context. I review the current status of panarthropod phylogenetic hypotheses and their implications for arthropod evolution, and propose an alternative developmental evolutionary scenario. I examine the signal present in existing fossil panarthropod morphological datasets using combined Bayesian and parsimony approaches, and discuss alternative strategies for the identification and coding of morphological features.

Chapter 4 details the outcome of continued field exploration within geologic time periods significant to the evolution of early animals. I present the discovery of precambrian sponge fossils co-occurring with the classic, macroscopic and enigmatic soft-bodied Ediacaran fauna. I provide a systematic description of fossil material from localities in both Nevada and southern Namibia.

Figure 1.1. (following page) The origin and diversification of animals as inferred from the geologic and genetic fossil records.
Cumulative first appearances of higher Linnean taxonomic ranks measure the rise of animal disparity (blue and yellow bars). The pattern of animal origination inferred by time-calibrated molecular clock analyses overlies the geologic record. Open circles indicate molecular clock calibrations, closed colored circles indicate divergence estimates of crown group animals. The first appearances of many animal groups occur concurrently near the Ediacaran-Cambrian boundary. Reproduced from (Erwin et al. 2011). Available as high-res file Additional I.

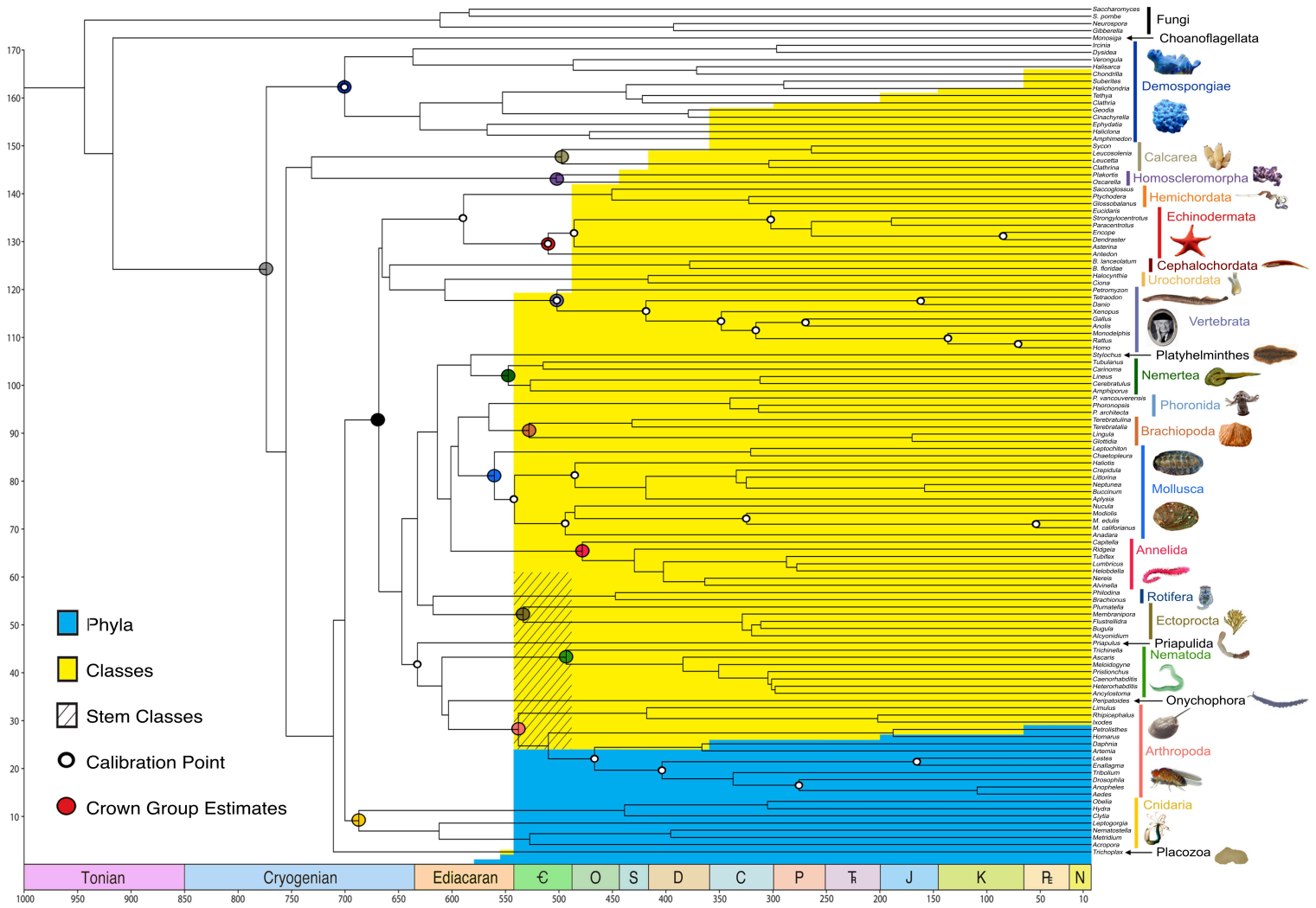

Figure 1.1. The origin and diversification of animals as inferred from the geologic and genetic fossil record.

Significance

The compilation and assessment of ancient animal molecular toolkits provides a broad, synthetic review of development in the early evolution of animals. Importantly, this work provides revised interpretations of LCA morphological capacities based on the quality and instructiveness of underlying comparative developmental and experimental data. Integration of this compilation with the fossil record – and in a phylogenetic context – reveals the existence of long macroevolutionary lags between the origin of developmental genetic tools and the origin of distinctive animal morphologies as documented in the fossil record. Such temporal lags in evolution point to the necessity of investigating non-uniformitarian mechanisms in the early evolution of developmental processes.

Re-analysis of basal panarthropod morphological datasets reveals that the long-touted hypothesis of the role of lobopods in arthropod origins has very little support. Relationships between lobopods and panarthropod crown groups are largely unresolved due to poor phylogenetic signal and potential taphonomic and coding biases. This lack of resolution may be a primary factor in shaping a "basal grade" of lobopod organization, leaving open the possibility that panarthropods independently evolved defining morphological features. This work discusses the importance of incorporating developmental genetic data in assessments of morphological homology, and highlights the role uncertainty should play in the estimation of fossil phylogenetic relationships.

The missing precambrian record of definitive sponge fossils has presented a major scientific conundrum and fueled widely differing opinions about earliest animal life. Evidence from comparative molecular biology holds that sponges were not only one of

the earliest-branching animal groups, but likely were present in oceans in some form since the Cryogenian, contrasting with the first fossil appearance of crown sponge fossils in the lower Cambrian. The fossil material presented in this work demonstrates the presence of spicule-producing sponges within latest Ediacaran communities, and is the oldest evidence, to date, of true sponges. Additionally, the stratigraphic overlap of these sponge fossils with enigmatic Ediacaran forms in two geographically separate environments indicates that the sponges were ecologically prominent, widespread, and may have significantly impacted these evolutionary communities, alluding to the macroevolutionary role sponges likely played as ecosystem engineers. The reliable age constraints on these fossils will also make them useful for testing fossil calibrations in future molecular clock models of animal genetic divergence.

Chapter 2: Origin of Metazoan Developmental Toolkits and their Expression in the Fossil Record

Abstract

Developmental regulatory genes (largely transcription factors and signaling pathways) were once viewed as tightly connected to the origin of the morphological features with which they are associated in bilaterians. With the increased study of basal metazoans (sponges and cnidarians) as well as other eukaryotic clades, it is now clear that many of these highly conserved genes arose much earlier in evolution, and served different biological purposes. This provides a new view of the nature of developmental toolkits associated with the early origin of Metazoa: ancient regulatory genes were only later co-opted for the various developmental roles associated with bilaterian morphology. Here we review the nature of the toolkits at the origin of Metazoa, the Placozoan-Eumetazoan last common ancestor (LCA), the Cnidarian-Bilaterian LCA, and the Protostome-Deuterostome LCA. Integrating this data with recent molecular clock results and data on the fossil record reveals long macroevolutionary lags between the origin of the molecular toolkits and their developmental potential, and the origin of crown group morphologies as documented in the fossil record.

Keywords: Metazoa, phylogeny, fossil record, genetic toolkit, Ediacaran, Cambrian, macroevolution

Introduction

Although multicellularity has evolved in many eukaryotic lineages (Knoll 2011), differentiated cell types and tissues are relatively rare, having evolved in fungi, algae

(including land plants) and animals. The production of differentiated body plans in these lineages requires a suite of developmental genes, cell-cell interactions, and dynamic regulatory signaling. These have been best studied among animals, where comparative studies of considerable phylogenetic breadth have been carried out, supplemented more recently by a growing number of whole-genome sequences. Although their phylogenetic coverage is not yet comprehensive, comparative evolutionary developmental studies have revealed deep conservation of key developmental tools. Indeed, recent studies of such early-branching groups as sponges and cnidarians have uncovered many genes and components of developmental gene regulatory networks (dGRNs) previously thought unique to bilaterians. The presence of these genes in early-branching metazoan lineages raises important questions about their ancestral role in early metazoans.

In this chapter we discuss the acquisition of metazoan developmental characteristics within a developmental framework, focusing on a series of key nodes, including the metazoan last common ancestor (LCA) and the cnidarian and bilaterian LCAs. At each node we evaluate the evidence based on genomic data, expression data, and conserved pathways or functions, each progressively a more robust basis for inferring ancestral development. The summary here updates earlier reviews (e.g. Rokas 2008; Erwin 2009). Data from the fossil record, particularly from the Ediacaran (635-542 million years ago [Ma]) and the Cambrian (542-488 Ma) provides one critical insight when combined with molecular clock and comparative developmental studies: a long macroevolutionary lag separates the acquisition of the developmental toolkit needed to form bilaterians and their appearance in the fossil record (Erwin et al. 2011).

Phylogenetic Context

A phylogenetic context is required to integrate fossil and developmental evidence to understand the early evolution of Metazoa. In this section we present the current basic framework of metazoan phylogeny provided by molecular sequence data, with fossil data integrated as appropriate. The dating of important nodes is provided by molecular clock analyses. Although molecular clock studies of early metazoan history have yielded highly variable results, there is increasing congruence between different studies. In this section we follow the phylogenetic structure and molecular clock results presented in Erwin et al. (2011) except where indicated. We also highlight where discrepancies persist about the placement of particular clades.

Molecular Phylogeny

Recent studies of metazoan phylogeny have produced discordant results for the base of the tree (e.g. Edgecombe et al. 2011; Philippe et al. 2011b; Erwin et al. 2011; Ryan et al. 2013; Nosenko et al. 2013; see also discussion on the history of metazoan phylogenetic studies in Edgecombe et al. 2011). These studies differ in taxon coverage, sequences, and analytic details, but all reported strongly supported tree topologies. Two recent analyses of these studies evaluated the methodological problems contributing to the discordant results, particularly those associated with short internal branches between nodes caused by rapid diversification and long-branch attraction (Philippe et al. 2011b; Nosenko et al. 2013).

Although we acknowledge areas of continuing uncertainty below, drawing from these studies we have adopted the topology shown in Figure 2.1 (based on Erwin et al. 2011), with choanoflagellates as the outgroup to Metazoa and paraphyletic sponges at the

base of the tree. Placozoans, represented by *Trichoplax adhaerens,* branch next followed by coelenterates, including both cnidarians and possibly ctenophores (not shown). The position of ctenophores is critical to evaluating the monophyly of triploblastic animals with nerve and muscle cells, and is discussed below. The crown of bilaterians is well supported by molecular studies, and is comprised of the deuterostomes and the two major protostome clades: Lophotrochozoa and Ecdysozoa. Acoel flatworms, historically part of the Platyhelminthes and more recently placed between cnidarians and the bilaterian LCA, have been suggested to group with *Xenoturbella* at the base of the deuterostomes based in part on microRNA (miRNA) data (Philippe et al. 2011a). However, other studies support acoel and nematodermatid flatworms + *Xenoturbella* as more basal metazoans (Edgecombe et al. 2011), and as yet this clade remains unresolved. Regardless, one of the surprising insights of recent studies of bilaterian phylogeny is that the basal clades in each of the three major groups are morphologically simple, and as will be discussed further below, may have been simplified from morphologically more complex ancestors. The most recent metazoan phylogenies suggest that the basal groups are acoels and xenoturbellids among the deuterostomes, priapulids among the ecdysozoans, and platyhelminths among the lophotrochozoans. This pattern has important implications for interpreting the developmental and morphological complexity of the PDA and the LCA of the three major bilaterian clades.

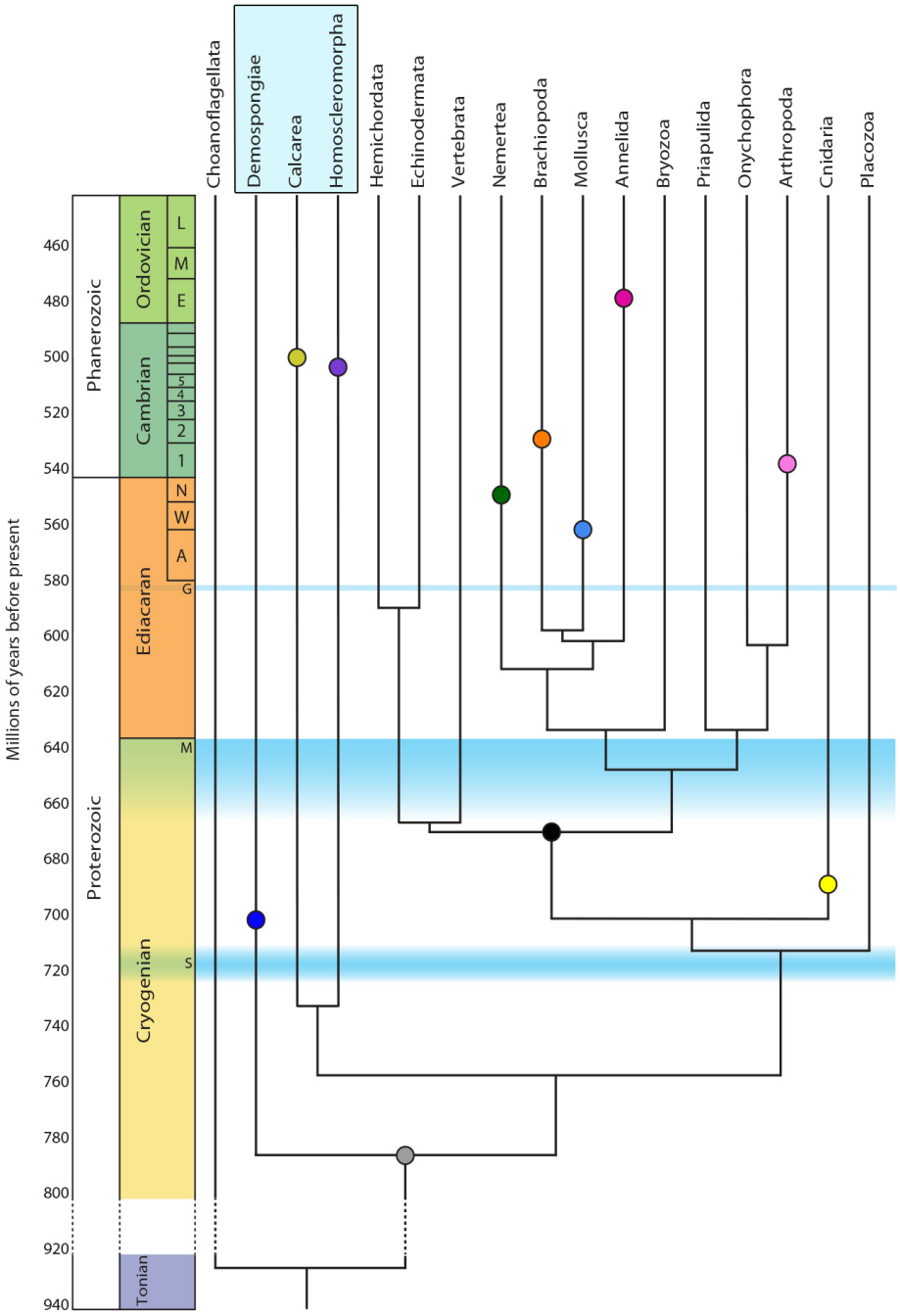

Figure 2.1. The origin of animals and major metazoan clades as inferred from molecular clock analyses, based on Erwin (2011).
Age estimates (in millions of years [Ma]) for major nodes are indicated by circles – grey (Metazoa), black (Bilateria) – while crown group age estimates are indicated by the colored circles on each branch. Sponge paraphyly is indicated by the blue box containing the major sponge groups. Horizontal blue bars represent glaciations, abbreviated as: S, Sturtian; M, Marinoan; G, Gaskiers. Major Ediacaran temporal/fossil assemblages are abbreviated: A, Avalon; W, White Sea; N, Nama. Early stages of the Cambrian period are labeled (1-5), and Ordovician stages abbreviated as E, Early; M, Middle; L, Late.

Several aspects of this topology remain uncertain. Some molecular studies indicate that living sponges are paraphyletic, with the demosponges, calcareous sponges and homoscleromorphs all distinct clades (Sperling et al. 2009), a result that receives support from studies of miRNA (Robinson et al. 2013). Yet the paraphyletic nature of sponges, though supported by molecular data, remains contentious and Nosenko et al. (2013) concluded that sponge monophyly vs. paraphyly depends on root placement. There are several groups of fossil sponges that may well represent additional distinct poriferan clades.

Ctenophores have proven difficult to place phylogenetically, and have been suggested to be the sister group to cnidarians as well as both basal to and above cnidarians in the analyses cited above. Less plausibly they have been placed at the base of the metazoan tree (Ryan et al. 2013), probably a consequence of long-branch attraction (Nosenko et al. 2013). Support for this basal position is not strong, and clearly more data is needed to resolve the ctenophore problem. The position of acoels, as discussed above, also remains contentious. Morphologic and developmental evidence suggested that they represent descendants of a basal bilaterian clade that branched before the PDA (Edgecombe et al. 2011), however, additional phylogenetic studies suggest a position as basal deuterostomes (Philippe et al. 2011a). Even if the latter hypothesis is correct, it is quite likely that acoelomorph-grade organisms, evidently now extinct, branched between cnidarians and the PDA. In this paper we follow the consensus phylogeny shown in Figure 2.1, noting where continuing topological uncertainties would affect our discussion.

Origin of Major Metazoan Clades and Crown Groups

Molecular clocks have been applied to dating early metazoan divergences for several decades, although with considerable spread in the results. The suite of available genes, the methods of analysis, and the variety of fossil calibration points have all improved and consequently different clock studies are beginning to converge. As outlined above, here we adopt a recent analysis that is largely consistent with other recent studies (Erwin et al. 2011). Its results are robust to a variety of tests, including root placement, choice of molecular clock model, and subsampling of the calibration points.

Results place the Metazoan LCA node at about 800 Ma, followed by the rapid divergence of sponge clades, the appearance of cnidarians, and their divergence into the Anthozoa and Hydrozoa by about 700 Ma (Figure 2.1). If these results are generally correct, they indicate that all of these divergences, as well as the appearance of the bilaterian LCA, occurred during the Cryogenian Period. As its name implies, the Cryogenian began with the Sturtian glaciation and ended, at about 635 Ma, with the end of the Marinoan glaciation. Each glaciation was global in extent, and each has been associated with possible 'Snowball Earths' in which the Earth's surface became entirely glaciated. Whatever the validity of the Snowball Earth hypothesis, growing geochemical and other environmental evidence confirms considerable environmental turmoil during the Cryogenian.

Bilaterian clades diverged during the Ediacaran Period, with the time of origin of most bilaterian crown groups clustered into a relatively narrow interval from the late Ediacaran into the Cambrian. The overall pattern, on which we elaborate in the discussion, indicates genetic divergence of major metazoan clades during the Cryogenian

and Ediacaran, but there is no evidence from the fossil record that representatives of these lineages had yet evolved Phanerozoic morphologies. After some 150-200 million years of evolution the relatively simultaneous appearance of new bilaterian morphologies is documented in the fossil record by the Cambrian explosion, and in the crown group nodes estimated via molecular clock analysis. A new study estimates major ecdysozoan divergences occurring in the Ediacaran, with the pancrustaceans diversifying during the early Cambrian (Rota-Stabelli et al. 2013).

Developmental Toolkits in a Phylogenetic Perspective

Genomic studies of many eukaryotic lineages have demonstrated that the widespread occurrence of multicellularity (Knoll 2011) reflects the broad distribution of many of the developmental tools required for the generation, organization, and maintenance of multicellular structure (Parfrey and Lahr 2013; Rokas 2008; Sebé-Pedrós et al. 2011). These tools include members of a variety of transcription factor families (Hox, Sox, T-box, Pax, ANTP, etc.), components of the major cell signaling pathways such as Wnt, Notch/Delta, Hedgehog, and TGF-β, as well as cell adhesion and structural molecules. Early information about the phylogenetic distribution of the developmental toolkit came from studying expression patterns in transcription factors and signaling systems, which turn out to display greater phylogenetic conservation than expected several decades ago. Although these studies initially considered only model animal systems, more recent work has engaged a phylogenetically more diverse array of organisms, providing a stronger basis for inferring the nature of developmental systems in early Metazoa. For our discussion of early metazoan developmental toolkits, four nodes on the tree in Figure 2.1 are of particular significance: the last common metazoan

ancestor, which documents the complexity of gene regulatory and developmental tools shared across all living animals; the node between placozoans and all higher metazoans; the cnidarian-bilaterian LCA; and the protostome-deuterostome ancestor (often considered the bilaterian LCA as well).

One theme that has emerged recently is that most of the developmental tools responsible for patterning bilaterians have much deeper roots and many developmental genes – and even gene pathways – appear to have achieved their current functions through gene co-option. Current function is thus often a poor guide to ancestral function, and can severely constrain inferences about the nature of ancestral clades (Erwin and Davidson 2002; Davidson and Erwin 2010). Reconstructing developmental tools and capabilities at various points along metazoan phylogeny depends upon an array of different evidence, including genomic data, expression data, and evidence for conserved developmental pathways and functions (in increasing order of the difficulty of obtaining the data). Genomic data (see Table 2.1) provides a baseline estimate of the shared developmental toolkit, and information about the presence of critical protein-binding domains at most may suggest potential function. Demonstrating spatiotemporal patterns of expression is often a first step in hypothesizing gene developmental roles, however, only data from experimental manipulation verifies conserved pathways and roles for toolkit components (Table 2.2). The strength of inferences about the nature of LCAs differs depending on the source of data; consequently, in this section we discuss evidence for each specific type of data. Tables 2.1 and 2.2 summarize a selection of the genomic and expression/functional evidence (respectively) discussed below. This approach provides a conservative basis for inferring the likely morphology at each key node.

Table 2.1. Genomic presence/absence of a selection of developmental tools integral to metazoan development. This subset of genes is representative of the evolving molecular capacity for core developmental processes, such as morphogenesis and patterning/differentiation. Summarized from (King et al. 2008; Srivastava et al. 2008; Fahey and Degnan 2010; Srivastava et al. 2010; Fairclough et al. 2013).

		Choano-flagellatea	Sponges	Placozoa	Cnidaria	Bilateria
Cell-cell adhesion	Integrins	○	•	•	•	•
	Fibrillar collagen	○	•	•	•	•
Cell polarity	Crumbs		○	•	•	•
	Stardust/MPP5 /Pals-1				•	•
	Bazooka/Par-3		○	○	•	•
	Par-1	•	•	•	•	•
	Lethal Giant Larva (Lgl)	○	•	•	•	•
	Discs Large (Dlg)	•	•	•	○	•
Adherens junctions	Cadherins	○	•	•	•	•
	Catenins		•	•	•	•
	Patj	•	•	•	•	•
	Vinculin	•	•	•	•	•
Basal lamina	Type IV collagen		○[a]	•	•	•
	Laminin	○	○	○	•	•
	Nidogen			•	•	•
	Perlecan			○	•	•
Tight junctions	Claudin					•
	Occludin					•
Septate junctions	Neurexin			○	○	•
	Neuroglian			•	○	•
	Contactin					•

(table continues on following page)

Table 2.1 (continued)

		Choano-flagellatea	Sponges	Placozoa	Cnidaria	Bilateria
Signaling pathways	Notch/Delta	○	•	○	○	•
	Hedgehog	○	○	○	•	•
	Wnt		•	•	•	•
	JAK/STAT	○	○	○	○	•
	RTK	○	○	•	•	•
	TGF-β		•	•	•	•
Transcription factor families	Sox	•	•	•	•	•
	Fox	•	•	•	•	•
	T-box		•	•	•	•
	POU		•	•	•	•
	LIM		•	•	•	•
	ANTP		•	•	•	•
	Six		•	•	•	•
	PRD		•	•	•	•

Closed circles represent the presence of gene homologs identified in one or more species of the clade. *Open circles* represent the presence of aberrant or incomplete homologous genes. In the case of signaling pathways, *closed circles* indicate homologs of a complete signaling pathway, and *open circles* indicate the absence of core pathway components. [a]indicates the presence of type IV collagen in one sponge group (Homoscleromorpha)

Metazoan LCA

The availability of choanoflagellate and sponge whole-genome sequences (King et al. 2008; Srivastava et al. 2010b; Fairclough et al. 2013) as well as genomic data from several additional sponges has greatly improved our ability to infer the shared genetic features of the metazoan LCA. However, function cannot be confidently assigned by sequence presence/absence data alone, and both gene expression data and experimental reconstruction of functional pathways lag behind that of both the eumetazoan and bilaterian LCAs.

Genomic Data

Choanoflagellates contain genes that encode conserved protein domains found in cadherins, some cell adhesion and polarity proteins, and components of signaling pathways used in cellular differentiation and patterning in metazoans (King et al. 2008; Fairclough et al. 2013). Representative domains of some metazoan transcription factor families are present as well, although these are less diverse than in metazoans. Of the seven major metazoan signaling pathways (Wnt, Hh, TGF-β, Notch/Delta, JAK/STAT, NHR, RTK), elements of four (Hh, Notch/Delta, JAK/STAT, RTK) are known from choanoflagellates, although the JAK/STAT pathway is represented by only a single gene (Larroux et al. 2008).

Reconstruction of the evolution of signaling pathway components between choanoflagellates and the metazoan LCA suggests that it largely involved the shuffling of ancient eukaryotic domains with completely new domains. For example, domains of key components of both the Wnt and Hedgehog pathways, although present in choanoflagellate genomes, are not found in the organizations known to be critical for pathway function in metazoans. Interestingly, although the pathways are incomplete, some signaling components shared between choanoflagellates and metazoans have been found to be disproportionately upregulated in both thecate cells and multi-cell colonies of the choanoflagellate *Salpingoeca rosetta* (Fairclough et al. 2013); perhaps the evolution of these domains may be related to the capacity to form these different cell morphologies and multi-cell associations.

Sponges have multiple cell types with some regional patterning and coherent body architectures. They possess homologs within most of the major transcription factor

families, including ANTP, Sox, Fox, T-Box (including Brachyury), and PRD-like (Larroux et al. 2008; Srivastava et al. 2010b). Although T-box genes have not been identified in choanoflagellates, they have been reported from the amoeba *Capsaspora owczarzaki* and other opisthokonts, including a Brachyury homolog (Sebé-Pedrós et al. 2013). Moreover, the T-box family appears to have diversified at the base of Metazoa. The developmental tools necessary to generate basic sponge-grade features are present, but sponges appear to lack many of the tools necessary for the level of developmental and regulatory control found in more derived clades, and most of the transcription factor families listed above have relatively few members. True Hox genes, responsible for regional identity establishment in bilaterians, have not been identified in sponge genomes, although this seems to be due to the secondary loss of Hox and ParaHox loci in the poriferan lineage (Ramos et al. 2012). Adamska et al. (2011) suggest that the Wnt, TGF-β and Notch/Delta signaling pathways were largely complete and probably functioned similarly to those of eumetazoans, while the Hedgehog and tyrosine kinase growth factor pathways were evidently still missing their key signaling ligands. The genome of the homoscleromorph sponge *Oscarella carmela*, as in the demosponge *Amphimedon queenslandica*, has components of six of the seven primary signaling pathways in metazoans (Nichols et al. 2006).

The evolution of epithelia is a critical innovation in metazoans, and there has long been debate over the extent to which sponges can be considered to have true epithelia (Leys and Riesgo 2012; Fahey and Degnan 2010). Part of the controversy reflects different definitions of epithelia, but critical to this subject is the extent to which sponges contain adherens and tight junctions as well as a basement membrane or lamina. The

Amphimedon genome has evidence for several orthologs of cell polarity genes and adherens junction components, but no evidence for orthologs of genes associated with either tight or septate junctions, or basal lamina (Srivastava et al. 2010b; Fahey and Degnan 2010; Nichols et al. 2012). Consistent with the pattern seen in other proteins, many of the domains that were eventually assembled to form septate and tight junctions and basal laminae are present in the *Amphimedon* genome and were likely present in the metazoan LCA (Fahey and Degnan 2010). In contrast, homoscleromorphs have long been known to have type IV collagen, a key component of basement membranes, and Leys and Riesgo (2012) have identified the sequence for it in a calcareous sponge as well. Leys and Riesgo (2012) also suggest that poriferan claudin-like genes indicate septate junctions were present in the metazoan LCA.

Cadherins are cell surface receptors involved in cell adhesion, polarity and developmental signaling. Although many cadherin protein domains have been identified in choanoflagellates, these do not include the conserved cytoplasmic domain found in metazoan cadherins (King et al. 2008; Fairclough et al. 2013). Analysis of sponges indicates that representatives of at least three cadherin families, lefftyrin, coherin and hedgling (a sponge and cnidarian-specific precursor to Hedgehog), were present in the metazoan LCA and, as discussed below, may have been able to participate in intracellular signaling (Nichols et al. 2012).

An expressed sequence tag (EST) comparison of sponge genes to those of other metazoans showed the greatest similarity between sponges, cnidarians and deuterostomes, with the lowest similarity among protostomes (Harcet et al. 2010). This result is consistent with earlier comparisons between *Nematostella vectensis* and other

lineages indicating extensive gene loss on the protostome line (Ogura et al. 2005, Chapman et al. 2010, Forêt et al. 2010).

Expression Data

The Sox genes are a family of HMG box transcription factors involved in the regulation of cell type specification and development in animals, and the family appears to have arisen between choanoflagellates and the metazoan LCA. Fortunato et al. (2012) identified seven Sox and four Sox-like genes in a calcareous sponge, and showed that they were dynamically and differentially expressed in unique patterns during embryonic development, or in specific adult sponge cell types. Similarly, *Amphimedon* embryos dynamically express the genes for a single Notch receptor and five Delta ligands, reflecting the multiple developmental roles of this signaling pathway (Richards and Degnan 2012). In bilaterians, Pax and Six genes are part of a regulatory network that is involved in development of many tissues and organs. Recent work has shown Pax and Six expression in cells located in active growth zone in the developing choanoderm of a freshwater demosponge (Rivera et al. 2013), and additional knock-down experiments (as discussed below) have elucidated some Pax/Six regulatory interactions.

The Wnt signaling pathway is absent in choanoflagellates, and the presence of almost all Wnt pathway components in multiple sponges indicates this to be a metazoan developmental innovation (Petersen and Reddien 2009; Adamska et al. 2010). Wnts carry out many functions in bilaterian development, including the establishment and organization of primary body axes. The dynamic expression patterns of Wnt signaling components during *Amphimedon* embryonic development suggest multiple, temporally

distinct regulatory roles. Adamska et al. (2010) observed early, polarized expression of Wnt pathway components suggestive of broad anterior-posterior (A/P) axis patterning in addition to later expression localized to a larval organ-like structure. Although these distinct spatio-temporal expression patterns are compelling, further study is needed to demonstrate the precise functional roles of the Wnt pathway in generating these sponge features.

The expression patterns of genes associated with more terminally differentiated cell types have also been investigated in sponges. Although sponges lack mesoderm or muscle cells, Steinmetz et al. (2012) identified orthologs of both striated muscle (ST) and non-muscle (NM) heavy chain myosin (MyHC) in two demosponges. Non-muscle MyHC was detected in many adult cell types, including the pinacocytes responsible for sponge peristalsis-like contraction, while ST MyHC was restricted to the outlet pores (apopyles) which house a sieve-like cell that controls water flow. Steinmetz et al. propose that an early metazoan contractile apparatus existed in the LCA, the components of which independently evolved to form distinct muscle types in the cnidarian and bilaterian lineages (see below). Though sponges lack neurons and photoreceptive opsin pigments, *Amphimedon* larvae possess posterior ciliated pigment rings that are believed to mediate phototaxis (Leys et al. 2002). Rivera et al. (2012) recently discovered two genes encoding cryptochrome (Aq-Cry1 and Aq-Cry2), one of which (Cry2) is expressed in the larval pigment ring eye and maximally absorbs blue light – the same wavelength corresponding to peak larval swimming activity. The LIM homeobox family of transcription factors are involved in the development of many organs in bilaterians, but notably all members of this family have roles in specifying neural cell fates. Lhx3/4 (lim-3), Lhx1/5 (lin-11) and

Islet are all expressed in developing *Amphimedon* embryos, including cells specific to the aforementioned eye pigment rings (Srivastava et al. 2010a). These expression studies suggest that molecular tools gained their developmental roles in multifunctional cells prior to the segregation of these functions in additional specialized cell types.

Conserved Pathways and Conserved Functions

Complex developmental GRNs have not yet been identified in sponges, and some workers have suggested that this may limit their morphologic complexity (Adamska et al. 2007; Fahey et al. 2008). Some evidence for conserved functions, however, has been described. In line with the observed polarized expression of Wnt in *Amphimedon* embryos (Adamska et al. 2010), Windsor and Leys (2010) have found that disruption of the canonical Wnt pathway effects aspects of sponge aquiferous system organization, suggesting a role of the Wnt pathway in establishing sponge axial polarity. And, although studies have yet to be done *in vivo*, based on amino acid domain comparisons Nichols et al. (2012) propose that the classical cadherin identified in *Oscarella carmela* may have had the ability to bind β-catenin, thus regulating cell-cell adhesion and contributing to other downstream signaling cascades. The regulatory interactions between Pax and Six genes have been established in the freshwater demosponge *Ephydatia muelleri*, indicating that a component of the network is present and may have been involved in the formation of a multifunctional epithelia (Rivera et al. 2013).

Extinct spongiform clades have been described from the lower Paleozoic fossil record, including archaeocyathids, chancelloriids and other groups. Archaeocyathids include a variety of early Cambrian fossils with a unique, double-walled and heavily

calcified skeleton. They have been assigned to a number of groups, from sponges to an extinct phylum, but the discovery of modern sclerosponges has confirmed that archaeocyathids were indeed sponges (Rowland 2001). It now appears likely that both sponge spicules and massive, sclerosponge-like skeletons evolved multiple times among the different sponge lineages; other fossil clades of equivalent rank may also exist (Sperling et al. 2007). Further study of the unique character combinations of some of these groups might shed further light on the evolution of developmental complexity (Erwin and Valentine 2013).

The paraphyletic nature of sponges indicates that the metazoan LCA was likely a simple filter-feeding organism, with genetic elements of what would eventually become elaborate signaling pathways and developmental GRNs. Multiple cell types with some regional body patterning would have been present, but although homologs of most major transcription factor families were present, these were likely utilized in cell-type specification rather than in establishing more sophisticated morphology. Any limited patterning may have included axial polarization / organization via Wnt signaling, for example, as there is little evidence that sponges were capable of more sophisticated regulatory control. Tight junctions and basal laminae may have been present, with cadherins mediating cell adhesion and signaling; thus, the metazoan LCA may have been a proto-epithelial, simply-patterned organism.

Placozoan-Eumetazoan LCA

The complete genome sequence of the placozoan *Trichoplax adhaerens* has provided insights into development in eumetazoans (Srivastava et al. 2008). The presence of epithelia in *Trichoplax* has led to the definition of placozoans plus all eumetazoans as

the epitheliozoa (Sperling et al. 2009), suggesting the presence of true epithelia in this basal group. However, while polar cells with zonula adherens are present in placozoans, in addition to genes encoding collagen and laminins, there is no underlying basal lamina and evidence for septate junctions is ambiguous. Thus, true epithelia seems to be absent (Fahey and Degnan 2010). Placozoans also lack nerve or muscle cells (although they do respond to external stimuli), organs, and anterior-posterior differentiation, but share members of the gene families associated with such patterning with eumetazoans. For an excellent discussion of the tribulations of *Trichoplax* since its discovery and an overview of its morphology see Schierwater et al. (2011). Some of the soft-bodied Ediacaran macrofossils may represent either placozoans or related lineages (Sperling and Vinther 2010).

Genomic, Expression & Functional Data

Evidence on the nature of the placozoan developmental toolkit is based largely on genomic data, with only a few papers providing information on gene expression. The genome of *Trichoplax* shows a high degree of conservation of gene structure and synteny, and little of the intron loss observed in other species (Srivastava et al. 2008). The whole-genome analysis identified a variety of transcription factors used by eumetazoans in regional patterning and cell type specification, despite the limited evidence for placozoan regional patterning and the presence of only four or five cell types (Srivastava et al. 2008). A total of 23 different transcription factor families have been identified, including homeobox members of the paired and ANTP classes and Brachyury from the T-box family. Within the ANTP class, representatives of the Hox/ParaHox, NKL and extended

Hox groups have been identified (Schierwater et al. 2011). A more recent analysis of orthologous genes syntenous to Hox and ParaHox loci indicates that the single Hox-like gene in *Trichoplax* is likely a ParaHox ortholog, with only remnants of a Hox locus remaining after the loss this gene in the lineage (Ramos et al. 2012).

Several signaling pathways are present, including Wnt, TGF-β, Notch and JAK/STAT, although some have lost key components for signal transduction. As some sponges appear to have these components, this suggests they were lost in the placozoan lineage. Some cell types in *Trichoplax* may have retained ancestral multifunctionality, which would explain why the genome contains evidence for ion channels, neurotransmitter and neuropeptide receptors but lacks evidence for the ability to generate either neurotransmitters or synapses. Srivastava et al. (2008) emphasize that the rich diversity of *Trichoplax* developmental control systems is consistent with the suggestion of Erwin and Davidson (2002) that these systems were co-opted in cnidarians and other eumetazoans for regional patterning.

Gene expression and functional data in *Trichoplax* is limited, but hints at a developmental complexity belied by the basic placozoan morphology. Trox-2, the single ParaHox gene described above, is expressed around the entire animal periphery in small cells between the upper and lower epithelial layers (Jakob et al. 2003). Disruption of this gene halts growth and binary fission, suggesting a role in the specification of a stem cell population. The T-box family genes Brachyury and Tbx2/3 are also expressed in *Trichoplax*, and because these genes show distinct localizations uncorrelated with anatomical features, Martinelli and Spring (2008) suggest the presence of undescribed cryptic cell types. The placozoan upper cell layer consists of monociliated cells, and

placozoans do possess a homolog to FoxJ1, a transcription factor involved in ciliogenesis. Ectopic expression of this placozoan homolog in zebrafish embryos induces the expression of known ciliogenic target genes, supporting a conserved role for placozoan FoxJ1 in the development of cilia (Vij et al. 2012). The transcription of other key toolkit components has been reported without localization information, via *in situ* hybridization (LIM homeobox genes; Srivastava et al. 2010a) and mass spectrometry of the proteome (Notch/Delta, Wnt and TGF-β pathway components, ECM-related proteins; Ringrose et al. 2013). The *Trichoplax* proteome analysis only increases ambiguity concerning the existence of basal lamina, for although many basement membrane proteins are translated there is no evidence for either classical cadherin expression or the associated catenins known to mediate adhesion at zonula adherens junctions (Ringrose et al. 2013).

As Sperling and Vinther (2010) note: "crown-group placozoans likely represent a limited and highly derived subset of [Ediacaran + placozoan clade] diversity" (p. 204). This seems to us quite likely, with *Trichoplax* a highly derived remnant of this clade. Ancestral members of this clade could have been more morphologically sophisticated, given the developmental complexity of elements found in *Trichoplax*, but in a pattern first observed in sponges (and that will recur in cnidarians) the developmental potential of these clades appears to be higher than their realized morphologic complexity.

Cnidarian-Bilaterian LCA

As described in the metazoan phylogeny section, we believe that the weight of the current evidence supports a topology with ctenophores as the sister group to cnidarians (Coelenterata hypothesis), and we view claims that ctenophores are basal to sponges as an artifact of long-branch attraction (Nosenko et al. 2013). The genome of the ctenophore

Mnemiopsis has been sequenced (Ryan et al. 2013), and recent papers suggest that it lacks a variety of developmental genes found in other eumetazoans. Among the missing elements in *Mnemiopsis* are five of the 11 defined homeodomain classes and several Hox class genes (Ryan et al. 2010), parts of the TGF-β signaling pathway (Pang et al. 2011), and both miRNAs as well as the Drosha and Pasha nuclear proteins required for miRNA processing (Maxwell et al. 2012). This has been interpreted as supporting a position for ctenophores basal to sponges (as in Ryan et al. 2013) and would imply that muscles, elements of the nervous system, and other attributes of ctenophores evolved twice, requiring sponges to be secondarily simplified from a more complex ancestor. Given the well-documented problems with establishing relationships among early-branching metazoans, it seems more plausible that crown ctenophores have secondarily lost many elements.

Cnidarians exhibit polarity along a primary body axis (oral-aboral) and are diploblastic, with two germ layers (ectoderm and endoderm) giving rise to two epithelial layers with myoepithelial cells, a non-centralized nerve net nervous system, and the highly specialized stinging cells (cnidocytes) which define the group. It is now evident that cnidarian body plans, morphologically simple in comparison to the diversity of bilaterian forms, are underlain by complex developmental programs that deploy many of the same molecular tools and regulatory pathways thought to be unique to bilaterians.

Genomic and Expression Data

The genomes of *Nematostella vectensis* and *Hydra magnipapillata* share a surprisingly greater number of linkage groups and conserved synteny with the human

genome than what may be expected given the estimated cnidarian-bilaterian divergence of 700 Ma (Putnam et al. 2007; Chapman et al. 2010; Steele et al. 2011, Erwin et al. 2011). And, although it has less conserved gene organization than in *Nematostella*, *Hydra* displays genomic conservation far beyond that of the more recently diverged protostomes *Drosophila melanogaster* and *Caenorhabditis elegans* (Chapman et al. 2010). Preliminary analysis of EST data from the hydrozoan *Clytia hemisphaerica* finds it has a higher proportion of unique, taxon-specific genes than either *Nematostella* or *Hydra*, perhaps owing to unique genetic requirements of both polyp and medusa life cycle stages (Forêt et al. 2010). Given the deep split between the cnidarian crown groups Anthozoa and Hydrozoa, the forthcoming *Clytia* whole-genome sequence should be enlightening.

Homologs for members of all of the major developmental transcription factor families seem to be present in cnidarians, with the possible exception of the NF-κB and NFAT families. The single *Nematostella* NFAT-like protein groups ambiguously with other NFAT genes, and the IκB C-terminal domain of all bilaterian NF-κB proteins is absent in the *Nematostella* homolog (but present in different protein sequence) (Sullivan et al. 2006). Sox, Fox, and T-box genes are found in the *Nematostella* genome (Magie et al. 2005; Putnam et al. 2007), and, like their homologs in bilaterians, appear to be associated with processes as diverse as regional patterning, germ layer and cell fate specification, and morphogenesis. Sox genes expressed in the blastopore region of *Nematostella* gastrulae may be functioning to restrict ectoderm vs. endoderm fate, while a repertoire of *Nematostella* Fox genes expressed along the oral-aboral axis may be involved in defining distinct domains along this primary axis (Magie et al. 2005).

Nematostella possesses representatives of all classes of homeobox transcription factors, barring *engrailed*, while the faster rate of evolution in *Hydra* has lead to the loss of many homeobox proteins in its genome (Chapman et al. 2010, Forêt et al. 2010). Members of the homeobox transcription factor LIM family are present in both taxa (e.g. Lhx, Lmx, islet), and as in bilaterians, may work in combination to specify specific neural cell fate. *Nematostella* LIM genes are combinatorially expressed in three major neuralized regions – the planula apical tuft and the polyp oral and pharyngeal nerve rings – but expression of these genes in neurons and similar expression in *Hydra* or *Clytia* have yet to be demonstrated (Srivastava et al. 2010a). And, while the staggered expression of *Nematostella* anterior and posterior-class Hox genes along the oral-aboral axis (Finnerty et al. 2004) is suggestive of a conserved "Hox code" between cnidarians and bilaterians, Hox homolog expression domains in *Clytia* do not demonstrate conservation of such a role across Cnidaria (Chiori et al. 2009), and a "true" Hox patterning system likely postdates the cnidarian-bilaterian split (Schierwater and Kamm 2010).

By the evolution of the cnidarian-bilaterian LCA, genes representing all of the major developmental signaling pathways are present and largely complete (Putnam et al. 2007, Chapman et al. 2010). Components of the non-canonical (PCP) Wnt pathway, absent in sponges (with the exception of atypical cadherin Flamingo in *Oscarella carmela* (Nichols et al. 2012)), are present in the *Nematostella* and *Hydra* genomes (Putnam et al. 2007, Chapman et al. 2010), along with eumetazoan BMP/Chordin signaling components and downstream TGF-β effectors. The first true Hedgehog proteins also arose in the cnidarian-bilaterian LCA lineage, which likely possessed both Hedgling and Hedgehog proteins. Interestingly, because the Hedgehog ligand requires polarized

cells and associations with basement membrane-related proteins for processing (Ingham et al. 2011), the evolution of this signaling pathway may have been dependent upon the evolution of true epithelia.

Cnidarian contractile myoepithelial cells comprise both striated and smooth muscle types, both of which express the highly conserved type II myosin heavy chain protein. Striated-type (ST) MyHC is expressed in cnidarian fast-contracting muscles and non-muscle (NM) MyHC broadly in both smooth and non-muscle cells in the endoderm. However, cnidarians lack defining features of bilaterian striated muscle, such as the troponin complex, which is completely missing, and z-disc components, which are expressed either ubiquitously or only in smooth muscle (Steinmetz et al. 2012). Steinmetz et al. (2012) propose that cnidarian and bilaterian striated muscle each evolved independently from an ancient shared contractile machinery based on ST and NM MyHC.

Conserved Pathways and Conserved Functions

Functional studies in cnidarians – primarily *Nematostella*, *Clytia*, and *Hydra* – increasingly point to an ancient conserved role for canonical Wnt signaling as a major developmental "organizer", contributing to axis establishment, germ layer specification, and gastrulation. Throughout Bilateria, early nuclear β-catenin localization via activation of canonical Wnt signaling is a major contributor to patterning the future posterior (and thus A/P axis), specifying endomesoderm cell fate, setting the site of gastrulation, and antagonizing anterior-patterning signals. The Spemann organizer in the frog *Xenopus*

provides a classic example: when transplanted to new regions of an embryo, cells that have received these signals induce a secondary axis.

A growing body of evidence indicates a conserved role for the canonical Wnt pathway in determining a similar cnidarian "organizer" and in patterning axial polarity. The cnidarian blastopore forms in the animal hemisphere of the embryo at the oral pole, and cells that ingress form the cnidarian endoderm. As in the formation of bilaterian posterior domains, oral pole fate seems to be determined by known bilaterian "posterior" cues. In *Nematostella* and *Clytia*, β-catenin stabilization specifies the oral-aboral axis by defining presumptive oral territory; inhibition of the canonical Wnt pathway disrupts gastrulation, while ectopic pathway activation favors endoderm formation (Momose et al. 2007, Lee et al. 2007, Röttinger et al. 2012). Transplantation of the *Nematostella* blastopore lip even induces the formation of a secondary body axis (Kraus et al. 2007). In *Hydra*, Wnt, downstream effector Tcf, and β-catenin are known to exhibit "head" organizer effects, and maintain adult polarity (Broun et al. 2005). These findings make a compelling case for the molecular homology of the cnidarian oral and the bilaterian posterior poles.

Many deuterostome embryos are "pre-loaded" with maternal transcripts to deploy this Wnt cascade, and a similar mechanism in *Clytia* has been identified (Momose et al. 2008). Maternal transcripts of the *Clytia* Wnt receptor Frizzled (CheFz1 and CheFz3) were found to be localized to the animal and vegetal halves of the egg, respectively, with CheFz1 forming a cytoplasmic gradient from animal to vegetal pole and CheFz3 tightly localized to the vegetal cortex. These receptors regulate β-catenin stabilization positively

(CheFz1 in oral pole) and negatively (CheFz3 in aboral pole), effectively establishing polarized Wnt activation (and oral tissue identity) along the oral-aboral axis.

Cnidarian orthologs of bilaterian "anterior" genes also appear to specify the cnidarian aboral pole, adding further evidence for a conserved primary axis patterning regulatory program (Sinigaglia et al. 2013). Six3/6, a key regulator of anterior patterning in all three major bilaterian clades, specifies the early identity of the *Nematostella* aboral region, and activates a suite of anterior-patterning homologs which set more finely-resolved regional boundaries. These include FoxQ2, FGFs (known to antagonize Wnt signaling and thus suppress posterior fate in bilaterians), and FoxJ1, which seems to specify development of ciliary cells in the apical organ (Sinigaglia et al. 2013).

Other cnidarian signaling pathways share more broadly related patterning and morphogenetic roles with bilaterians. BMP2/4/Dpp and Chordin establish endodermal molecular asymmetry along the *Nematostella* directive (perpendicular to oral/aboral) axis (Saina et al. 2009). The bilaterian dorsal/ventral axis is also specified by BMP signaling, but though it is tempting to homologize these pathways, Saina et al. (2009) point out that differences in wiring make it likely that BMPs were first used for axial patterning before being modified in bilaterians for specific D/V formation. The non-canonical Wnt pathway (planar cell polarity [PCP] pathway), well-studied in *Drosophila* and vertebrates, is involved in the generation/lateral orientation of cellular structures (including cilia) in epithelial sheets, and through this mechanism, planar-oriented cell divisions. Momose et al. (2012) have demonstrated that the PCP pathway is necessary for ciliogenesis and the oral/aboral orientation of cilia in the *Clytia* planula larva in addition to the oriented cell divisions necessary for embryo elongation, supporting an ancient role

in cellular organization. Notch/Delta signaling in *Nematostella* appears involved in the oriented cell division, cell shape change, and cell fate partitioning required for embryonic tentacle elongation (Fritz et al. 2013), and though these reflect a subset of Notch/Delta roles in bilaterians, it is also notable that tentacle outgrowth does not seem to employ a Distal-less/Dlx-based signaling circuits as does many bilaterian outgrowths/appendages.

By the evolution of the cnidarian-bilaterian LCA, metazoans possessed a large and functionally diverse repertoire of developmental signaling pathways and transcription factors. These animals had the capacity to establish both a primary and an orthogonal body axis, as well as organize sensory and other anatomical structures in relation to these axes. A mouth and gut were probably present, in addition to multifunctional cells necessary for navigating and responding to the environment. Developmental components seemed to have participated in roles similar to, but less specific than, those in bilaterians, contributing to broad fate restriction and patterning but not yet to the extensive segregation of function in bilaterian germ layers, organs, and tissues.

Protostome-Deuterostome LCA

Developmental biologists initially had little reason to expect that the developmental pathways, and even the genes controlling development in organisms as different as flies and vertebrates, would be related. The discovery of extensive conservation of both genes and pathways led to early proposals on the nature of the protostome-deuterostome LCA (Arendt and Nubler-Jung 1994; Shenk and Steel 1994; De Robertis and Sasai 1996) and more detailed discussions as additional data accumulated (Knoll and Carroll 1999; Baguñà et al. 2001; Carroll et al. 2001; Valentine et al. 1999). As described in the preceding sections, however, the identification of many of these

highly conserved genes in phylogenetically more distant clades called into question many of the earlier inferences about developmental homologies (Erwin and Davidson 2002; Davidson and Erwin 2010).

As the cnidarian-bilaterian LCA was characterized by general body patterning produced by conserved organizing pathways well-described in bilaterians, we will limit our discussion of the PDA toolkit to those components contributing to more urbilaterian-specific features.

Genomic Data

Inferring the structure of the bilaterian LCA genome and developmental toolkit requires comparisons between the three major bilaterian clades: the protostome groups Ecdysozoa and Lophotrochozoa, and Deuterostomia. Early work with model ecdysozoans *Drosophila* (fruit flies) and *Caenorhabditis elegans* (nematode worm) seemed to indicate that Ecdysozoa had undergone extensive gene loss, but with the addition of many more taxa it is clear that gene loss is more a function of divergence time and high rates of evolution regardless of lineage (Wyder et al. 2007; Miller and Ball 2009). Data from lophotrochozoans still lags behind the other clades. A preliminary analysis of three lophotrochozoan genomes - owl limpet *Lottia gigantea*, marine polychaete *Capitella teleta*, and freshwater leech *Helobdella robusta* – finds that these genomes exhibit greater similarity in organization and content to basal deuterostomes than to other protostomes, and the authors suggest that these genomes may more accurately approximate the ancient bilaterian condition (Simakov et al. 2013).

Table 2.2. Comparison of functional roles of a subset of metazoan developmental tools. Summary of experimental evidence demonstrating the likely developmental functions of select genes/pathways in extant groups, and by extension, the potentially ancient origin of some of these roles. See text for full discussion.

	Sponges	Placozoa	Cnidaria	Bilateria
Canonical Wnt Pathway	Early polarized expression in *Amphimedon* larvae suggests axial patterning; disruption affects aquiferous system organization	Pathway components present in genome	"Organizer" role in *Nemtaostella, Clytia, Hydra*; specification of oral/aboral axis, oral regional fate and endoderm fate	"Organizer" in many bilaterians; anterior / posterior axial patterning, specification of posterior fate, gastrulation site, endomesoderm
Notch / Delta pathway	Dynamical expression in *Amphimedon*	Pathway components present but incomplete; lacking key domains	Oriented cell division and shape change, cell fate partitioning in tentacle elongation in *Nematostella*	Many roles, including morphogenesis, boundary formation, cell fate partitioning
Pax/Six	Pax/six expressed in *Ephydatia* choanoderm active growth zone; involved in aquiferous system organization, cell type differentiation	Six3/6 and second Six family transcription factor present in genome	Six3/6 involved in early identity of aboral region; activates "anterior" Fox gene homologs	Pax/six involved in development of tissues and organs; six3/6 involved in anterior patterning
FOX	Fox genes present in genome	Ectopic expression of *Trichoplax* FoxJ1 in zebra-fish induces expression of ciliogenic target genes	FoxJ1 may be involved in specification of ciliary cells in *Nematostella* apical organ	FoxJ1 regulates ciliogenesis in vertebrates; expressed in sea urchin larvae apical tuft
HOX	True Hox genes absent; likely secondary loss	Expressed in interstitial cells around periphery of animal; disruption halts binary fission/growth	Exhibits staggered expression along *Nematostella* oral/aboral axis	Involved in regional patterning across Bilateria
LIM	Lhx3/4 (lim-3) and 1/5 (lin-11) expressed in cells specific to *Amphimedon* larval "eye" pigment rings	Lhx 1/5 and other LIM family genes present in genome; 3 of 6 expressed in cultured *Trichoplax*	Potential involvement in neural cell fate; expressed in neuralized regions	Lim-3, lin-11 involved in organ development, specification of neural cell types

Gene Expression and Conserved Pathways and Functions

As in cnidarians, the Wnt pathway is utilized for axial patterning across Bilateria, from ecdysozoans (e.g. *C. elegans*, insects) and lophotrochozoans (planarians, nemerteans) to both basal deuterostomes (urochordates, echinoderms, cephalochordates) and chordates. Canonical Wnt signaling is utilized by all groups for specifying posterior fate, but it appears that the Hedgehog pathway takes on a more prominent role in antagonizing Wnt signals in the developing bilaterian anterior (Petersen and Reddien 2009; Ingham et al. 2011). Wnt and Hedgehog signaling interactions also establish and maintain A/P segmental boundaries in arthropods, and possibly annelids as well (Dray et al. 2010; Ingham et al. 2011). In *Xenopus*, the endo- and mesodermal fate-specifying signals that set up early organizer and A/P cell fates also induce BMP antagonist expression, initiating the dorsal/ventral patterning pathway (De Robertis and Kuroda 2004), although in *Drosophila* this is achieved by maternal factors localized prior to fertilization, making an ancestral Wnt signal input for this pathway less likely.

Regardless of input, a "true" BMP/BMP antagonist-based D/V patterning circuit (see preceding discussion of cnidarian D/V patterning above) was in place in the PDA. BMP2/4 and antagonist Chordin (Dpp and Sog in *Drosophila*) establish dorsal-ventral polarity in all model organisms (with the exception of *C. elegans*) as well as in the hemichordate *Saccoglossus kowalevskii* (Lowe et al. 2006). The leech *Helobdella* additionally utilizes BMP5-8 and antagonist Gremlin for D/V axis specification, demonstrating both the conservation of BMP D/V signaling in Lophotrochozoa as well as a change in the regulatory logic of this circuit (Kuo and Weisblat 2011).

It increasingly appears that the bilaterian LCA had more finely tuned axial and regional patterning afforded by the pathways discussed above as well as expanded and diversified Hox and ParaHox gene clusters. Bilaterian Hox and ParaHox genes are involved in providing regional specification of cell fate in many developing tissues and structures, from the nervous system and gut to muscles and appendages. These genes are often deployed in spatial arrangements mirroring their genomic arrangement, and this collinear expression (or "Hox code") was likely present in the bilaterian LCA (Chiori et al. 2009). Any deviations from colinearity commonly occur in quickly evolving lineages with disintegrated Hox/ParaHox clusters (Hui et al. 2009; Ikuta 2011). An accounting of the various spatiotemporal expression patterns and functional roles of these genes across the Bilateria is beyond the scope of this chapter, and the determination of specific ancestral function is complicated by their extensive, lineage-specific duplication, loss, break-up, and divergence. The bilaterian LCA may have had seven or eight Hox genes and three ParaHox genes. Although the smaller acoelomorph set has been proposed to approximate the ancestral bilaterian condition (Hejnol and Martindale 2009), the potential placement of acoels at the base of deuterostomes (Philippe et al. 2011a) makes a better case for gene loss in this group. As reviewed by Holland (2013), the taxonomically widespread role of bilaterian Hox genes in A/P patterning of ectoderm/mesoderm and the role of ParaHox genes in the A/P patterning of the gut has fueled the hypothesis that these were their ancestral functions, but more work is needed to resolve this question.

The conserved utilization of the Distalless/Dlx pathway in proximal/distal patterning of vertebrate and arthropod appendages as well as other body outgrowths has lead to the expectation that the PDA possessed, if not appendages, similarly specified

body protrusions (e.g. Knoll and Carroll 1999). However, conflicting expression patterns and the lack of Distalless and Dac homologs in the distal region of developing parapodia in the polychaete *Neanthes arenaceodentata* suggests that these tools did not pattern appendages in the ancestral bilaterian (Winchell et al. 2010). Additional work by Winchell et al. (2013) indicates that the LIM homeobox (Lhx) transcription factors *apterous* and *lim1*, required for proximodistal patterning in fruit flies and the flour beetle *Tribolium*, are expressed in developing nervous/sensory structures and parapodial muscle precursor cells and not in a proximodistal fashion. As protostome limb development does not seem to be produced by a conserved molecular pathway, the authors posit that Distalless and Lhx pathways originally patterned sensory outgrowths, and that these were independently co-opted in different lineages for proximodistal patterning.

The presence of Pax6 (or Pax6-like genes) in many bilaterians, and its role in eye specification in both vertebrates and *Drosophila*, has long been regarded as evidence of eyes in the bilaterian LCA. Studies of photoreceptors across bilaterian lineages, however, presents a more complicated picture. Molecular characterization of visual-system related cell types across metazoans indicates that both rhabdomeric and ciliary opsin predates the cnidarian and bilaterian split, and that these were independently modified in the different bilaterian lineages for either photoreceptive or non-visual sensory roles (Arendt 2008). While Pax6 seems to be involved in specifying cephalic eyes generated from brain outgrowths, a recent study (Backfisch et al. 2013) has demonstrated that noncephalic photoreceptors are specified by another Pax system (Pax2/5/8) and may predate the origin of cephalic eyes. Photoreceptive cells in the nerve cord and notopodia of annelids may be related to r-opsin-expressing organs of the amphioxus neural tube, and interestingly,

orthologs of annelid r-opsin are expressed in both zebrafish retinal ganglia and neuromasts – the specialized mechanosensory cells of the fish lateral line system. Backfisch et al. (2013) suggest that an ancient type of r-opsin photoreceptive cell participated in many sensory roles in the ancestral bilaterian. This may mean that multifunctional sensory apparatuses were more likely to have existed in the bilaterian LCA than cephalic eyes, again suggesting a pattern of ancient multifunctionality to derived specialization of metazoan cell types (Arendt 2008).

While the structure of the brain/CNS of the bilaterian ancestor is still unclear, there is increasing evidence for conserved molecular pathways in establishing CNS signaling centers in the PDA (e.g. Cañestro et al. 2005; Pani et al. 2012); additionally, the discovery of innervated stalked eyes and a presumptive optic lobe in the arthropod *Fuxianhuia* (Ma et al. 2012) suggests that the brain and CNS were highly specialized by the early Cambrian. This may not have been the case for the ancestral bilaterian circulatory pump. A discussion of bilaterian pumping organ homology by Xavier-Neto et al. (2007) posits that rather than a heart or peristaltic pump itself being ancestral to bilaterians, a common tissue specification machinery (which included the "heart" gene tinman/Nkx2-5) was independently modified in the bilaterian lineages to produce different pumping organs. This is yet another demonstration of conserved GRN components not necessarily indicating conserved morphology.

Thus, the ancient bilaterian, as compared to more basal metazoans, was an animal tuned for interaction with its environment. The PDA possessed A/P and D/V axial patterning capacities necessary for arranging morphological structures in a fashion conducive to directed movement, the genetic underpinnings for more specific control of

regional patterning, as well as molecular pathways that could establish anatomical outgrowths for exploring the environment. Though the bilaterian LCA may not have possessed recognizable structures for sensation, movement, and feeding, it clearly had the developmental machinery needed for these systems in place, and different lineages may have elaborated these developmental capacities in different ways.

Discussion

The rapid expansion of work on basal metazoans continues to challenge our understanding of the evolution of developmental complexity. Additional whole-genome sequences of sponges and cnidarians are in progress and the first ctenophore genome has very recently been published. Combined with further comparative developmental studies on other clades, these will lead to ongoing revision of the work presented here. Yet in many ways the general pattern now appears unambiguous: (1) much of the developmental toolkit was present among basal metazoan clades and (2) the early origin of these clades was evidently decoupled from the origin of the morphologies that characterize the crown groups. This provides a basis for evaluating the changing views on the nature of the LCAs at critical nodes in metazoan evolution, for integrating with data from the fossil record, and for inferring the implications for evolutionary processes.

Changing Views of the Last Common Ancestors

As comparative sequence data accumulated from *Drosophila*, *Caenorhabditis* and *Mus* during the 1990s, and molecular phylogeny provided a new view of metazoan relationships (Aguinaldo et al. 1997) several authors realized that it could be used to infer the nature of the bilaterian last common ancestor, or *Urbilateria* (Shenk and Steel 1994;

De Robertis and Sasai 1996). Previous efforts at ancestral reconstruction were based primarily on morphological comparisons and many pre-dated the spread of phylogenetic approaches as more rigorous analysis of shared characters. Evidence for shared developmental genes, and eventually shared complex developmental pathways, led to numerous discussions of the morphological complexity of the bilaterian LCA (Valentine et al. 1999; Knoll and Carroll 1999; Carroll et al. 2001; Erwin and Davidson 2002).

By 2003 the accumulated studies suggested that the bilaterian LCA was morphologically complex. A minimal reconstruction would include (see Erwin and Davidson 2002; Erwin 2009; Carroll et al. 2001 for citations): seven to eight Hox genes controlling anterior/posterior differentiation; a larger cluster of ANTP-class genes including the ParaHox and NK genes; dorsal-ventral patterning controlled by sog/chordin/dpp/BMP2/4*;* anterior patterning via ems/Emx and otd/Otx; a tripartite brain; posterior patterning of the developing embryo via evenskipped/evx, caudal/cdx; segmentation controlled through engrailed and Delta-Notch ligands; eye formation controlled by Pax6 and ey; a regionalized gut and endoderm produced through GATA transcription factors, brachyury and goosecoid; a heart with development controlled via Nkx2.5/tinman; and possible appendage formation moderated through distalless. The fossil record posed a significant challenge to this interpretation. Most molecular clock studies of that time suggested that the bilaterian LCA dated to over 750 Ma, and such a complex bilaterian would necessarily have left evidence in the trace fossil record of Cryogenian and Ediacaran-aged rocks (Valentine et al. 1999; Erwin and Davidson 2002).

Yet even by 2003 there were greatly differing views of how to interpret the occurrence of highly conserved developmental control genes across bilaterians. The

dominant view was that the conservation of the genes necessarily implied conservation of function, and specifically, the conservation of the morphogenetic pathways documented in extant metazoans. In other words, for example, the presence of Pax6 and ey in flies and mice was evidence that eyes were present in the bilaterian LCA (Callaerts et al. 1997; Arendt and Wittbrodt 2001). But at the time there was little data from basal metazoan clades and seemingly little reason to question such conclusions. Indeed, some authors continue to favor a morphologically and developmentally complex bilaterian LCA (De Robertis 2008; Baguñà et al. 2008). The alternative is that at least some of the bilaterian conserved developmental genes may have been co-opted from other developmental roles, suggesting a potentially much simpler bilaterian LCA. Erwin and Davidson (2002) argued that many of these conserved genes were responsible for cell specification and regional patterning rather than complex morphogenetic pathways, with more precise spatial and developmental control systems intercalated into smaller, less connected simpler networks. As discussed earlier in this chapter, the identification of much of the bilaterian developmental toolkit in more basal metazoan clades basically supports this view. Sponges, placozoans, and cnidarians all possess developmental genes that appear capable of generating more complex morphologies than occur in these clades. The integration of evidence from the fossil record with molecular clock results may help to resolve this apparent conflict.

Fossil Record of Early Metazoa

Although molecular clock estimates suggest that Metazoa originated by about 780 Ma, and the Bilateria by about 660 Ma (Fig. 2.1), there is scant fossil evidence of animals before the appearance of the Ediacaran biota after 579 Ma. Despite many reports, the

only plausible earlier records are of a putative sponge biomarker (a diagnostic lipid) in rocks older than 635 Ma from Oman (Love et al. 2009) and a possible sponge fossil of about the same age (Maloof et al. 2010). For recent reviews of the fossil record of early metazoan diversification see Erwin et al. (2011) and Erwin and Valentine (2013).

After 579 Ma there is abundant evidence of metazoans, including some body fossils known as the Ediacaran macrobiota, fossil embryos, and a variety of trace fossils (horizontal burrows). The Ediacaran macrobiota (579 to 542 Ma) encompasses a number of independent clades, only two of which may have been bilaterian (*Kimberella* and the dickinsoniomorphs). The remaining suite of fronds, discs and other entities are almost entirely soft-bodied, and have no apparent mouths, guts, appendages, and with a few exceptions, evidence of motility. The phylogenetic affinities of the Ediacaran macrofossils beyond the two potential bilaterians remains a subject of considerable discussion. The fossil embryos, from the Doushantuo Formation in southern China, probably represent members of basal metazoan clades and possibly some other extinct lineages. Trace fossils of the Ediacaran are largely superficial graces, but increase in complexity and diversity toward the base of the Cambrian.

The Cambrian Explosion *sensu stricto* began about 542 Ma with the appearance of penetrating, vertical burrows, denoting the presence of a coelom in the burrower, and of a diverse array of spines, plates and other skeletal elements known as the small shelly fauna. These fossils are quickly followed by the appearance of a variety of bilaterian lineages, with the order of first appearances largely controlled by preservational issues. By about 520 Ma all the major clades of durably skeletonized marine organisms had appeared with the exception of the Bryozoa (which first appear in the fossil record during

the Early Ordovician, although they probably originated earlier). Many other clades, such as lobopods, priapulids, and various early arthropods, appear in extraordinarily well-preserved assemblages such as the Burgess Shale and the Chengjiang faunas.

Molecular clock estimates of divergence times clearly establish a gap of 200-100 million years between the acquisition of many elements of the metazoan developmental toolkit and the appearance of these clades in the fossil record (Erwin et al. 2011). This explosion of bilaterian fossils during the early Cambrian coincides with the origins of bilaterian crown groups based on molecular clock evidence (Erwin et al. 2011). From this decoupling of the origin of the clades and their appearance in the fossil record we have concluded (see Erwin et al. 2011) that the early phase of metazoan evolution involved numerous lineages, probably of small body size, and lacking the morphologies that characterize the later crown groups. This also suggests that the highly conserved developmental tools may have been operating in different ways than later in the history of these clades (in simple patterning and for cell-type specification, rather than in complex regulatory pathways leading to regional patterning) (see Erwin and Davidson 2002; Davidson and Erwin 2010). Thus the emerging evolutionary pattern is one of early divergence of major metazoan clades during the Cryogenian, followed by divergences of metazoan phyla in the latest Ediacaran and Cambrian. The latter was associated with the class 'Cambrian explosion' as described from the fossil record (Erwin and Valentine 2013).

Importance of Marcoevolutionary Lags

The long, macroevolutionary lag between the origin of much of the developmental toolkit and its utilization in a wide array of bilaterian bodyplans is not

unusual (Jablonski and Bottjer 1990). Indeed macroevolutionary lags between the origin of a clade and the ecological success of elements of the clade are not infrequently associated with major macroevolutionary innovations. The evolution of grasses, for example, predated the spread of grasslands by some 15-20 myr, during which grasses were virtually invisible in the fossil record (Stromberg 2005). Macroevolutionary lags highlight an important feature of evolutionary dynamics. In contrast to the views of Ernst Mayr (Mayr 1960) and others, evolution is not always highly opportunistic, taking advantage of new possibilities as they arise. Rather, there may be a long delay between the origin of a novelty, and even the diversification of the resulting clade into several lineages, and the time when the clade becomes ecologically and evolutionarily important. This feature of evolution parallels the longstanding distinction among historians of technology between invention (the creation of something new, often as recorded by patents) and innovation (the economic success of an invention). In evolution, changes in the physical environment or in ecological interactions are often required before an innovation may succeed and spread (Erwin and Valentine 2013; Erwin 2008). In the case of the grasses studied by Stromberg, it appears that changes in climate and water availability triggered the spread of grasslands during the Miocene. With the origin of animals a plausible case has been made that increased oxygen levels in the ocean were an important contributory cause to the diversification of Bilateria beginning about 550 Ma (Erwin and Valentine 2013).

What macroevolutionary lags emphasize, however, is that data on the origin of developmental novelties alone is insufficient to fully understand the dynamics of

evolutionary innovation. Ultimately the success of developmental novelties such as those discussed here is dependent upon environmental context and ecological opportunities.

Summary

1. Developmental genes originally thought to be exclusive to bilaterians and linked to specific bilaterian features are deeply conserved, and the number of these genes identified in early-branching metazoans, particularly sponges and cnidarians, continues to grow.
2. Although much of the metazoan developmental toolkit was present among basal metazoans, these genes were only later co-opted for the various developmental roles associated with bilaterian morphology.
3. The prevalence of co-option means the current function of developmental genes in living groups is a poor guide to ancestral function. A wide array of comparative developmental data is required to infer the nature of ancestral metazoan development; gene functional data derived from experimental manipulation provides the strongest evidence for these inferences.
4. A current metazoan phylogenetic framework is presented to contextualize and polarize fossil and developmental information related to the evolution of metazoan development.
5. We evaluate current available comparative developmental data to make conservative inferences for likely morphology at each key basal metazoan node.
6. The acquisition of metazoan developmental characteristics likely proceeded with the evolution of more precise spatial and developmental control via the evolution of gene regulatory networks.

7. A long macroevolutionary lag exists between the origin of much of the metazoan developmental toolkit and its utilization in the wide array of bilaterian body plans observed in the fossil record. This decoupling of invention and innovation emphasizes the importance of environmental context and ecological opportunity in explaining the success of developmental genetic potential in the Cambrian explosion.

Acknowledgements

We acknowledge financial support from the NASA Astrobiology Institute Foundations of Complex Life MIT/Harvard research node.

Chapter 3: Morphology, homology, and resolution at the base of the fossil panarthropods

Abstract

The Cambrian fossil lobopods play a central role in hypotheses about the origin and evolution of the Panarthropod clade, and many consider these 'legged worms' to be primitive forms demonstrating step-wise evolution of defining arthropod characteristics. In this study, I review the status of panarthropod phylogenetic hypotheses and their implications for arthropod evolution, and propose an alternative evolutionary scenario in which lobopods may represent the outcome of rapid parallel diversification. I examine the signal present in three recently published fossil panarthropod morphological datasets using combined Bayesian phylogenetic analyses and parsimony character mapping, and show that relationships between lobopods and panarthropod crown groups are largely unresolved due to poor phylogenetic signal and potential taphonomic and coding biases. This lack of resolution may be a primary factor in shaping a "basal grade" of lobopod organization, leaving open the possibility that panarthropods independently evolved defining morphological features. I discuss alternatives strategies for morphological character coding that may help link new genetic developmental information to the evaluation of fossil morphology and morphological evolution.

Keywords: Panarthropoda, Cambrian, lobopod, phylogeny, homology, development

Introduction

The most ubiquitous and diverse animals on earth – nematodes and arthropods – are united with a number of other invertebrates in the monophyletic Ecdysozoa, a clade

now widely supported by molecular analyses and named for the shared, characteristic cuticle molting (ecdysis) of its members (Aguinaldo et al. 1997; Philippe et al. 2005; Telford et al. 2008). Within Ecdysozoa, three limb-bearing phyla – Tardigrada (tardigrades), Onychophora (velvet worms), and Euarthropoda (arthropods) – comprise the Panarthropoda (Nielsen 1995; Dunn et al. 2008). Broad interest in the panarthropod clade has been motivated and sustained largely because the group, at some point in its evolutionary history, gave rise to the last common ancestor (LCA) of all true arthropods. These familiar sclerotized and jointed animals are a major ecological component of the Cambrian Explosion (Conway Morris 1986; Hou and Bergström 1991), and their famously strange and unique fossil forms have inspired numerous questions about morphological disparity and developmental evolution in deep time (e.g. Gould 1991; Hughes 1991; also reviewed in Erwin 2007). As the polarity of evolutionary change in any group is informed by the identity of its closest relatives as well as its ancestral forms, an accurate fossil panarthropod phylogeny is critical for understanding the origin of the arthropods, and has implications for understanding the pace and structure of the Ediacaran-Cambrian radiation. In this study, I review the status of panarthropod phylogenetic hypotheses and their implications for arthropod evolution. I examine the signal present in recently published fossil panarthropod morphological datasets, and discuss alternatives to current approaches utilized in fossil panarthropod phylogeny estimation.

Panarthropoda: Molecular Consensus and Fossil Placement

Panarthropod monophyly has been broadly accepted based on morphological and molecular data for some time, but the relationships between its constituent phyla

remained less certain (e.g. Schmidt-Rhaesa et al. 1998; Mallatt et al. 2004; Telford et al. 2008). All possible panarthopod relationships have been suggested, if not advocated, and retrieved in molecular phylogenetic analyses with varying degrees of support: Onychophora and Tardigrada as sister groups (e.g. Waggoner 1996; Mallatt and Giribet 2006); or, euarthropods as either sister to Tardigrada (e.g. Garey et al. 1996; Budd 1996; Giribet et al. 2001) or Onychophora (e.g. Peterson and Eernisse 2001; Dunn et al. 2008). Recently, an analysis of expressed sequence tags (ESTs) and new microRNA (miRNA) libraries demonstrated strong support for an onychophoran-arthropod clade (Campbell et al. 2011). As miRNAs are less likely to exhibit convergent evolution, the discovery of distinct miRNAs unique to only Onychophora and Euarthropoda seems to have solidified panarthopod genetic relationships for now (Campbell et al. 2011).

Despite new molecular resolution, few morphologies in highly derived living onychophorans and arthropods unambiguously inform their primitive condition, making the panarthropod fossil record indispensable for understanding the evolution of these groups (e.g. Edgecombe 2009; Edgecombe 2010). The fossil 'lobopods' in particular have played a central role in hypotheses of both panarthropod and arthropod origins. Lobopods are a group of soft-bodied 'legged worms' primarily found in the exceptionally preserved Sirius Passet, Chengjiang, and Burgess Shale Cambrian faunas (Figure 3.1) (e.g. Ramsköld and Chen 1998; Bergström and Hou 2001; Liu et al. 2008). Hypotheses of lobopod affinities have varied widely since the original description of the Burgess lobopod *Aysheaia pedunculata* Walcott 1911 as an annelid worm. Many workers, citing the outward resemblance of lobopods to living velvet worms, have suggested a close lobopod-onychophoran relationship, with the fossil forms representing marine

onychophoran ancestors (e.g. Walcott 1931; Hutchinson 1930, 1969; Robison 1985; Ramsköld and Hou 1991; Ramsköld and Chen 1998). If this is true, lobopod fossils would have little bearing on the origin of the arthropod clade. Others, mirroring Snodgrass's (1938) hypothesis that an ancestral lobopod grade gave rise to both proto-onychophorans and arthropods, have supported lobopods as basal progenitors of any (or every) crown panarthropod group (e.g. Delle Cave and Simonetta 1975; Whittington 1978; Dzik and Krumbiegel 1989). As described below, this general view has been most prominent, and implies that lobopod fossils represent transitional forms linking crown phyla to a lobopod-like primitive condition. Fewer studies have rejected the notion of Cambrian lobopods as basal precursors, but those that do stress the uniqueness of derived lobopod characters and the chance that broad panarthropod similarities are the result of convergent evolution (e.g. Bergström and Hou 2001).

Lobopod Affinities: Current Views

More than two decades of work on early arthropod evolution has adopted or adapted the lobopod-arthropod transition hypothesis proposed by Budd (e.g. Budd 1993, 1996, 1999; although see Zhang and Briggs 2007). In a series of descriptive papers, Budd postulated that the lobopods represent a paraphyletic grade of basal panarthropods whose members progressively evolved defining arthropod characteristics, such as sclerotized cuticle and jointed biramous limbs. Budd also suggested that biramous limbs may have evolved via the fusion of lobopod appendages with the lateral lobes observed in some stem euarthropods. This hypothesis hinges on similarities between *Kerygmachela* Budd 1993 and *Pambdelurion* Budd 1997, which may possess both lobopodous walking legs and lateral gilled lobes, to the stem arthropods *Opabinia* Walcott 1912 and *Anomalocaris*

Whiteaves 1892 (Budd 1999; Budd and Daley 2012). Such a limb transition is more uncertain, since *Opabinia* and anomalocaridids lack walking limbs (Zhang and Briggs 2007; although see Budd and Daley 2012), but the 'gilled lobopods' are nonetheless cited as key fossils supporting a lobopod-arthropod transition (e.g. Liu et al. 2008; Edgecombe 2009).

As new lobopod fossils are discovered, and established taxa redescribed and reanalyzed, it is increasingly clear that group as a whole a possesses a mélange of characters, many of which resemble features in tardigrades, onychophorans, or arthropods (e.g. Liu et al. 2006; Liu et al. 2011; Liu and Dunlop 2014; Smith and Ortega-Hernández 2014; Smith and Caron 2015). Some features, such as pharyngeal teeth in *Jianshanopodia* or *Hallucigenia*, are even similar to structures in more basally-branching vermiform ecdysozoans (Edgecombe 2009; Smith and Caron 2015). The successive addition of new taxa and character combinations to cladistic analyses has yielded significantly different lobopod trees and uncertainty regarding lobopod interrelationships, but workers generally agree that results support 1) a basal lobopod paraphyletic grade, with different lobopod taxa more closely related to different crown panarthropod groups, and 2) the involvement of a lobopod progenitor in the gradual evolution of euarthropod characteristics (e.g. Liu et al. 2011; Mounce and Wills 2011; Legg et al. 2011). Importantly, this lobopod consensus accepted by paleontologists has motivated and shaped experimental developmental research into arthropod origins and panarthropod evolution more broadly (e.g. Shubin et al. 1997; Eriksson et al. 2009; Eriksson et al. 2010).

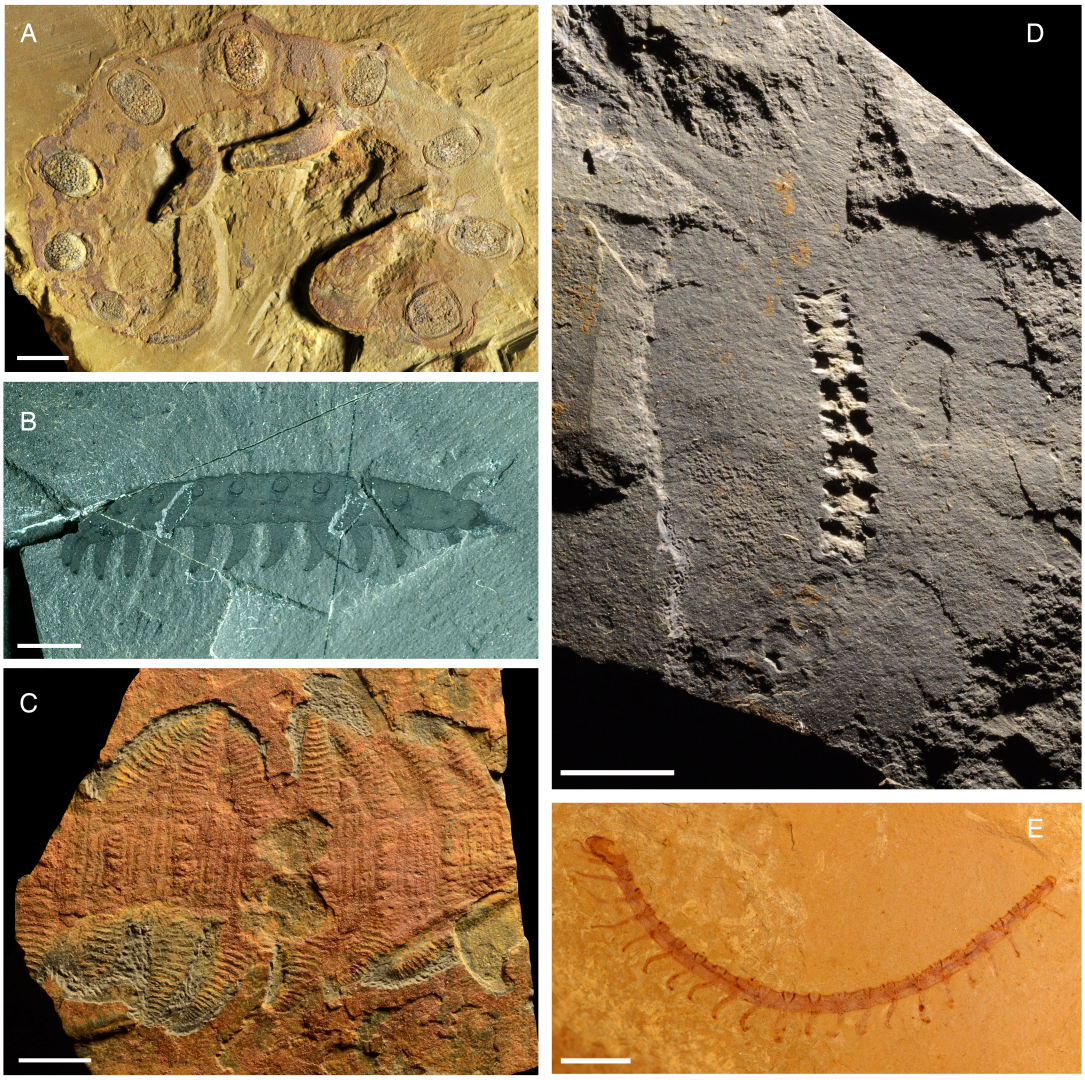

Figure 3.1. Lobopod fossils from exceptionally preserved Cambrian faunas. A) *Microdictyon sinicum* from the Chengjiang, ELRC 30008, photo courtesy of Han Zeng. B) *Aysheaia pedunculata* from the Burgess Shale, USNM 83942, photo by Mike Eklund. C) *Hadranax augustus* from the Sirius Passet, MGUH 24.527. D) *Kerygmachela kierkegaardi* from the Sirius Passet, MGUH 22.084. E) *Cardiodictyon catenulum* from the Chengjiang, photo by Han Zeng. Scale bar in A: 2 mm; B: 5 mm; C: 1 cm; D: 1 cm; E: 5 mm. Available as high-res file Additional II.

Panarthropod Radiation: Geologic Context

The evolution of the lobopods themselves is rarely discussed within a temporal framework (Liu et al. 2008). Fossil representatives of lobopods, stem euarthropods, and even potential crown arthropods appear concurrently in the Cambrian, preceded only by

disarticulated lobopod sclerites (within the earliest Cambrian 'small shelly fauna'; Bengtson 1991) and possible *Rusophycus*-like arthropod traces (Benton et al. 2009). Genetic divergence estimates for panarthropod phyla indicate even older origins. A time-calibrated molecular analysis of the panarthropod tree specifically places the genetic radiation of tardigrades, onychophorans, and arthropods within a geologic timeframe (Rota-Stabelli et al. 2013), and age estimates derived in this study appear robust to changes in calibration bounds and priors. Panarthropods are estimated to have diverged from sister ecdysozoans approximately 565 million years ago (Ma), with a maximum and minimum bound of 593 Ma and 537 Ma, respectively. The Onychophora + Euarthropoda group diverged ~561 Ma (585, 537) and the Euarthropoda ~543 Ma (567, 514) (Rota-Stabelli et al. 2013). Two observations are apparent from these estimates: 1) Ancestral panarthropods, including the panarthropod LCA and the onychophoran-arthropod LCA, diverged in the Ediacaran, tens of millions of years before their first fossil appearances, and 2) confidence intervals on these divergence time estimates overlap, suggesting the possibility of a rapid panarthropod genetic diversification.

When constrained by a mid-late Ediacaran divergence, a lobopod-arthropod transition would require a complex limb transformation to have occurred in a time interval that records no conclusive fossil evidence for macroscopic limbed bilaterians (Budd and Jensen 2015; Buatois and Mángano 2016). Additionally, broad patterns in animal developmental evolution suggest that although clade LCAs may possess the genetic tools necessary for building descendent morphologies, they need not have deployed these tools in the same way or constructed comparable features (Tweedt and Erwin 2015). An alternative hypothesis for panarthropod evolution could involve rapid

diversification in cryptic, and perhaps even limbless, Ediacaran panarthropod ancestors sharing a common genetic capacity for major clade-defining characteristics (Figure 3.2). In this view, ancestral gene regulatory networks involved in limb development, cuticle modification, and anterior patterning could have diverged prior to their manifestation in early Cambrian forms, and observed fossil morphologies may reflect the parallel recruitment of developmental modifications to a shared genetic blueprint.

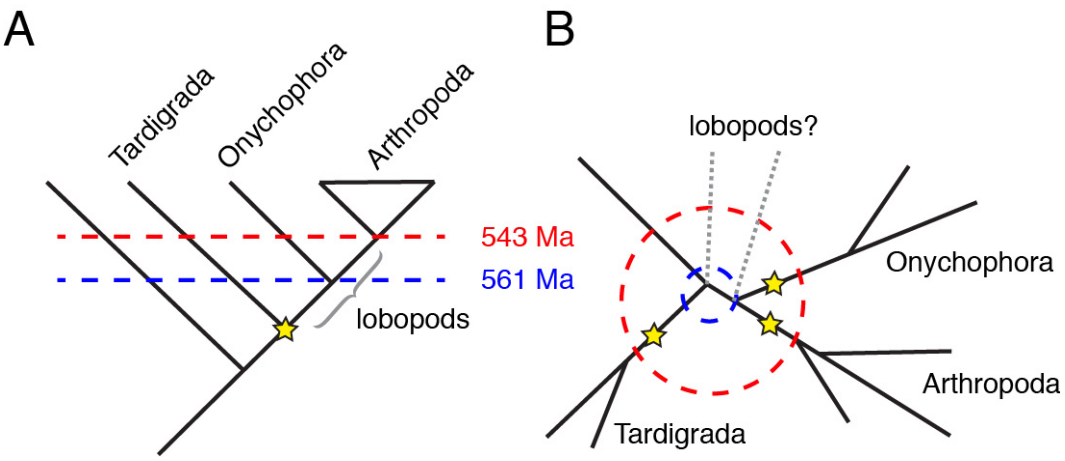

Figure 3.2. Two hypotheses for panarthropod evolution.
A) The major features of panarthropods, including limbs, evolve in the LCA (yellow star) and are present from ~565 Ma onward. Lobopods form a grade of ancestral panarthropod organization (grey bracket). B) Gene regulatory networks present in the LCA are independently modified and evolve (yellow stars) closer to the Cambrian ~543 Ma. Lobopods may represent independent lineages (grey dashed lines). Blue dashed line, Onychophoran-Euarthropoda divergence at ~561 Ma (Rota-Stabelli et al. 2013); red dashed line, Euarthropoda divergence at ~543 Ma (Rota-Stabelli et al. 2013).

Examples of parallel recruitment in animal developmental evolution are becoming increasingly common (reviewed in Chipman 2010; Tweedt and Erwin 2015), and this evolutionary phenomenon need not be restricted to cases of 'deep homology', such as the parallel evolution of limbs and segments from shared genetic networks across bilaterian

phyla (e.g. Panganiban et al. 1997; Arthur et al. 1999; Shubin et al. 2009). Disparate limb morphologies within Panarthropoda suggest an alternative hypothesis in which Cambrian fossil lobopods may not represent arthropod progenitors or even the basal panarthropod condition, but rather one (or multiple) distinct sister panarthropod lineage(s). Adopting phylogenetic methods that incorporate uncertainty provide one way of exploring whether current morphological data support the hypothesis of a lobopodous euarthropod LCA, suggest a rapid parallel evolution of panarthropod lineages, or are insufficient to discriminate between either scenario.

Lobopod Phylogeny: Applying New Methods

Current approaches to fossil panarthropod phylogeny estimation do not explicitly incorporate topological uncertainty, and may not be able to accommodate or distinguish potential convergent evolution. To date, all fossil panarthropod morphological datasets have been analyzed using maximum parsimony, which is operationally designed to reduce homoplasy. The conventional use of limbless ecdysozoan sister taxa (e.g. priapulid worms or nematodes) to root fossil panarthropod trees may also introduce biases *a priori*, especially as the majority of morphological traits are either absent or inapplicable in these taxa (e.g. Jenner 2002). Given the topological variation in reported fossil panarthropod trees and the assumptions made by parsimony-based analysis, re-examination of fossil panarthropod data within a probabilistic, model-based framework may help evaluate long-held views of arthropod origins.

Likelihood-based methods for estimating phylogenetic trees from discrete morphological character data have not been widely adopted by the paleontological field, but they provide a number of benefits not afforded by parsimony (Clarke and Middleton

2008; Wright and Hillis 2014). In a likelihood framework, all characters – including autapomorphies – contribute to branch length estimation and are phylogenetically informative (Lewis 2001). This may be particularly useful for fossil groups possessing relatively few total characters and many uniquely derived states, like the Cambrian lobopods (Gould 1991). Additionally, likelihood models may be structured to allow rates of change to vary among characters, permitting a dimension of biological reality in character evolution, and providing a mechanism for testing hypotheses about morphological character change (Wagner 2012; Harrison and Larsson 2015).

The goals of this study are: 1) to determine if basal panarthropod morphological data are better modeled by allowing rate heterogeneity among characters, rather than a parsimony-like assumption of equal rates 2) to determine whether published lobopod-stem arthropod phylogenies are reproducible and supported by a Bayesian approach, 3) to assess the impact of outgroup choice and inclusion of transitional 'gilled lobopod' taxa on stem panarthropod trees, and 4) to understand which morphological features may drive particular topologies. I discuss character homology within a developmental framework, and propose alternative strategies for the accurate application of developmental information to character coding.

Methods

Datasets

For this study, three fossil lobopod and stem arthropod discrete morphological character datasets were selected to test most recent lobopod phylogenetic hypotheses and to minimize parent-daughter matrix overlap (Table 3.1). However, the majority of published stem arthropod phylogenetic studies largely draw from a shared pool of

characters and taxon coding, so rather than representing independent analyses, these data represent variation within a research paradigm. One dataset (Legg et al. 2013) did not focus on lobopod-arthropod relationships, but recapitulates the ubiquitous basal lobopod paraphyly hypothesis, and was analyzed in full as well as with reduced taxon sampling comparable to the other two datasets (Table 3.1). Preliminary analyses found that basal topologies of interest estimated for the full Legg dataset were identical to those estimated using a subset of the taxa, so a reduced dataset was used for all subsequent analysis. Original character coding for each dataset was maintained.

Table 3.1. Morphological datasets analyzed in this study.

Dataset	Abbreviation	Taxa	Lobopod Taxa	Characters
Ma et al. 2014	M	27	16	42
Smith and Caron 2015	SC	40	20	84
Legg et al. 2013	L	311	15	753
Legg et al. 2013 'pared'[1]	LP	44	15	753

[1]dataset with reduced taxon sampling

Model Selection

All phylogenetic analyses were conducted using the MrBayes (Ronquist et al. 2012b) implementation of the Lewis (2001) Mkv model for discrete morphological characters, which applies a correction to the Mk model to adjust for character ascertainment bias common in morphological data collection (details in Lewis 2001). To determine an appropriate model for rates of character change, three candidate models – equal rates (EQ), gamma-distributed rates (GM), and lognormally-distributed rates (LN) – were compared for each data set. The default prior on rate distribution shape parameters

implemented in MrBayes is an exponential prior, so to assess the impact of prior choice on model fit, two priors were tested for models employing rate heterogeneity: an exponential prior with a mean of 1.0 (MrBayes default), and a uniform prior on the interval [0.001, 100], which has been shown to cover the range of effective variability in rate distribution shape parameters (see Fig. 1 in Harrison and Larsson 2015).

In Bayesian approaches, marginal likelihood – the probability of a model given the data, averaged over its parameters with respect to the prior – is used for model comparisons (Nylander et al. 2004; Ronquist et al. 2012). Stepping-stone methods estimate marginal likelihood by sampling a series of power posterior distributions that connect the prior to the posterior, providing a more consistent and accurate estimation than the harmonic mean (Xie et al. 2011; Baele et al. 2012; Ronquist et al. 2012b). Marginal likelihoods for each model-dataset combination were therefore derived from both harmonic mean (details below) and stepping-stone estimates. Stepping-stone analyses were conducted in MrBayes v. 3.2.6 on the CIPRES Science Gateway platform (Miller et al. 2010). Each analysis comprised four independent runs of at least 12 million generations, and up to 52 million generations for datasets where increased sampling provided more confident convergence in likelihood estimates. Stepping-stone sampling utilized default MrBayes parameters of 50 steps from the posterior to the prior, with the first step sampling the posterior and successive steps selecting power posterior quantiles from a beta distribution with $\alpha=0.4$. The first 25% of samples from each step were discarded as burn-in. Convergence in marginal likelihood values was assessed by visual inspection of step and joined plots (Ronquist et al. 2012b).

Bayes factors are routinely used to assess relative model support, and because they take priors into account they naturally penalize model complexity (e.g. Baele et al. 2012; Bergsten et al. 2013). Bayes factors for all pairwise model comparisons were calculated as twice the log difference in mean marginal likelihood, following methods employed by Nylander et al. (2004), Clarke and Middleton (2008), and Harrison and Larsson (2015). Marginal likelihood means were derived from four independent runs per model for both standard Markov Chain Monte Carlo (MCMC) or stepping-stone runs. While interpretation of Bayes factors is subjective, guidelines set forth by Kass and Raftery (1995) are most commonly used: for the Bayes factor of model 1 over model 0 (B_{10}), $2 \cdot \ln(B_{10}) < 2$ indicates no support for model 1 over model 0; $2 < 2 \cdot \ln(B_{10}) < 6$ indicates positive support; $6 < 2 \cdot \ln(B_{10}) < 10$ strong support; and $10 < 2 \cdot \ln(B_{10})$ very strong support.

Parsimony-based Estimation of Character Rate Distributions

Likelihood and parsimony methods are fundamentally different phylogenetic approaches, but their combined use can help characterize morphological datasets (Harrison and Larsson 2015). Following methods described by Harrison and Larsson (2015), empirical distributions of character rates for each dataset were generated using parsimony to calculate total number of changes per character across Bayesian posterior topology samples. Characters were mapped to every topology sampled from the EQ model marginal posterior distributions of trees (>40,000 trees) using ACCTRAN optimization in PAUP* v.4b10 (Swofford 2002). Distributions of character change were combined and summarized in R using the APE and reshape packages (R Core Team

2015; Paradis et al. 2004; Wickham 2007). Scripts to conduct PAUP analyses within the R framework were provided by Luke Harrison (Harrison and Larsson 2015).

Tree Estimation

Tree topologies was estimated using either the best-fitting rate model, or, if model comparisons were equivocal, model(s) with highest marginal likelihoods. Topological analyses were conducted on the CIPRES platform with MrBayes 3.2.6 (Miller et al. 2010; Ronquist et al. 2012b). For each phylogeny estimation, four independent runs of four chains sampled model and tree space every 1000 generations, for total of at least 10 million generations and up to 50 million generations. The first 25% of samples were discarded as burn-in. Mixing between chains was found to be low for all datasets under a default temperature setting, so temperature values between 0.05 and 0.025 were used for heated chains. Convergence was confirmed by inspection of generation plots, average standard deviations of split frequencies (ASDSF), and parameter potential scale reduction factors (PSRFs). Estimated sample size (ESS) and marginal distributions of all parameters were visualized using Tracer (Rambaut et al. 2014). Marginal likelihood harmonic means estimates (HMEs) for converged runs were utilized in model comparison.

To determine how the inclusion of limbless ecdysozoan outgroups and key 'transitional' gilled-lobopod fossils influence topology, analyses with these taxa removed individually or in combination were conducted for each dataset under its best-fitting rate model. Character transitions supporting different topologies were examined with parsimony character mapping under both ACCTRAN and DELTRAN optimizations in PAUP* v.4b10 (Swofford 2002).

Results

Model Comparison

Harmonic mean and stepping-stone marginal model likelihoods for each dataset, model, and prior combination are reported with Bayes factor comparisons in Tables 3.2 and 3.3. Variation in harmonic mean likelihood estimates between four independent runs was relatively high (Table 3.2), reflecting the poor reliability of this method (Fan et al. 2011; Xie et al. 2011; Baele et al. 2012). In contrast, variation in stepping-stone marginal likelihoods was much lower (Table 3.2), with the Ma dataset (M) exhibiting an average range of 0.14 log-likelihood units between replicate runs, and the Smith and Caron dataset (SC) an average range of 0.82 log-likelihood units. Replicate stepping-stone runs for the reduced-size Legg dataset (LP) also ranged 0.82 log-likelihood units, with the exception of the EQ model, which exhibited higher variation between runs and a range of almost 12 log-likelihood units. Stepping-stone analyses under the equal-rates model (EQ) for the M and SC datasets exhibited considerable instability, such that convergence was impossible and marginal likelihoods could not be accurately estimated (NA values in Table 3.2).

The inability of EQ models to adequately explore parameter space is itself an indication that an equal character rates assumption for these data is problematic. Lacking stepping-stone likelihood estimates for the M and SC data, Bayes factors comparing rate heterogeneous models (LN and GM) to the EQ model were calculated using likelihood harmonic means. As the harmonic mean can produce erroneously high likelihoods, only values of $2 \cdot \ln(B_{10}) > 6$ were taken as potential positive evidence for model preference. The M dataset exhibited support for the LN + exponential prior (Exp) model over equal

rates, as demonstrated by a value of $2 \cdot \ln(B_{10})$ above 6. For the SC dataset, Bayes factor comparisons also suggested support for the highest likelihood model (GM+Exp) over the EQ model. LP dataset Bayes factor comparisons were calculated from stepping-stone estimates, and showed very strong support for the LN+Exp over EQ model. For this dataset, given the large differences in likelihoods between the rate heterogeneous models (LN and GM) and the EQ model (>40 log-likelihood units), the marginal likelihood variability between EQ runs was not considered large enough to impact the Bayes factor interpretation.

As expected, harmonic mean marginal likelihood estimates were much higher than estimates successfully obtained in stepping-stone analyses, reflecting known HME likelihood overestimation (Xie et al. 2011; Baele et al. 2012). Stepping-stone Bayes factor comparisons between rate heterogeneous models are summarized in Table 3.3. For all datasets, the LN model with an exponential prior yielded the highest marginal likelihoods, and Bayes factor comparisons with this model show strong evidence over the LN+Uni and GM+Uni models. Low values of $2 \cdot \ln(B_{10})$ for the LN+Exp / GM+Exp model comparison, however, indicate no evidence that the LN model better represents underlying character rate distributions than the GM model under the same prior (Table 3.3). In one dataset (LP), the GM model with a uniform prior performed slightly better than the LN-uniform model, but a value of $2 \cdot \ln(B_{10})$ close to 2 coupled with variation in likelihood estimates makes this difference equivocal. Bayes factors comparing exponential versus uniform priors for each rate model demonstrate broad support for the exponential prior in the M and LP datasets, and only slight support in the SC dataset (LN model only).

Table 3.2. Harmonic mean and stepping-stone model likelihood estimates with Bayes factor comparisons.

		Model likelihoods				Bayes Factors	
		Harmonic Mean (HME)		Stepping-stone (SS)		HME	SS
Dataset	Model	LnL	Range	LnL	Range	$2 \cdot \ln (B_{10})$	$2 \cdot \ln (B_{10})$
M	Equal	-380.94	3.69	Na	Na	6.7	Na
M	Lognormal + Exp[1]	-377.59*	2.24	-418.99*	0.29	---	---
M	Lognormal + Uni[2]	-380.92	1.43	-422.08	0.08	6.66	6.18
M	Gamma + Exp	-388.80	13.07	-419.12	0.09	22.42	0.26
M	Gamma + Uni	-381.49	3.39	-422.07	0.09	7.8	6.16
SC	Equal	-592.72	5.94	Na	Na	7.72	Na
SC	Lognormal + Exp	-592.37	7.21	-690.98*	0.76	7.02	---
SC	Lognormal + Uni	-590.44	5.38	-692.47	1.08	3.16	2.98
SC	Gamma + Exp	-588.86*	2.33	-691.44	0.92	---	0.92
SC	Gamma + Uni	-591.09	6.97	-691.55	0.54	4.46	1.14
LP	Equal	-921.23	2.8	-1105.81	11.6	4.02	85.62
LP	Lognormal + Exp	-920.27	5.35	-1063.00*	0.42	2.1	---
LP	Lognormal + Uni	-927.39	9.72	-1066.14	1.02	16.34	6.28
LP	Gamma + Exp	-919.22*	5.73	-1063.24	0.76	---	0.48
LP	Gamma + Uni	-928.34	12.43	-1065.06	1.03	18.24	4.12

[1]Exp = exponential prior on rate distribution parameters

[2]Uni = uniform prior on rate distribution parameters

* = highest likelihood model in each dataset; used as model 1 (M_1) in Bayes factor calculation

Table 3.3. Stepping-stone model likelihoods and Bayes factor comparisons between LN and GM models.

		SS ln (marginal likelihood)		Bayes Factor	
Dataset	Model comparison (M_1 / M_0)	M_1	M_0	$2 \cdot \ln (B_{10})$	Support
M	Lognormal + Exp / Lognormal + Uni	-418.99	-422.08	6.18	Strong
M	Gamma + Exp / Gamma + Uni	-419.12	-422.07	5.9	Positive
M	Lognormal + Exp / Gamma + Exp	-418.99	-419.12	0.26	No
M	Gamma + Uni / Lognormal + Uni	-422.07	-422.08	0.02	No
SC	Lognormal + Exp / Lognormal + Uni	-690.98	-692.47	2.98	Positive
SC	Gamma + Exp / Gamma + Uni	-691.44	-691.55	0.22	No
SC	Lognormal + Exp / Gamma + Exp	-690.98	-691.44	0.92	No
SC	Gamma + Uni / Lognormal + Uni	-691.55	-692.47	1.84	No
LP	Lognormal + Exp / Lognormal + Uni	-1063.00	-1066.14	6.28	Strong
LP	Gamma + Exp / Gamma + Uni	-1063.24	-1065.06	3.64	Positive
LP	Lognormal + Exp / Gamma + Exp	-1063.00	-1063.24	0.48	No
LP	Gamma + Uni / Lognormal + Uni	-1065.06	-1066.14	2.16	Equivocal

[1]Exp = exponential prior on rate parameters
[2]Uni = uniform prior on rate parameters

Character Rate Distributions

Character rate distributions estimated across all posterior tree topologies are summarized as relative frequency histograms (Figure 3.3). Each dataset distribution illustrates total changes per character across a pool of >40,000 marginal posterior topologies sampled in the EQ model analyses. The M dataset (Figure 3.3A) exhibited a more evenly-distributed number of characters changing between one and three times on a topology, with a drop-off occurring at four changes and decreasing to very few characters changing more than seven times. Datasets SC (Figure 3.3B) and LP (Figure 3.3C) have higher maximum changes per character, but show much more asymmetric distributions, with many more characters exhibiting single changes and a rapid decrease in total changes per character.

Bayesian Consensus Topologies

Figure 3.4 depicts, for each dataset, the original publication's primary consensus cladogram alongside the corresponding 50% majority-rule consensus tree estimated with the highest likelihood rate model (LN). For all topology analyses, PSRFs were 1.0 and ESS above 200 for all parameters. Final ASDSFs were below 0.005, indicating convergence for all runs.

Notably, in both M and SC Bayesian consensus topologies (Figures 3.4B and 3.4D), tardigrade, onychophoran, stem euarthropod and lobopod taxa generally collapse in a basal polytomy, with strongest topological support indicating their distinction from priapulid outgroup(s). Across all datasets, posterior probabilities for fossil panarthropod relationships are extremely low, with only the stem euarthropod fossil clades and a single

lobopod phylogenetic pairing (*Luolishania* with Collins' monster) consistently sampled in more than 90% of Bayesian posterior topologies (posterior probability (PP) > 90%). *Kerygmachlea*, *Pambdelurion*, and the stem euarthropods *Opabinia* and *Anomalocaris* are found grouped in every analysis, but with more variable clade probabilities and branching order (Figure 3.4).

Relationships between panarthropod crown representatives of the M dataset are all unresolved, in contrast to a Tardigrada-Onychophora group suggested by the consensus cladogram (Figures 3.4A, 3.4B). The position of the lobopods is similarly uncertain. A monophyletic clade consisting of all but five lobopod taxa was originally reported (Figure 3.4A), but a single lobopod clade in the Bayesian analysis consists of fewer taxa and has no support (55% PP). The basal position of *Megadictyon* and *Jianshanopodia* relative to *Kerygmachela* and *Pambdelurion* in the Bayesian consensus tree mirrors the original cladogram, but also with low posterior probability (65% PP).

The SC consensus topology retrieves a lobopod + crown Onychphora clade very similar in taxonomic composition to one in the original cladogram (Figures 3.4C, 3.4D). Although support for the clade as a whole is negligible, within this group close sister relationships between *Antennacanthopodia* and onychophorans, and between *Luolishania* and Collins' monster, are well resolved (92% and 98% PP respectively) and reflect the parsimony results. Notably, no lobopods branch with the *Kerygmachela* + stem euarthropod clade in the new consensus tree (Figure 3.4D), and those originally depicted as more closely related to total-group arthropods remain unresolved in a basal polytomy.

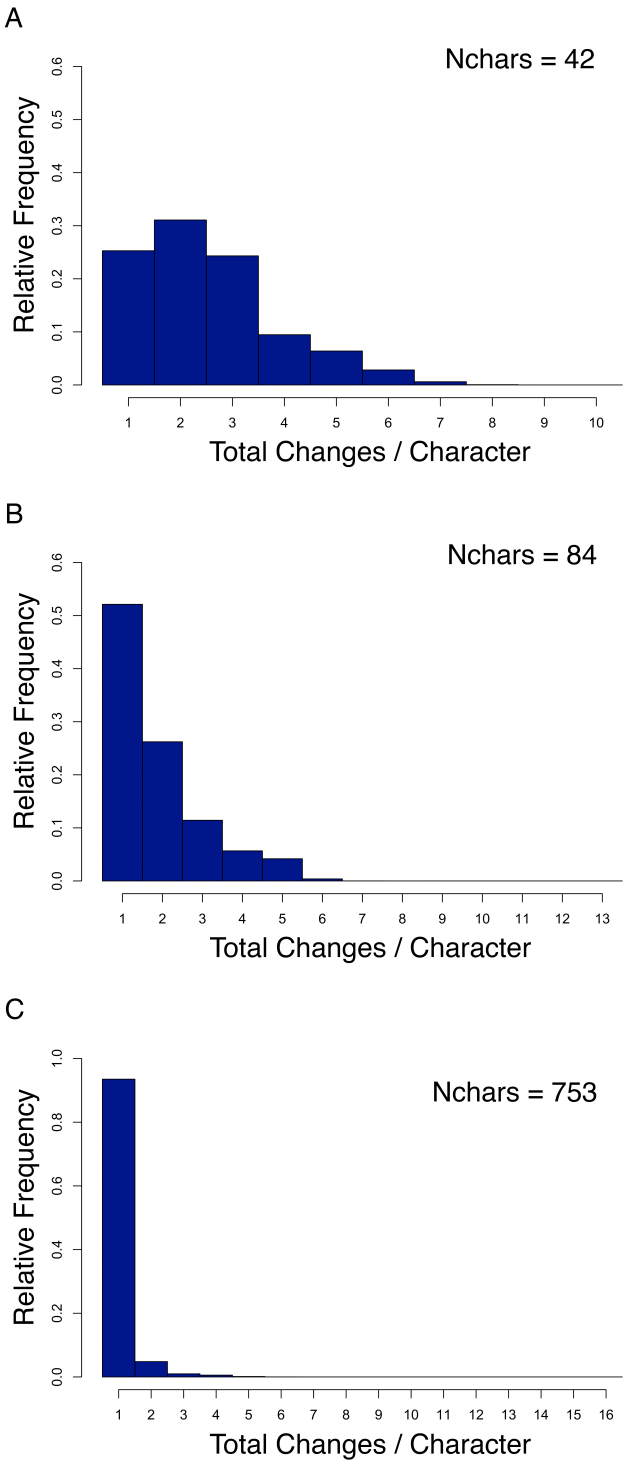

Figure 3.3. Relative frequency histograms summarizing the distribution of total changes per character across Bayesian marginal posterior topologies.
Character changes were mapped to every EQ model topology in a sample of >40,000 trees using PAUP* parsimony reconstructions (see methods) and pooled for each dataset: A) M dataset, B) SC dataset, and C) LP dataset. Available as high-res file Additional III.

Figure 3.4. Original parsimony cladograms and Bayesian 50% majority-rule consensus trees.

Topologies show either parsimony cladograms (A, C, E) or the posterior distribution of phylogenies inferred under the LN model (B, D, F) for datasets M (A, B), SC (C, D), and LP (E, F). Posterior probabilities are reported as percentages in Bayesian majority-rule consensus trees. Crown panarthropod groups are indicated by colored boxes: green, Tardigrada, blue, Onychophora; pink, Euarthropoda. Cladograms redrawn from Ma et al. 2014; Smith and Caron 2015; Legg et al. 2013. Available as high-res file Additional IV.

In contrast to the first two datasets, the LP consensus tree closely resembles the original study cladogram, showing step-wise branching of basal lobopods leading to more derived forms, and a highly supported separation of tardigrades from an onychophoran-arthropod clade. The exact sister-group relationships between onychophorans, a subset of lobopods, and a long euarthropod stem clade, however, are not resolved as they are in the original study (Figure 3.4F). Posterior probabilities are variable, with lowest values occurring at basal lobopod branches, but are generally higher than those in the other datasets.

Little to no topological difference was observed between trees estimated with the LN and GM models. M and LP consensus trees from the two rate models were identical and found to have very similar posterior clade probabilities (not figured). SC topologies estimated with the GM model differed mainly in the collapse of the lobopod-Onychophora clade (Figure 3.5), with only the *Antennacanthopedia* + Onychophora subclade sampled in more than 90% of trees (92% PP). Fully resolved SC consensus trees illustrating all compatible clades (Figure 3.5) indicate broadly similar results between the LN and GM models.

Outgroups, Transitional Taxa, and Character Change

Distant ecdysozoan outgroups (e.g. *Priapulus*, *Caenorhabditis*) and hypothesized lobopod-arthropod 'transitional taxa' (e.g. *Kerygmachela*, *Pambdelurion*) were removed individually or in combination in LN model analyses to assess their impact on tree topology. Removal of outgroups from the M and LP dataset had no impact beyond slightly lower support values for most clades (not figured). For the SC dataset, removing both the priapulid *Tubiluchus* and palaeoscolecid worm *Cricocosmia* also had no impact

on topology (not figured); however, removal of only *Cricocosmia* resulted in the collapse of the lobopod-Onychophora clade and an overall consensus topology similar to that estimated with the GM model (Figure 3.6C).

Removal of 'transitional' gilled-lobopods did not shift LP topology (not figured), but caused distinctive topological changes for the M and SC datasets. Excluding *Kerygmachela* and *Pambdelurion* from the M dataset resulted in dramatic loss of phylogenetic signal, with all lobopods forming a basal polytomy, and the lateral-lobed *Opabinia* and *Anomalocaris* positioned as most derived within the arthropod group (Figure 3.7A). Fully-resolved consensus topologies derived for the M taxonomic exclusion analyses suggest that lobopod + arthropod clades are not sampled without the presence of intermediate fossil forms (Figures 3.7B, 3.7D).

Exclusion of transitional fossils from SC analyses largely resulted in higher support for clades grouping lobopods closely with tardigrades and onychophorans, but also a *Megadictyon* + *Jianshanopodia* position at the base of euarthropods (Figures 3.6A, B, D). When *Cricocosmia* is removed along with transitional taxa (Figure 3.6D), tardigrades and onychophorans form a monophyletic clade at the exclusion of the euarthropods entirely.

Parsimony character mapping for each dataset and consensus topology revealed characters that consistently supported particular relationships. In general, monophyletic lobopod clades retrieved in the Bayesian analyses share papillae, terminal claws on lobopodous limbs, and unique character states representing distinctive dorsal sclerite features. Clades containing *Hallucigenia* species, *Cardiodictyon*, and *Luolishania* + Collins' monster occur in both M and SC consensus trees, and are grouped by variations

on sclerite morphology in combination with differentiated anterior trunk regions. The highly supported sister relationship retrieved for *Luolishania* and Collins' monster across all datasets appears primarily driven by the presence of spinose appendages in these taxa, in combination with anterior-posterior bipartite trunk differentiation (e.g. M character 9[1] "spines/appendicules on lobopodous limbs" and char. 38[1] "two long body tagmata"; SC char. 71[1] "cirrate limbs on anterior trunk"; LP char. 4[1] "two body tagmata").

Of all the (non-gilled) lobopods, *Megadictyon* and *Jianshanopodia* are the only taxa frequently positioned at the base of stem euarthropods. These fossils share some mouth/frontal appendage character states and serial midgut glands with the euarthropod clade (e.g. M 22[1] "radially arranged circumoral structures"; LP 535[1] "oral cone"; M 42[1] and SC 53[1] "serially repeating midgut glands"; LP 565[1] "gut caecae"). The grouping of *Antennacanthopodia* with crown onychophorans in two datasets (SC and LP) is supported in both analyses in part by the interpretation of eyes in this fossil, and the resulting applicability of onychophoran-specific pre-ocular appendage characters. Where lobopod relationships remain unresolved, character mapping indicates that the taxa share a common lack of papillae, sclerites, spines, or other character-rich modifications to a basic lobopodous body plan.

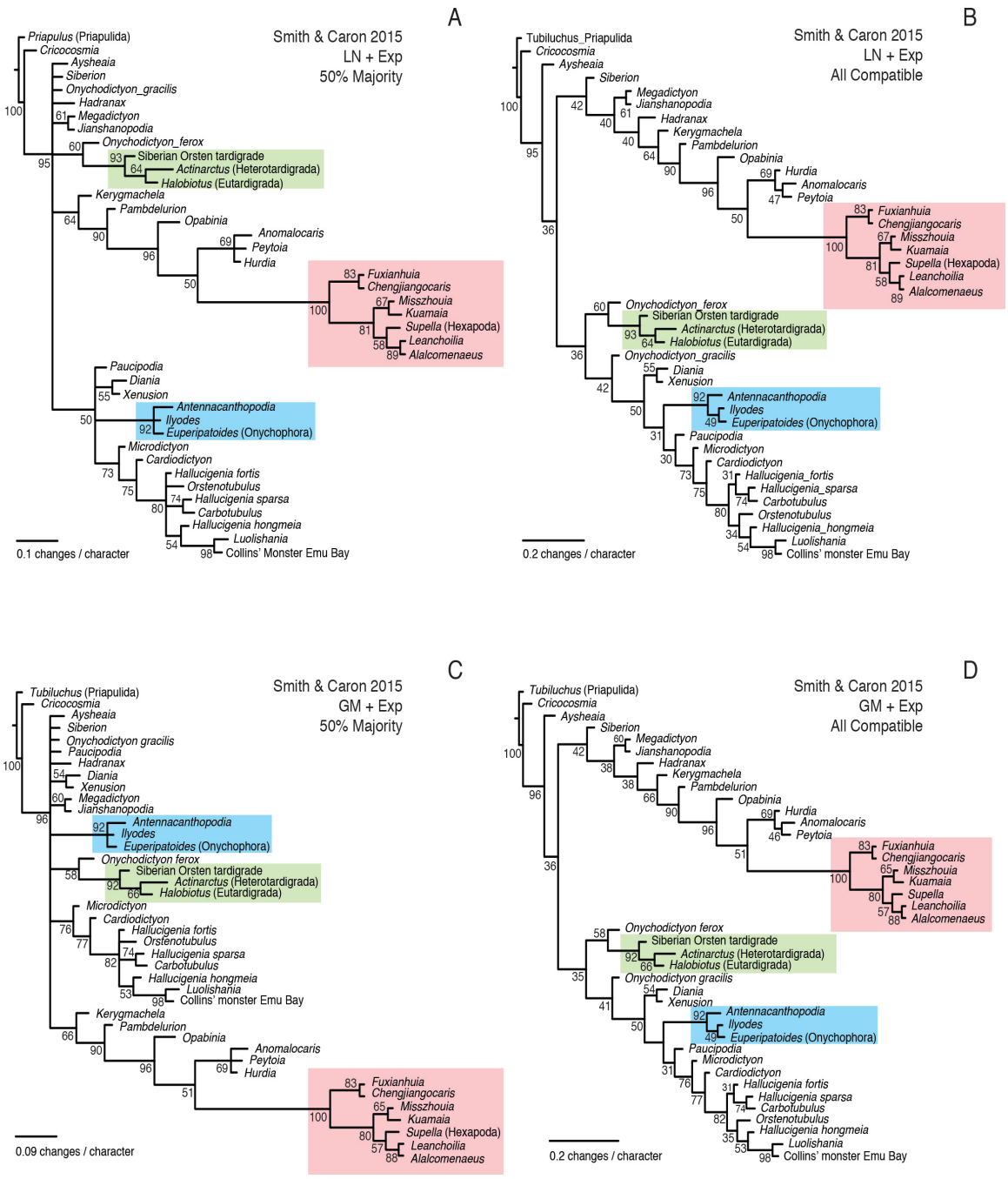

Figure 3.5. SC dataset topologies estimated with the LN+Exp or GM+Exp model. A) and B) SC topologies estimated with the LN+Exp model. C) and D) Topologies estimated with the GM+Exp model. A and C are 50% majority-rule consensus topologies, while B and D show fully resolved consensus trees depicting all compatible clades. Crown panarthropod groups are indicated by colored boxes: green, Tardigrada, blue, Onychophora; pink, Euarthropoda. Posterior probabilities are reported in percent. Available as high-res file Additional V.

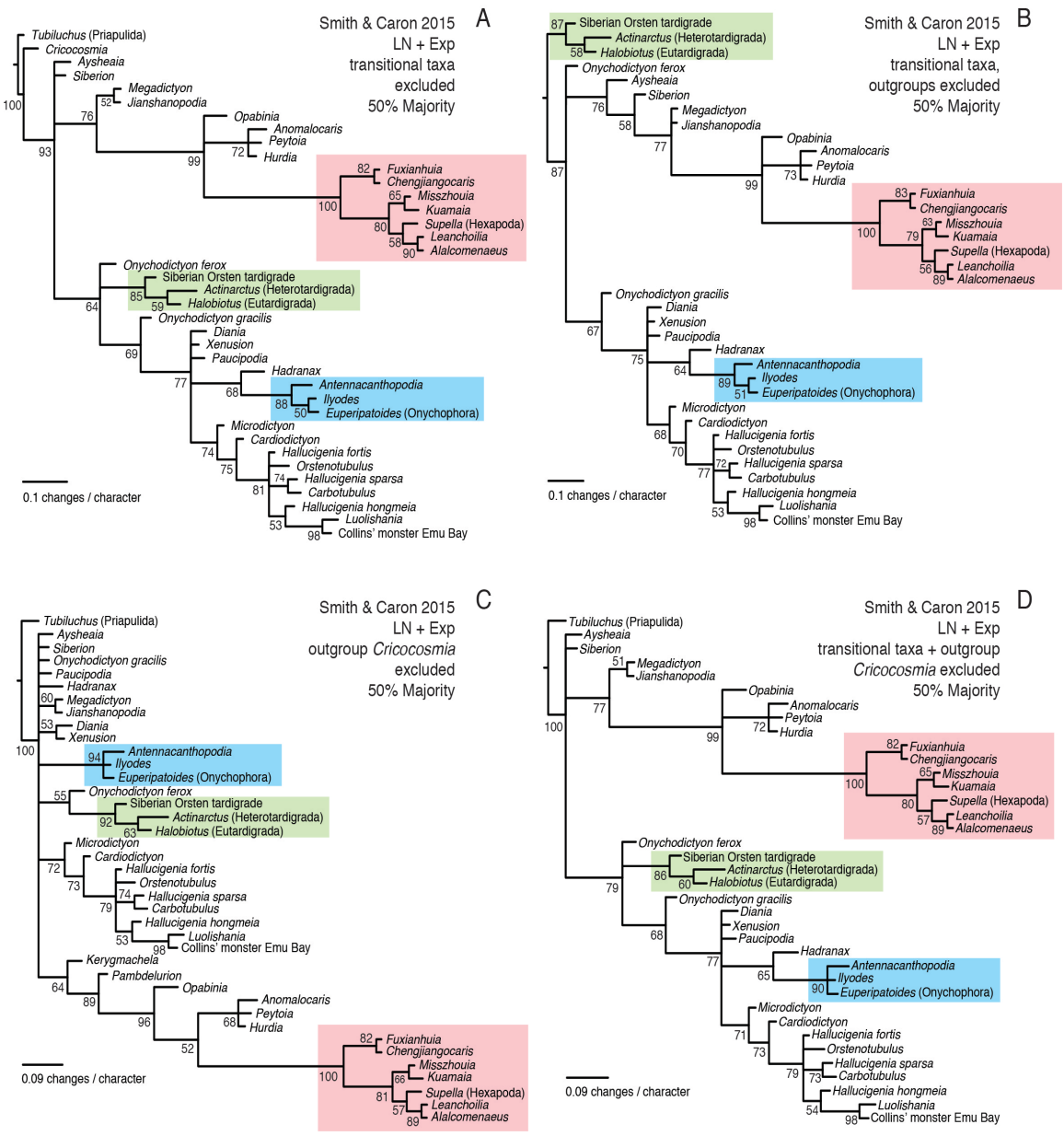

Figure 3.6. 50% majority-rule consensus trees derived from SC dataset taxonomic exclusion analyses under the LN+Exp model.
A) Transitional taxa *Kerygmachela* and *Pambdelurion* excluded. B) Transitional taxa and outgroups *Tubiluchus* and *Cricocosmia* excluded. C) Only *Cricocosmia* excluded. D) Transitional taxa and *Cricocosmia* excluded. Crown panarthropod groups are indicated by colored boxes: green, Tardigrada, blue, Onychophora; pink, Euarthropoda. All posterior clade probabilities reported in percent. Available as high-res file Additional VI.

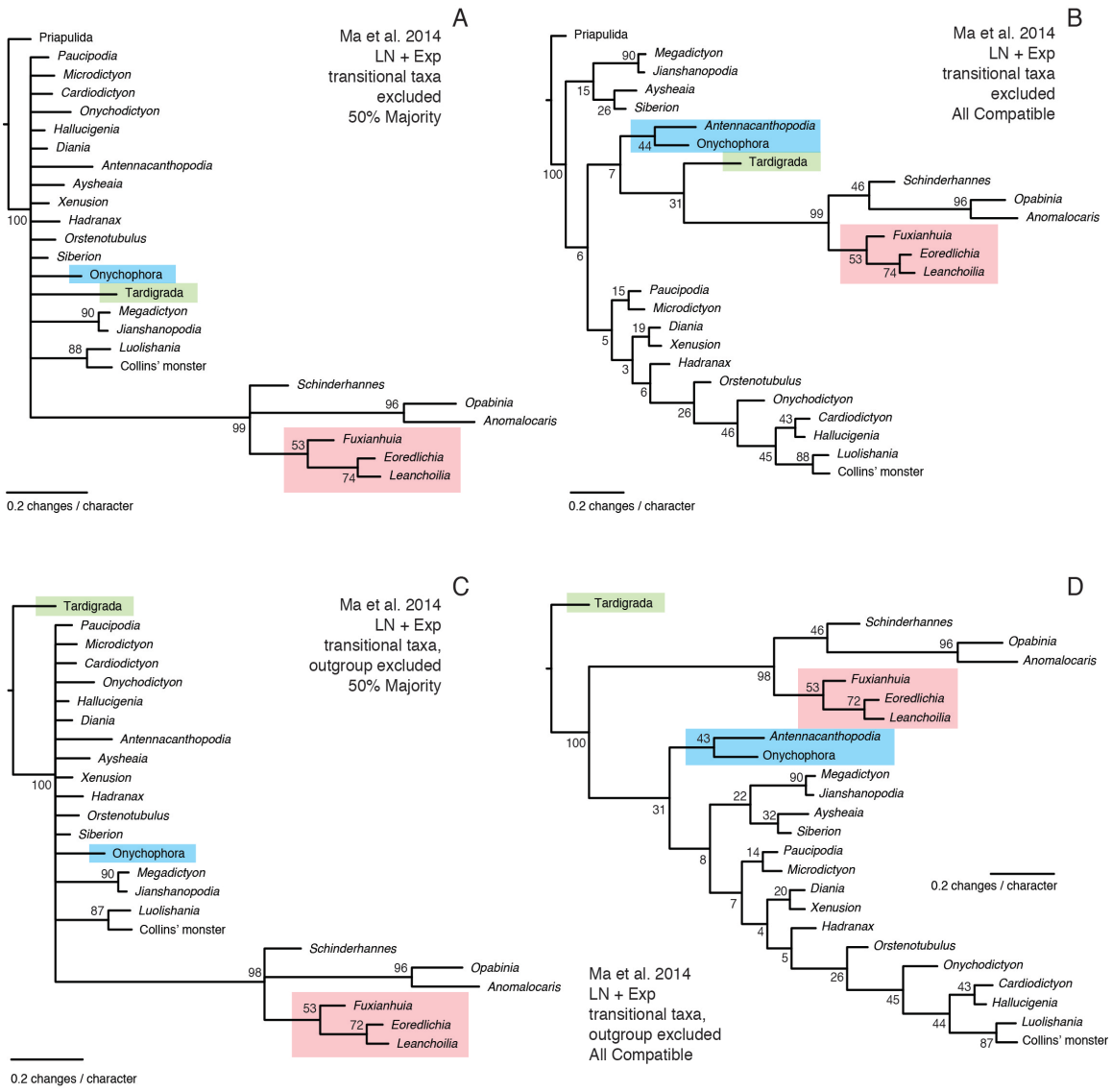

Figure 3.7. 50% majority-rule and all compatible clade consensus trees derived from M dataset taxonomic exclusion analyses under the LN+Exp model.
A) and B) Transitional taxa *Kerygmachela* and *Pambdelurion* excluded, 50% majority-rule tree in A and all compatible clades tree in B. B) and C) Transitional taxa and Priapulida outgroup excluded, 50% majority-rule tree in C and all compatible clades in D. Crown panarthropod groups are indicated by colored boxes: green, Tardigrada, blue, Onychophora; pink, Euarthropoda. Available as high-res file Additional VII.

Discussion

Modeling Character Rate Heterogeneity

The application of likelihood models to discrete morphological character data has been criticized due to concern that *a priori* decisions regarding appropriate models and rates of morphological character evolution will misrepresent phylogenetic signal (e.g. Spencer and Wilberg 2013; Xu and Pol 2014). However, Bayesian analysis of morphological characters using the widely implemented Lewis Mk model has been shown to outperform parsimony, even in scenarios with large amounts of missing data (Wright and Hillis 2014). Additionally, previous work has demonstrated that discrete character data from a wide range of empirical studies and taxonomic groups is best fit by models accommodating rate heterogeneity (e.g. Clarke and Middleton 2008; Wagner 2012; Harrison and Larsson 2015), and Harrison and Larsson (2015) argue that not accounting for character rate variation may pose the greater risk to accurate phylogeny estimation. This seems to be the case for at least two of the panarthropod fossil datasets (M and SC), as stepping-stone analyses under an equal-rates model were unable to adequately sample parameter space or converge on a likelihood estimate.

All three lobopod-stem arthropod datasets exhibit detectable character rate heterogeneity based on Bayes factor evidence for unequal- over equal-rates models and the observation that unequal-rates models generated highest HME and stepping-stone model likelihoods. Bayes factor support for rate heterogeneity is positive for the M and SC datasets (see Table 3.2), and very strong for the LP dataset. Thus, across a range of morphological dataset sizes (Table 3.1), accommodating variable rates in fossil panarthropod phylogenetic analyses appears to better represent underlying evolutionary

processes than an equal-rates approach, and indicates that parsimony-like assumptions are inappropriate for these data.

Rates of morphological character change are governed by complex interactions resulting from the hierarchical organization of developmental genetic networks, biomechanical constraints, and external selective forces (Wagner and Altenberg 1996; Erwin and Davidson 2009). Wagner (2012) argued that morphological character interdependence resulting from these interactions should make rates of character evolution fit a lognormal distribution. This appears to be the case for the three panarthropod fossil datasets, which exhibit highest model likelihoods under the LN rates model. Although Bayes factor evidence for lognormal over gamma-distributed rates is equivocal, distributions of character rates across all Bayesian posterior topologies (Figure 3.3) lends support to the choice of lognormal-distributed rates for modeling panarthropod character change. Overall character rate distributions show proportionally more characters with slow rates of change, and a long tail of few characters with faster rates, similar to results described by Harrison and Larsson (2015). These underlying character distributions may be better approximated by a lognormal distribution, which when implemented in MrBayes has several slow and one fast rate category, versus a gamma distribution, which has more evenly spaced rate category means (Figure 1 of Harrison and Larsson 2015). Likelihood differences observed between exponential and uniform priors under the same unequal-rates model (Table 3.3) show that the priors exert a large influence on likelihood, and suggest that low signal in all three datasets may not effectively update prior distributions.

Bayesian Topologies and Signal in Lobopod Datasets

Parsimony-generated consensus topologies originally reported for the M and SC datasets are not reproducible using a Bayesian approach. Across all topologies, clade posterior probabilities for clades were extremely low, and fall far below a 90-95% PP cutoff generally used as indication of good clade support (Cummings et al. 2003; Holder et al. 2008). Very few phylogenetic groups were consistently retrieved with high posterior probability; of these, the grouping of stem euarthropods, crown onychophorans, and crown tardigrades reflects the greater number of characters that may be coded unambiguously for extant animals and character-rich fossils. Conversely, lobopods that are frequently unresolved are united by a lack of modifications to a lobopodous body plan, such as papillae and epidermal specializations. Decay experiments in living velvet worms have demonstrated that many of these features, including gut morphology, eyes, papillae, and annulations are susceptible to significant taphonomic loss, and character preservation may be especially biased by body juxtaposition (Murdock et al. 2014). It is therefore quite probable that the "simplest" lobopod forms exhibit non-random decay and taphonomic stemward slippage (Sansom et al. 2010) rather than an actual primitive phylogenetic position. The description of taphonomically labile characters, such as the interpretation of eyes in *Antennacanthopodia*, or the absence of midgut glands in most small lobopods, must likewise be treated with caution, especially when these characters contribute to highly supported relationships with crown groups.

Recent studies revealing new characters in classic and well-studied taxa like *Hallucigenia* appear to produce some increase in phylogenetic information, as Bayesian analyses more frequently sample unique lobopod clades from these datasets (Smith and

Caron 2105). However, rather than informing crown panarthropod relationships – as unique fossil character combinations may do (Edgecombe 2009; Legg et al. 2013) – the conflicting characters and ambiguous coding in fossil lobopods produce greater overall topological uncertainty. Indeed, the collapse of many parsimony-supported clades to a basal polytomy in both M and SC analyses demonstrates that there is very little signal in these data to resolve the position of lobopods relative to crown panarthropods, or even crown panarthropods to one another. This absence of phylogenetic signal starkly contrasts with recent interpretations of parsimony-based panarthropod trees. For example, cladograms derived from the SC character matrix have been cited as evidence for a monophyletic tardigrade-arthropod clade (Tactopoda) (Smith and Ortega-Hernández 2014). Tactopoda was never retrieved in this study, and across all SC analyses the tardigrades were either unresolved relative to other crown panarthropods or more closely related to crown Onychophora. Clearly, by not accommodating uncertainty, parsimony-based approaches may suggest strong phylogenetic relationships from data that is equivocal at best, and evolutionary mechanism should not be inferred from such results. Together, the unresolved Bayesian consensus topologies and low support for lobopod groupings suggest that a paraphyletic "grade" of lobopods may not be a grade at all, but a result of poor phylogenetic signal.

Although M and LP Bayesian consensus trees showed no topological change with the removal of distant outgroups, taxonomic exclusion analyses did reveal the potential for outgroup choice to influence basal panarthropod topology. Smith and Caron (2015) specifically included the fossil palaeoscolecid *Cricocosmia* to mitigate long-branch attraction, and this study confirms that removal of this taxon causes topological change:

character-poor or character-ambiguous lobopod taxa shift to more basal phylogenetic positions (Figure 3.6C). Expanded and careful taxonomic sampling of outgroups – a common practice in molecular studies for minimizing long-branch attraction (e.g. Smith 1994; Rota-Stabelli and Telford 2008) – should therefore be regularly employed in fossil panarthropod phylogenetic studies. Given the efficacy of including *Cricocosmia* as an additional outgroup (Smith and Caron 2015), continued discovery and description of vermiform ecdysozoan fossils should provide suitable candidates for broader outgroup sampling.

Panarthropod Character Assessment

Taxonomic exclusion analyses illustrated the significant impact 'transitional' gilled-lobopod taxa have on basal panarthropod relationships. Without these fossil taxa, all lobopod phylogenetic structure in the M consensus tree disappears, suggesting that 'transitional' character combinations have a large role in shaping basal panarthropod topology. Interestingly, for the SC dataset, removal of *Kerygmachela* and *Pambdelurion* divides the lobopod clade into two distinct groups, with lobopod taxa possessing robust frontal appendages and midgut glands branching with stem-euarthropods, and all others forming a monophyletic clade with Onychophora and/or Tardigrada. This division between lobopods distinguishes those that possess features interpreted as "arthropod-like" from the remaining taxa, and alludes to a greater underlying issue in basal panarthropod phylogenetic analysis: character coding and homology assessment.

Systemic biases in character coding were most prominently realized in analyses of the LP dataset. Bayesian topologies estimated for these data closely resembled the original parsimony cladogram and generally exhibited higher clade posterior

probabilities. Unlike the M and SC consensus trees, which did not resolve character-poor lobopod taxa, close relationships between some of these lobopods (*Aysheaia*, *Siberion*, *Hadranax,* and *Xenusion*) and the euarthropod stem group were retrieved with relatively high posterior probabilities (i.e. <85%). The LP topology was also unexpectedly robust to outgroup and 'transitional' fossil exclusion, which may – at face value – suggest strong support for a paraphyletic lobopod grade linking crown panarthropod groups, as well as an increase in resolution due to greater taxonomic and character sampling.

Character mapping to the LP Bayesian consensus tree, however, revealed that the basal lobopod-panarthropod signal was produced by only ~50 morphological features, and that lobopod phylogenetic position was greatly influenced by a combination of inconsistent absence/inapplicable character coding and biased homology assessment. The former problem is pervasive in the construction of morphology character matrices designed to estimate relationships between higher taxonomic clades (Jenner 2002). Incorrect absence state [0] coding subsumes meaningful variation and erroneously homologizes character absences that are not equivalent, and can have significant impacts on topology estimation (Jenner 2002).

For example, lobopod taxa forming the "grade" of morphological organization between tardigrades, onychophorans, and euarthropods were positioned, in part, based on whether they possessed "isolated" dorsal sclerites or "nodes" (LP character 5). *Aysheaia*, *Siberion*, *Xenusion*, and *Hadranax* were retrieved as sister to stem euarthropods in the LP consensus tree, whereas the same taxa in M and SC datasets are unresolved at the total-panarthropod base. Characters supporting this LP lobopod-arthropod group include a shared sclerite/node absence state [0]. However, euarthropods presumably lack isolated

sclerites because their epidermal cells produce sclerotized cuticle globally (Schmidt-Rhaesa et al. 1998), and the "isolated sclerites/nodes" character is most appropriately coded as inapplicable for arthropods. Additionally, *Aysheaia*, *Siberion*, *Xenusion*, and *Hadranax* are coded as lacking "isolated" nodes (character 5[0]), although they are indicated as possessing the character "more than two plates/nodes on each segment" (6[1]). Character mapping indicates that the first character favors grouping these lobopods with euarthropods, while the second only favors a relationship between them.

Re-analysis of the LP dataset with character 5 revised to reflect the inapplicability of these epidermal specializations in arthropods produces a shift in the position of *Aysheaia* away from the euarthropod stem and collapses much of the basal lobopod "ladder" (Figure 3.8A-B). Re-defining character 5 to subsume all epidermal specializations, and character 6 to specify elaborations of this character, results in a coding of 5[1] for the four lobopods and draws them closer to other lobopod taxa (Figure 3.8C). Interestingly, uniting epidermal specializations as one unordered multi-state character by combining 5 and 6 completely flattens the basal lobopod "ladder" (Figure 3.8D). This suggests that within a probabilistic framework a decision to utilize multi-state versus binary characters can have significant topological impacts, and character coding should be assessed when using parsimony-based character matrices in total-evidence approaches. Additional revisions of character states (detailed below and in Appendix I) produce a broad collapse of these "arthropod-like" lobopods to an unresolved panarthropod polytomy (Figure 3.8E-D).

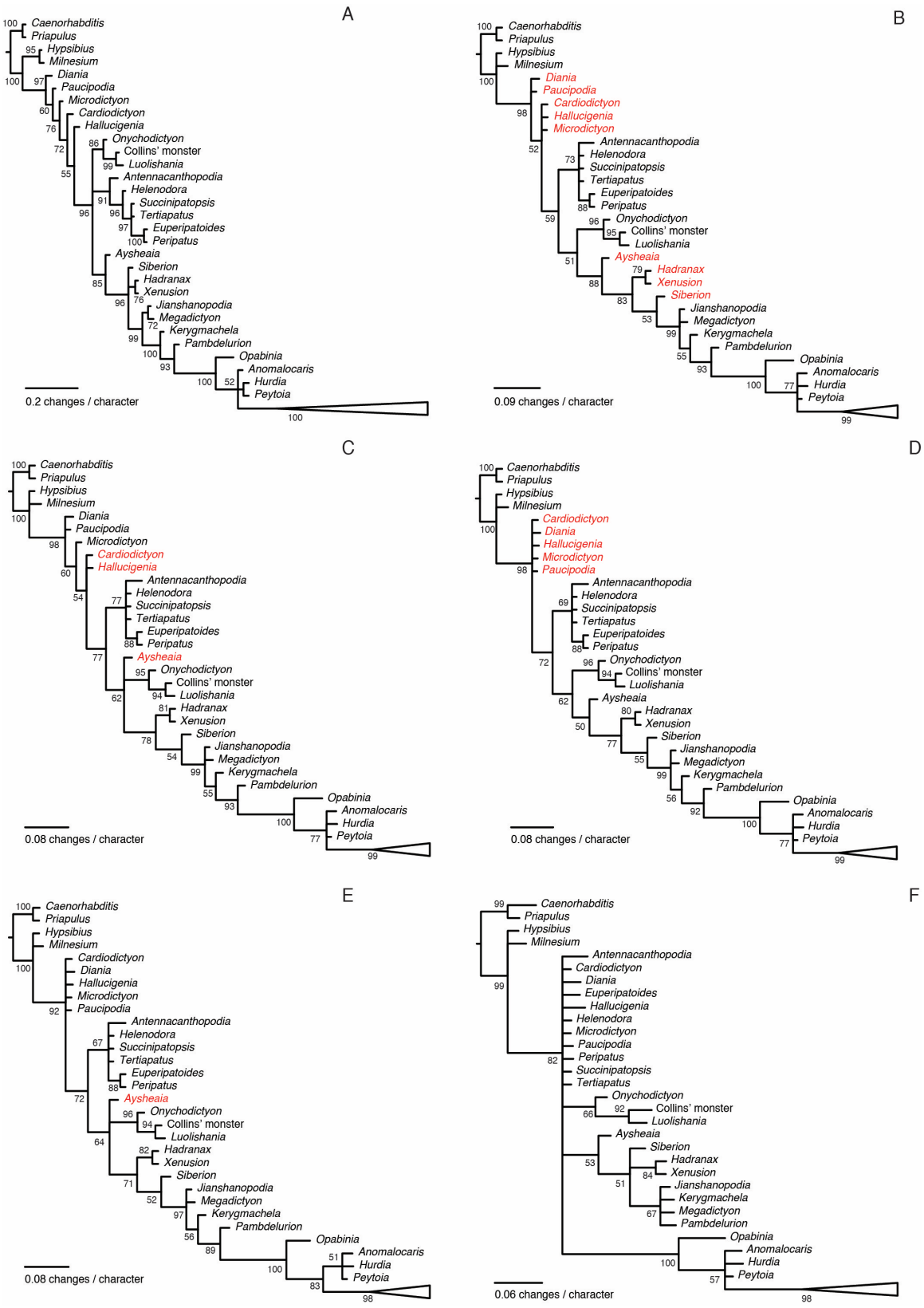

Figure 3.8. 50% majority-rule consensus trees inferred for the LP dataset with step-wise character revisions.

Figure 3.8. (previous page) 50% majority-rule consensus trees inferred for the LP dataset with step-wise character revisions.
All topologies estimated with the LN+Exp model. A) Consensus tree with original character coding, Figure 3.4E. B) Recoding character 5 as inapplicable for arthropods results in new positions for taxa in red. C) Recoding character 5 as [1] for all taxa possessing character 6 draws *Aysheaia* away from the arthropod stem. Taxa in red indicate topological change. D) Combining characters 5 and 6 into one multi-state character collapses basal lobopods into one polytomy (red). E) Recoding lobopods as lacking "grasping appendages" results in a topology similar to (C). F) Broad revision of characters (Appendix I) yields an unresolved panarthropod polytomy. All clade posterior probabilities indicated in percent. Available as high-res file Additional VIII.

Choices between an absence [0] or ambiguous state [?] in the LP dataset also reflect coding biases for particular taxa. Character 472 specifies the presence/absence of "multi-faceted eyes", referring to the description of ocelli in some lobopod taxa, and is defined by the authors as distinct from character 473, which specifies the presence of compound eyes (Legg et al. 2013). All lobopods are coded as lacking compound eyes (473[0]), however, transitional gilled-lobopods believed to be closely related to arthropods are designated as ambiguous (473[?]). Compound eyes are distinctive, easily recognizable features, and type material of *Kerygmachela* lacks any evidence for these structures. An ambiguous character state provides no information in a Bayesian analysis, and effectively subtracts from signal distancing gilled-lobopods from arthropods, reinforcing *a priori* hypotheses of lobopod-arthropod relationships.

Other characters present questionable homology assessments, although in the LP dataset this is due in part to a lack of knowledge of new lobopod characters and developmental information at the time of the original study. For instance, character 532 lumps all possible "radially arranged circumoral structures" – including papillae, plates, and lamellae – as one homologous feature. Neuronal tracing experiments in

onychophorans, however, indicate that lip papillae surrounding the mouth exhibit complex morphological development and innervation patterns, implying that these structures are not equivalent to pharyngeal teeth or other oral characters, and suggesting a similar distinctiveness in some lobopod features (Martin and Mayer 2014; Smith and Caron 2015). Segmental and/or appendage identity between onychophorans, lobopods, and arthropods may likewise prove to be less straightforward. Currently, paleontological workers treat the robust frontal appendages in some lobopod taxa as homologous to spinose, jointed frontal appendages in arthropods (e.g. chars. 202-204). These hypotheses not only impact basal panarthropod topology (supporting lobopod-euarthropod relationships), but carry broad developmental assumptions that may not hold across panarthropod phyla.

Morphological Homology: A Developmental Perspective

Networks of developmental regulatory genes (transcription factors and signaling pathways) control the construction of morphology and, by extension, underpin morphological homology. For many decades, evidence of shared developmental genes across wide-ranging bilaterian species, and the consistent expression of these genes in particular morphological features, led to the expectation that various animal LCAs possessed complex morphologies (reviewed in Tweedt and Erwin 2015). This paradigm generated a broad tendency to homologize morphological features based on gene expression patterns (Tweedt and Erwin 2015). Indeed, expression pattern data is frequently utilized in homology assessment within paleontology, and particularly the panarthropods (e.g. Scholtz and Edgecombe 2006).

Morphological features, however, are not the product of individual genes, but rather the complex hierarchical connections between multiple genes and signaling pathways (e.g. Erwin and Davidson 2009). Additionally, different hierarchies of these developmental gene regulatory networks (GRNs) relate to morphological homology in distinct ways. Highly conserved, recursively wired genetic circuits ("kernels" of Davidson and Erwin 2006; "Character Identity Networks (ChINs)" of Wagner 2014) appear to be tightly associated with specific body features, and Wagner (2014) posits that the genetic integration and cross-taxic conservation of ChINs forms the basis of morphological homology. In a similar fashion to individual genes, ChINs function as evolutionary units, and Wagner (2014) argues that the duplication and modification of ChINs can give rise to paralagous morphologic features, or "paramorphs". Paramorph regulatory networks may share core genetic components, such as the involvement of *eyes absent* and *sine oculis* in the generation of both compound eyes and ocelli in *Drosophila*, however, differences between these ChINs are responsible for organ-specific morphology (reviewed in Wagner 2014). The compound eye and ocelli are thus not homologous structures, although they share components of an ancient visual core regulatory system. The diversity of arthropod limbs may reflect a similar relationship of morphological paralogy, whereby shared limb regulatory networks were duplicated and diverged independently to give rise to unique appendages.

In contrast, GRN components that establish spaciotemporal organization of body structures or specify downstream cellular differentiation exist more peripherally in relation to ChINs, and are fundamentally decoupled from the identity of a morphological feature (Wagner 2014). Classic ectopic expression experiments (e.g. Halder et al. 1995)

exemplify the independence of character identity from character position, as the expression of *eyeless* (*ey*) and additional ChIN components are necessary and sufficient for the development of the *Drosophila* compound eye regardless of location (reviewed in Wagner 2014). Recognition that morphological character identity is linked to specific genetic circuits as opposed to single genes, and that these circuits may be largely independent from the positional inputs that deploy them, has wide-ranging implications for the assessment of character homology. More immediately, this developmental paradigm exposes issues with character coding in panarthropod fossils.

Assessment of limb homology in panarthropods, and particularly for specialized anterior appendages, has long been based on appendage segmental identity and specific innervation patterns, reflecting a reliance on topological correspondence to define homologs (discussed in Budd 2002; Scholtz and Edgecombe 2006). Elucidation of the Hox positional identity system in arthropods has shifted the conception of segmental identity to one in which Hox gene expression domains define segments and their corresponding limbs, and diverse crown arthropod limb types and/or tagmata have been united between major clades based on this system (e.g. Akam 2000). Recently, a Hox segmental identity framework was expanded to include panarthropods more broadly. A study delimiting onychophoran Hox gene expression patterns concluded, based on comparison of orthologous Hox spatial domains, that onychophoran antennae and jaws correspond to arthropod proto- and deutocerebral head segments (Eriksson et al. 2010). The authors also tentatively suggest that shared expression of the anterior-specific transcription factor *six3* supports homology of the onychophoran antenna and the arthropod (insect) labrum (Eriksson et al. 2010). Numerous fossil panarthropod studies

have incorporated these molecular homology assessments (e.g. Smith and Ortega-Hernández 2014; Smith and Caron 2015).

As outlined above, however, the developmental identity of morphological characters is likely to be distinct from the genetic instructions designating character position, and is not reducible to the expression of individual genes. In arthropods, the deployment of various appendage types is modulated by combinatorial spatial inputs from Hox and segmentation patterning (*engrailed*) networks, but this does not mean that a particular Hox gene is both necessary and sufficient for the generation of a specific appendage. Hox gene data support a homology of positional context, rather than the homology of appendages themselves. In order to properly define appendage homology, it will be necessary to elucidate genetic circuits responsive to, and downstream of, specific Hox positional inputs, as well as determine how circuits that generate distinct – and perhaps 'paralagous' – structures compare.

The common expression of *Distalless* genetic circuitry in panarthropod developing limb buds is frequently cited as evidence for limb homology in these groups (Sholtz and Edgecombe 2006). The *Distalless* (*Dll*) regulatory network, however, is involved in body wall outgrowths across all bilaterians (Panganiban 1997), and homology assessment should be made based on the composition and organization of *Dll*-based ChINs. It is quite possible that fleshy, lobopodous limbs are constructed by different ChINs than arthropodized appendages, which would support a scenario of parallel *Dll* recruitment across panarthropods, followed by independent modifications to paralogous limb-building circuits in each lineage. If panarthropod appendage ChINs are distinct, the

euarthropod LCA may not be lobopod-like at all, and limb transformation hypotheses requiring the step-wise addition of arthropod characters to lobopod legs would not hold.

In the absence of well-resolved gene regulatory network data, it may be most appropriate, then, for paleontologists to weigh similarity in structure above topological correspondence when assessing morphological character homology. I advocate the primary recognition of complex structure for fossil homology definitions, and propose that positional information should be subsumed within character states coded for these characters. The shared presence of a distinct sensory appendage in lobopods, for example, is likely to be more instructive than whether this appendage is positioned in a region presumed to correspond to a first or second segment. Likewise, the construction of epidermal papillae should be coded as homologous, and the location of these papillae on the body subsumed within this character as a positional state. Robust frontal appendages in large lobopod taxa may represent the elaboration of a limb type that is genetically distinct from those in arthropods, and if so, these morphologies should be represented as independent from the jointed and sclerotized frontal appendages of arthropods.

Minimally, this alternative character-coding scheme should be used to test the effects of potential bias in homology assessment, and will provide an additional strategy for examining how phylogenetic assumptions shape the outcomes of phylogenetic analyses. As this study demonstrates, the low signal in panarthropod morphological datasets, revealed by a Bayesian approach, is the most likely cause for lobopods forming a "grade" of organization, and these fossil may not exhibit a gradual evolution of crown panarthropod characters. Additionally, those characters uniting some lobopods with euarthropods are subject to taphonomic and worker coding biases, adding uncertainty to

the claim that specific lobopod taxa represent euarthropod precursors. Thus far, the soft polytomies inferred in these analyses represent poor data, and the discovery of new lobopod taxa and characters may help resolve lobopod-arthropod relationships. However, if – as time-calibrated molecular analyses suggest – a rapid genetic diversification occurred in cryptic panarthropod ancestors, it may be possible that lobopods represent multiple distinct lineages within the panarthropod clade, and no amount of morphological data will resolve the hard panarthropod polytomy. Elucidating the composition of gene regulatory networks that build panarthropod morphology will help determine which scenario of lobopod evolution is most likely.

Conclusion

Fossil panarthropod morphological data is poorly modeled by parsimony-like assumptions, and reanalysis of recently published character matrices shows that broadly accepted lobopod-arthropod relationships are not reproducible by a Bayesian approach. Accommodating uncertainty in model-based analyses demonstrates that 'basal' lobopods possess few characters that inform their phylogenetic position, while others may group with crown panarthropods based on coding and homology assessment bias. Signal within these datasets is unable to confidently resolve any lobopod relationships with respect to crown panarthropods, indicating that the mix of panarthropod characters these fossils possess lead to phylogenetic ambiguity rather than highly supported positions as transitional forms. It is therefore possible that the euarthropod LCA was not lobopod-like, and that lobopods represent separate lineages with paralagous panarthropod features.

Progress in basal panarthropod phylogeny will likely be made by future discovery of new fossil taxa and characters in both panarthropods and ecdysozoans more broadly,

particularly given the impact of additional fossil outgroups and key 'transitional' forms on panarthropod phylogenetic structure. As character homology is revised to reflect current uncertainty and future genetic regulatory insight, the position of the lobopods within Panarthropoda should hopefully become more clear. However, it may well be the case that the radiation of basal panarthropods occurred so rapidly in the Ediacaran that no amount of additional morphological data will resolve basal panarthropod relationships, and if so, the origin of the arthropods may reside in a true hard polytomy.

Acknowledgements

I thank Arne Nielsen and Jacob Walløe Hansen of the Geological Museum, Natural History Museum of Denmark for arranging accommodation and access to Sirius Passet specimens in Copenhagen. I also thank Maoyan Zhu and Han Zeng of the Nanjing Institute of Geology and Paleontology, Chinese Academy of Sciences, for their collaboration, gracious hospitality, and access to Chengjiang fossil lobopods. Peter Wagner, Rachel Warnock and Graham Slater provided valuable input and methodological advice. This work was funded by the NASA Astrobiology Institute Foundations of Complex Life MIT/Harvard node research grant, and a Cosmos Scholars grant awarded by the Cosmos Club of Washington, D.C.

Chapter 4: Sponge biofabrics from the late Ediacaran of Namibia and the Southwest United States

Abstract

Ecological assemblages that include the oldest animal lineages undoubtedly preceded the Cambrian Period. The missing precambrian record of definitive sponge body fossils or spicules has therefore prompted questions about the nature of ancestral sponges and potential preservation bias. We report biogenic fossil fabrics, herein interpreted as the oldest known spicule-bearing sponges, from the latest Ediacaran of Namibia and the southwest United States. Specimens of *Luthiera alomari* n. gen. n. sp. exhibit sponge walls with embedded longitudinal spicules similar to Cambrian protomonaxonid sponges as well as living hexactinellids, and evidently constructed tall, cylindrical bodies. Stratigraphic overlap between these sponges and enigmatic Ediacaran soft-bodied and tubular fossils indicates that mixed ecological assemblages of the late Neoproterozoic included animals integral to shaping the oceans for the Cambrian Explosion of bilaterian diversity.

Keywords: Ediacaran, Cambrian, sponges, ecosystem engineering

Introduction

The Ediacaran-Cambrian transition has been viewed in two distinct ways: as a phase shift between pre- and post-metazoan ecologies (e.g. Antcliffe et al. 2014); or, as an overlapping evolution of biotas, in which animals co-occur with, and begin to impact, Ediacaran communities (e.g. Narbonne 2005; Laflamme et al. 2013). Although a literal reading of the fossil record supports the former, growing evidence demonstrates that the biological and ecological foundations for the Cambrian Explosion are found in the

Ediacaran (Tweedt and Erwin 2015). Time-calibrated molecular phylogenies estimate that most animal genetic diversity was established in the Neoproterozoic, with the divergence of sponges (Porifera) in the Cryogenian, and both eumetazoans (Bilateria + Cnidaria) and bilaterians by the Ediacaran (Erwin et al. 2011; dos Reis et al. 2015).

While their exact phylogenetic position is debated, there is broad support for the placement of sponges as the earliest-branching animals (e.g. Pisani et al. 2015). Fossil sterols produced by modern demosponges occur in Cryogenian deposits and support their early evolution and ecological presence (Love et al. 2009). However, uncontested precambrian sponge spicules or body fossils have not been found, despite the fact that major extant sponge lineages produce readily-preservable skeletal material, and that ancestral sponges likely had spicules (Mehl-Janussen 1999; Sperling et al. 2010). Late Ediacaran structures from the Tsagaan Oloom Formation (Fm) in Mongolia (Brasier et al. 1997), initially considered the oldest hexactine spicules, were recently reexamined and determined to be arsenopyrite crystals (Antcliffe et al. 2014). Other possible sponge candidates, including bioclasts from the Cryogenian in South Australia (Maloof et al. 2010), calcified chambered structures in the Cryogenian of South Australia and Namibia (Wallace et al. 2014), and the Ediacaran fossils *Thectardis* (Sperling et al. 2011) and *Paleophragmodictya* (Gehling and Rigby 1996), although interpreted as potential sponges based on morphology, lack recognizable spicules or ostia. The phosphatized, mm-sized *Eocyathispongia* from the Ediacaran of South China provides an example of sponge-grade cellular organization (Yin et al. 2015), but spicules or body fossils are not found until the lower Cambrian, when representatives of the major crown lineages Hexactinellida and Demospongiae appear in the rock record (e.g. Steiner et al. 1993). The

~200 million year 'spicule gap' between the origin of Porifera based on molecular clocks and the first fossil appearance of the group *sensu stricto* has thus begged either taphonomic or evolutionary explanation (Xiao et al. 2005; Sperling et al. 2010).

Here we report the discovery of biological structures, which we interpret as fossil sponge biofabrics, from the latest Ediacaran of Namibia and the southwest United States. These fossils provide evidence of spicule-producing sponges in the precambrian, broaden the search image for early sponge remains, and demonstrate the existence of mixed communities, comprising metazoans, soft-bodied Ediacaran enigmatica, and dominant terminal Ediacaran tubular organisms, at the close of the Neoproterozoic.

Geologic Setting

Southern Namibia

Sponge biofabrics occur in the Ediacaran-Cambrian (E-C) Nama Group at Farm Swartpunt in Southern Namibia (Figure 4.1). Exposures at Farm Swartpunt include ~130 m of the Spitskopf Member (Mb) of the uppermost Schwarzrand Subgroup and contain Ediacara-type fossils, such as *Pteridinium* and *Swartpuntia*, as well as the skeletonized *Cloudina* and *Namacalathus* and the complex trace fossil *Streptichnus narbonnei* (Figure 4.1) (Saylor and Grotzinger 1996; Narbonne et al. 1997; Jensen and Runnegar 2005).

The fossil biofabrics at Swartpunt are found between horizons containing soft-bodied Ediacaran taxa. *Pteridinium* and *Swartpuntia* occur in several horizons within a ~22 m-thick sequence of siliciclastic mudstone and fine-grained sandstone, the lower parts of which are steeply dipping and interpreted as a post-depositional "megaslump" (Saylor and Grotzinger 1996; Narbonne et al. 1997). *In situ* sponge fossils occur ~1 m

above the principal fossil horizon atop the megaslump (fossil bed "A", Narbonne et al. 1997; "ridge 1", Darroch et al. 2015) within a recessive unit of thinly interbedded planar and locally ripple cross-laminated siltstone, sandstone and limestone (Figure 4.2). Float specimens were recovered from talus above and below "ridge 2" (Darroch et al. 2015; fossil bed "B", Narbonne et al. 1997). The environment is interpreted as open marine shelf, between wave- and storm-wave base, and likely within the euphotic zone (Saylor and Grotzinger 1996; Narbonne et al. 1997).

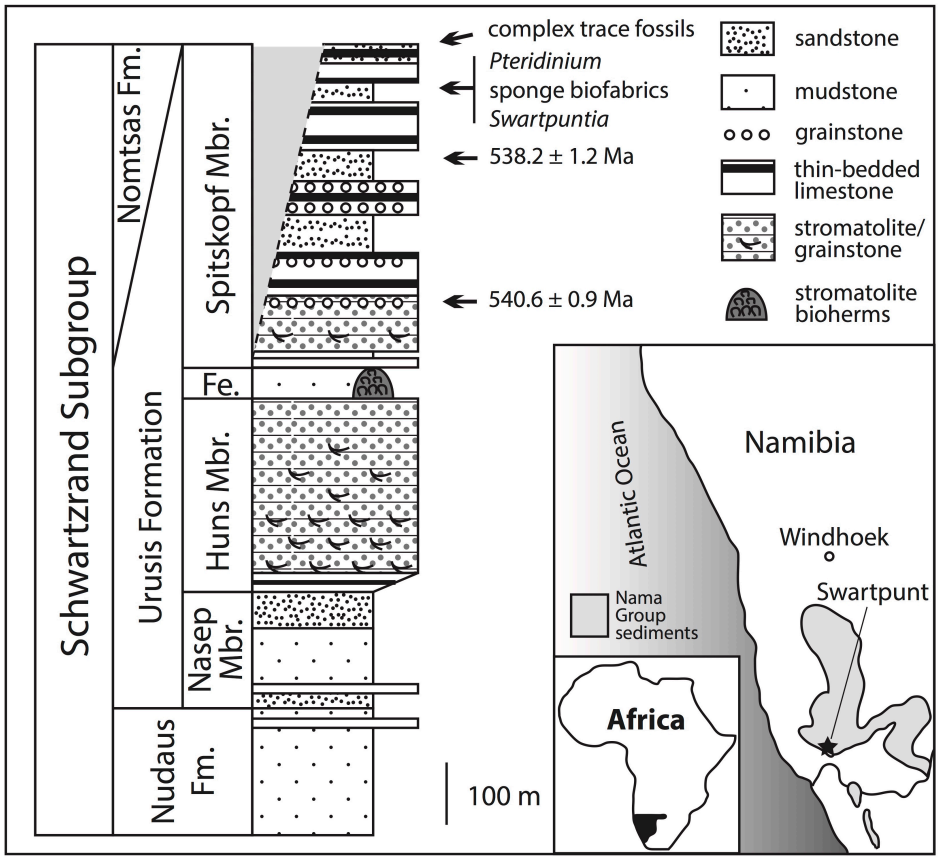

Figure 4.1. Generalized stratigraphy of the Schwarzrand Subgroup in southern Namibia, modified from Darroch et al. (2015).
The Cambrian Nomstas Fm rests unconformably on the Spitskopf Mb. U-Pb dates from Schmitz 2012. Inset: Nama Group sediments of southern Namibia, modified from Darroch et al. (2015). Black star = Farm Swartpunt (27°29' S, 16°41' W). Available as high-res file Additional IX.

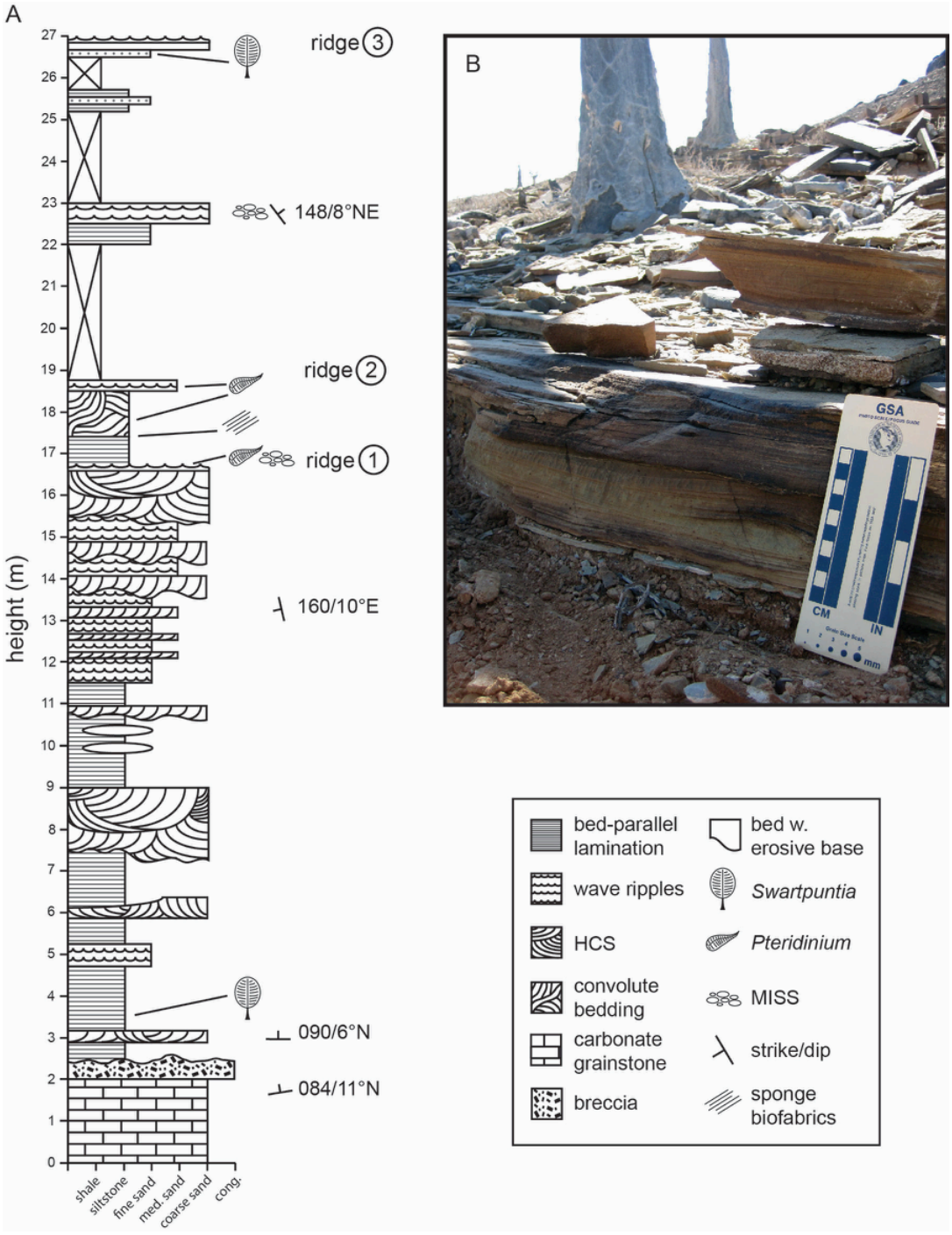

Figure 4.2. Sedimentology at Farm Swartpunt, southern Namibia.
A) Stratigraphic section through fossiliferous horizons, modified from Darroch et al. 2015. Sponge biofabrics occur between horizons containing *Pteridinium* and *Swartpuntia*. B) Fossil-bearing calcareous sandstone horizon preserving sponges on bed base. Available as high-res file Additional X.

Fossils at Swartpunt are bracketed by U-Pb zircon ash ages of 540.6±0.9 Ma from an ash that is ~90 m below the fossiliferous interval and 538.2±1.2 Ma from the overlying Nomstas Fm (Schmitz 2012; revised from Grotzinger et al. 1995) (Figure 4.1). Carbon isotope ($\delta^{13}C$) chemostratigraphy in the Nama Group is consistent with E-C chemostratigraphy and other radiometric constraints globally (e.g. Amthor et al. 2003; Zhu et al. 2006).

Nevada, United States

Sponge biofabrics were also found in latest Ediacaran strata at Mt. Dunfee, Nevada, USA (Figure 4.3). The fossils reported herein occur in the lowermost Dunfee (lower) Mb of the Deep Spring Fm, in the same stratigraphic interval as the *Gaojiashania, Wutubus,* and other vermicular fossils from Smith et al. (2016b). The fossils are preserved in a transgressive sequence, just above a karstic exposure surface (Smith et al. 2016b).

Although there are no U-Pb ash ages in E-C strata in the southwest USA, the fossils are temporally constrained using $\delta^{13}C$ chemostratigraphic correlation and biostratigraphy. The basal to middle part of the Dunfee (lower) Mb of the Deep Spring Fm records the late Ediacaran positive 3-5.5‰ $\delta^{13}C$ plateau (Smith et al. 2016b) that is thought to be characteristic of latest Ediacaran $\delta^{13}C$ values globally (e.g. Amthor et al. 2003; Smith et al. 2016a; Zhou and Xiao 2007). In Oman and Namibia, U-Pb ash ages of 546.7±0.7 Ma and 547.3±0.7 Ma, respectively, temporally constrain this positive $\delta^{13}C$ plateau (Bowring et al. 2007; Schmitz 2012). At Mt. Dunfee, the E-C boundary has been placed ~450 m above the fossiliferous interval in the upper part of the Esmeralda (middle) Mb of the Deep Spring Fm, where the first appearance datum of *Treptichnus*

pedum was found above the nadir of the 'basal Cambrian' large $\delta^{13}C$ excursion and the last appearance of a cloudinid (Corsetti and Hagadorn 2013; Smith et al. 2016b).

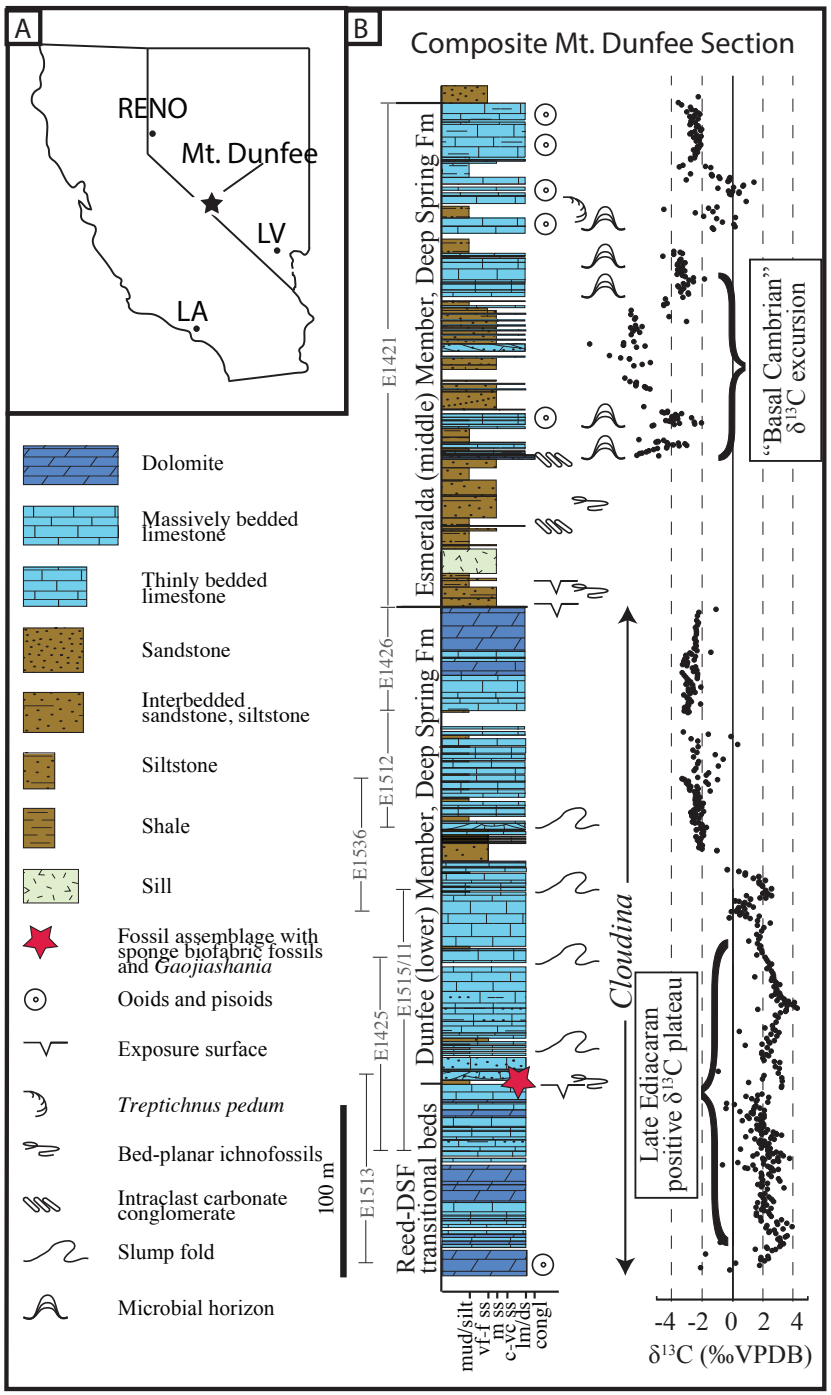

Figure 4.3. Geology of Mt. Dunfee, Nevada, USA.
A) Locality map. B) Composite stratigraphic column (37° 20' 32.52" N, 117° 19' 17.27" W). Figure modified from Smith et al. (2016). Available as high-res file Additional XI.

Methods

All specimens collected from Farm Swartpunt were photographed, assigned accession numbers (F-), and housed in the National Earth Science Museum at the Geological Survey of Namibia (Ministry of Mines and Energy, Windhoek). Slabs too large to transport were photographed in the field and left at outcrop. Nevada specimens were photographed and are currently housed at the National Museum of Natural History, Washington, D.C. Specimen measurements were obtained from high-resolution photographs using ImageJ software (Schneider et al. 2012) image analysis tools. Absolute distance in each specimen photograph was determined by calibrating length in pixels to photo scale bar length. ImageJ measurements may vary slightly with a user's manual pixel selection. To account for this variation, multiple data points were taken for every measurement. Based on scale bar calibrations, an average of ten separate measurements proved sufficient to provide accurate absolute measurements.

Fossil Structure and Biological Origin

More than 90 specimens were documented from Swartpunt and Mt. Dunfee localities. Fossils found *in situ* at Swartpunt are impressions preserved in positive hyporelief on a thin layer of micaceous fine sandstone forming the bases of 8-10 cm-thick finely laminated and occasionally rippled calcareous sandstone slabs. Swartpunt float specimens and Nevada specimens are preserved in siltstones and fine sandstones as positive relief impressions.

Fossils consist of straight, sub-cylindrical striations, preserved in either parallel longitudinal sets or slightly radiating groups (Figure 4.4). Striations are sub-mm in width, ranging from less than 0.1 mm up to 0.7 mm, and comprise approximately two to three

size orders (Figures 4.6, 4.7). Parallel striations are regularly spaced 0.1-2.0 mm apart. Sets span 3.5-188 mm in length (incomplete) and 0.6-40 mm in width, and may occur as both single- (Figures 4.4A, 4.5D) and double-parallel striation arrays (Figure 4.4F). In some Swartpunt specimens, arrays are preserved in walls of higher-relief cylinders (Figure 4.4G). Smallest-scale striations average 0.075 mm in width, are preserved as densely packed thatch or in isolation, and possibly taper at termini (Figures 4.4C, 4.6C). Thatch orientation varies but may lie transverse to larger striation arrays (Figure 4.6). "Vein"-like ridges 0.5-7.5 mm-wide co-occur with striation sets in Swartpunt fossils, either bounding parallel arrays or lying obliquely over/under smaller-scale structure (Figures 4.4A, 4.5D, 4.6). Veins are rectilinear to sub-cylindrical, and unlike striation arrays, cylindrical veins may show gentle curvature or deformation (Figure 4.4D). Often, veins bounding parallel arrays form 2-4 cm-wide and up to 28 cm-long rectangular tracts (Figure 4.5). Some veins are themselves striated (Figure 4.4D, 4.5C), indicating that they are constructed of bundles of the smaller cylindrical units.

Figure 4.4. (following page). *Luthiera alomari* biofabrics from Swartpunt and Mt. Dunfee.
A) Paratype F1241 detail showing multiple spicule size orders and overlapping structure. B) Sub-mm parallel spicule rods with discrete edges, Mt. Dunfee specimen. C) < 0.1 mm monaxons (arrows) exhibit possible tapering at termini, detail from F1238. D) Curved vein composed of bundled rods (arrows), paratype F1237. E) Fragmented and overlapping monaxon arrays, F1410. F) Double-parallel spicule array, F1556. G) High-relief cylindrical array indicating possible tubular form, F1426. Scale bar in A, B, D-G: 1 cm; C: 2 mm. Available as high-res file Additional XII.

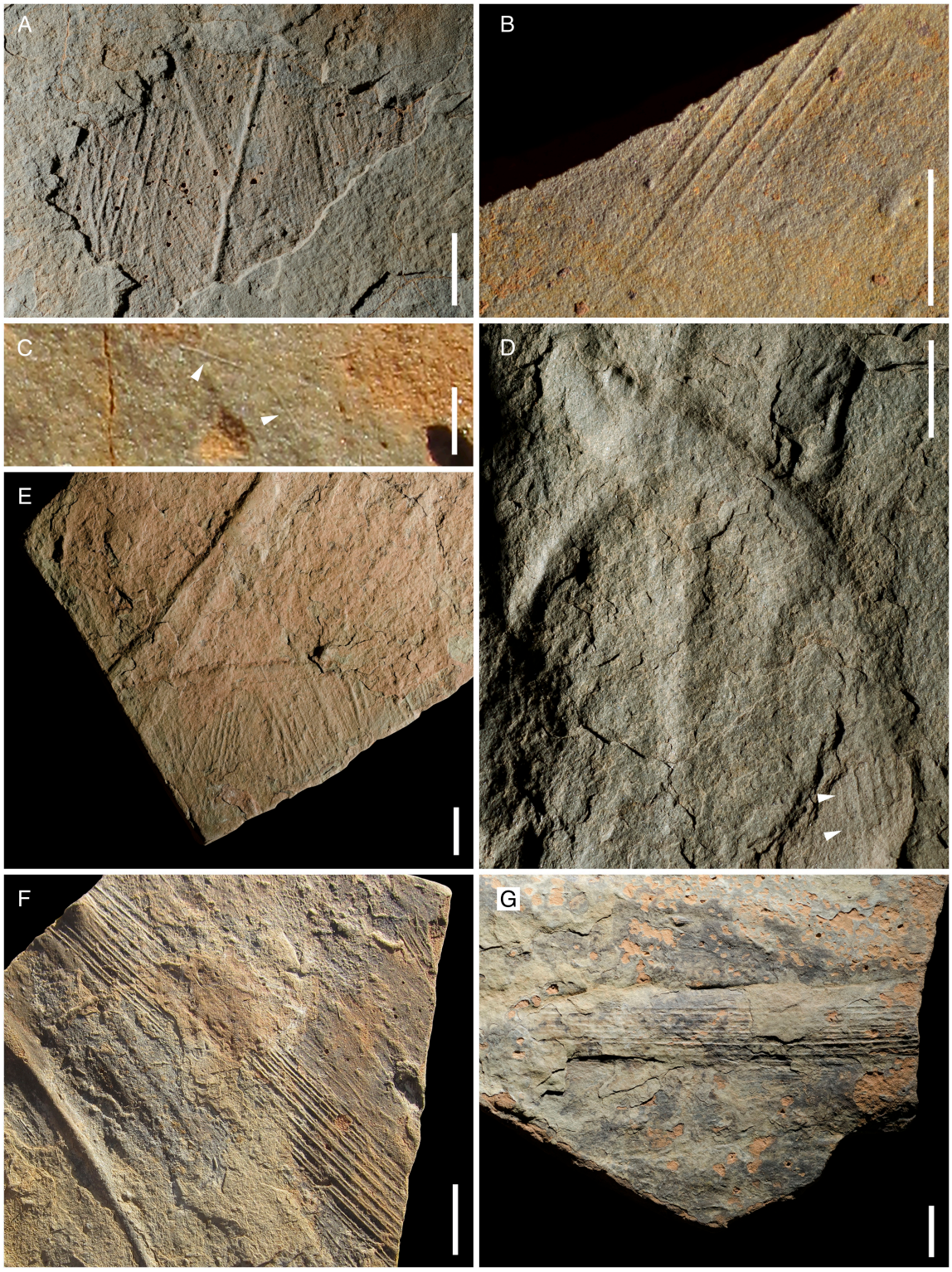

Figure 4.4. *Luthiera alomari* biofabrics from Swartpunt and Mt. Dunfee.

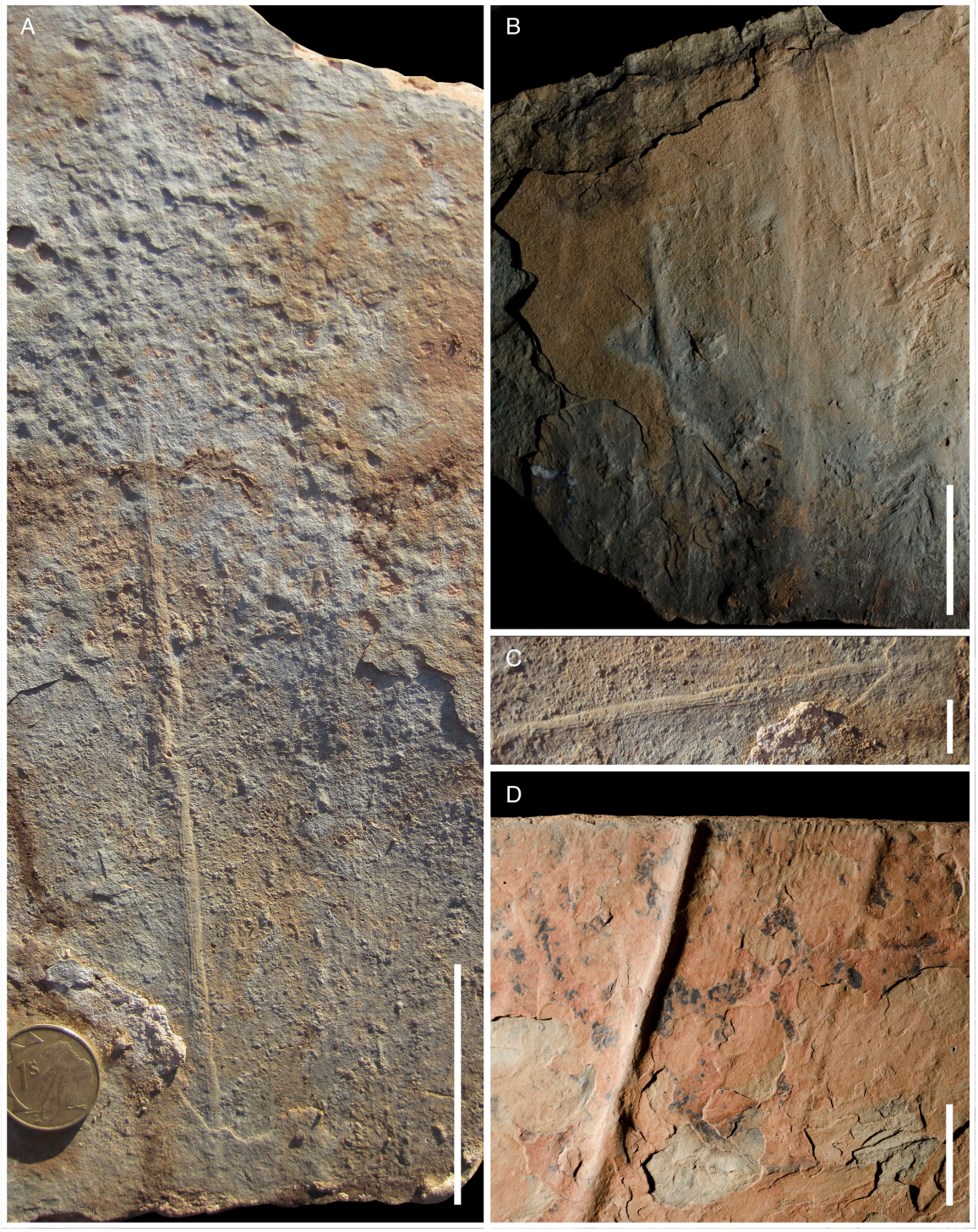

Figure 4.5. Specimens of *Luthiera alomari* with spicule tracts suggesting cylindrical / tubular bodies.
A) Field specimen with ~28 cm-long, 3.7 cm-wide rectangular impression. Left bounding vein (C) is comprised of bundled rods. B) Paratype F1407 with ~2 cm-wide, ~10 cm-long sub-triangular/cylindrical weathered impression. D) Paratype F1411 with veins bounding 3.8 cm-wide parallel array of 18+ spicule rods. Scale bar in A: 5 cm; B: 2 cm; C: 1 cm; D: 2 cm. Available as high-res file Additional XIII.

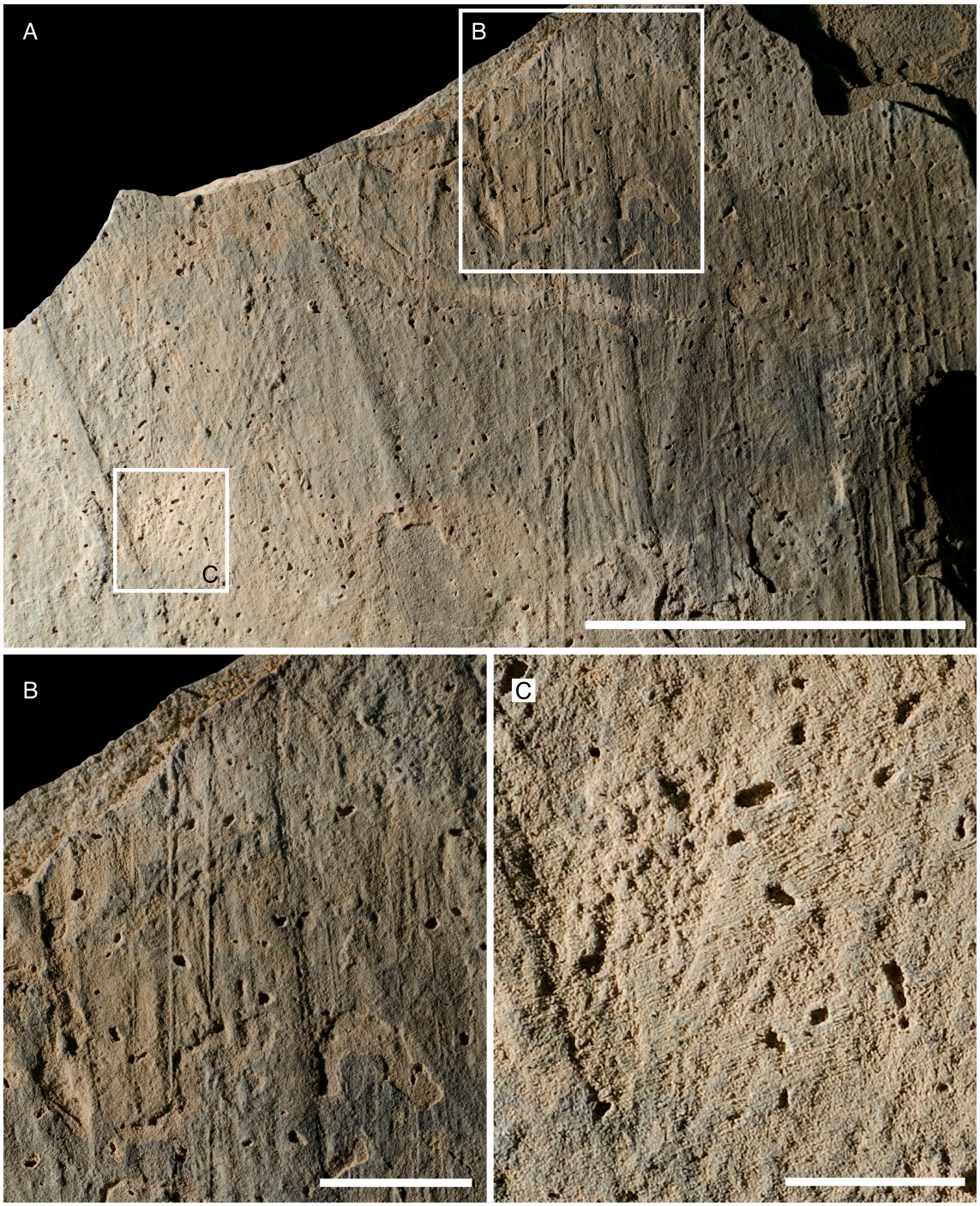

Figure 4.6. *Luthiera alomari* holotype (F1460).
A) Slab base with overlapping spicule arrays from fragmented sponge wall fabrics. Rectilinear/sub-cylindrical veins bound spicule tracts, and three size orders of spicules present. B) Detail of box B with well-defined rods and vein likely demonstrating edge thickening due to compression of stacked tissue. C) Detail of box C showing smallest-scale thatch. Spicule termini are not visible due to close grouping, but widths appear to narrow, suggesting elongate fusiform shapes. Scale bar in A: 5 cm; B: 1 cm; C: 5 mm. Available as high-res file Additional XIV.

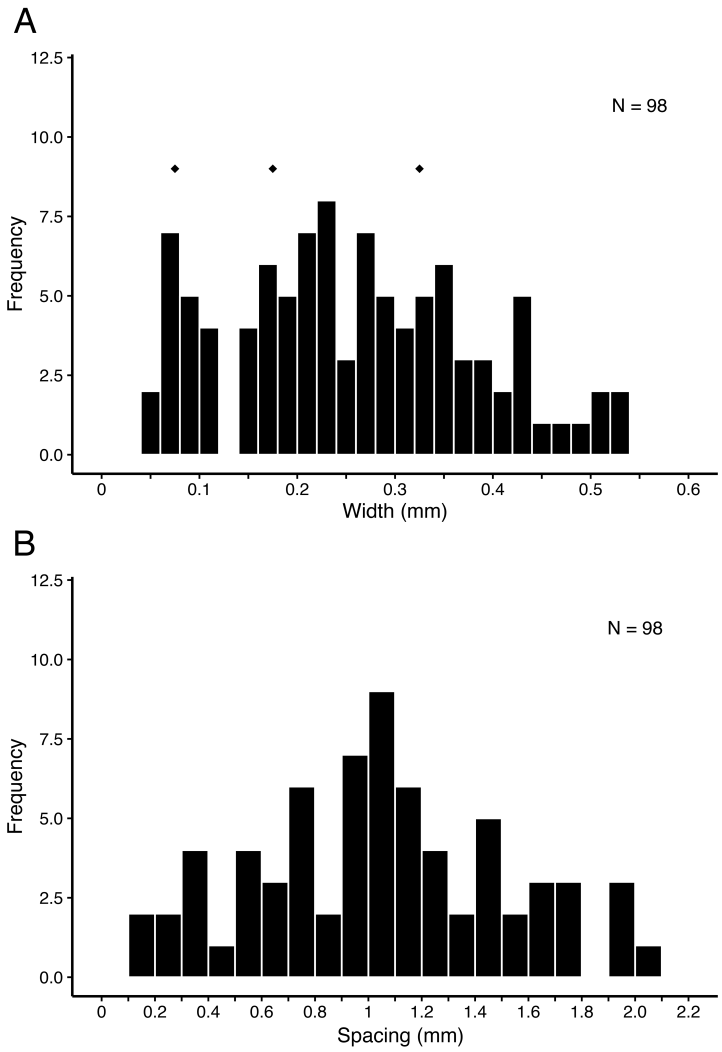

Figure 4.7. Frequency distribution of *Luthiera alomari* monaxon diameters and spacing in parallel arrays.
A) Monaxon diameter distribution. Diamonds in are local maxima of 0.075, 0.175, and 0.325 mm, suggesting at least two spicule size orders. B) Distribution of spacing between monaxons.

Although the generation of subparallel, rectilinear ridges and grooves on bed surfaces by erosional flow has been demonstrated experimentally (e.g. Allen 1969), multiple factors rule out a mechanical interpretation for these fossils. Overlapping arrays of parallel striations comprise multiple size orders and orientations, and exhibit no destruction that would be expected if directional shift in flow resulted in cross-cutting

grooves. In fact, slight bulging is often observed where one unit overlies another (Figure 4.4A), suggesting that the fossils record overlapping three-dimensional structures. Slightly radiating sets and arrays exhibiting sharp discrete edges are also incompatible with a sedimentary interpretation. Rectilinear grooves produced experimentally rarely exhibit spacing < 2 mm (mean 5-6 mm) and show random bifurcation or convergence (Allen 1969), whereas mean spacing of the fossil striations is 1.1 mm and structures do not bifurcate or rejoin. Local sedimentology indicating lower-energy depositional regimes in both Namibia and the SW US also rules out sedimentary interpretation. At Swartpunt, fossils occur in sub-mm laminae of fine sand or in silts, in strata interpreted to represent quiet open marine shelf deposition between larger storm deposits. At Mt. Dunfee, the fossils occur in a ~5 m stratigraphic interval of siltstones and micaceous sandstones with flat, sub-rounded mudchips and vermicular fossils (Smith et al. 2016b). The mud chips and fossils often occur on the same bedding surfaces, consistent with an interpretation that the biofabrics are the result of minimal transport of light, planar, biogenic material rather than the grooving and scouring of a bed surface by flow.

Fossil Fabrics and Sponge Affinity

In addition to ruling out a sedimentary interpretation, the scale and regularity in these fossils supports biological origin. Parallel rods most likely represent structural elements regularly arrayed within a thin tissue, and fossils preserve overlapping impressions of these biofabric fragments.

We interpret the < 0.1 mm striations and parallel-arrayed sub-cylindrical striations as monaxon spicules and larger spicule rods, respectively. Smallest-scale, thatch-like and isolated spicules fall within the lower diameter range of fine monaxons reported from

Cambrian sponges (Table 4.1). Rods spanning 0.1-0.5 mm in diameter are likewise comparable to larger structural monaxons (Table 4.1). Original spicule composition cannot be determined from these impression fossils, but comparison to other fossil spicule morphologies (Table 4.1) suggests siliceous or potentially biminerallic spicules (Botting et al. 2012). Faithful preservation of regular sub-mm spacing of spicule rods indicates binding by organic tissue, and we thus interpret longitudinal parallel arrays as sponge wall fragments. Variations in vein structure likely reflect separate features: 1) Curved, cylindrical veins may represent the bundling of monaxons into fibrous "rope" as in hexactinellid rooting tufts; and 2) veins bounding parallel spicule arrays may be thickened edges resulting from the stacking of spiculate tissue during compression of an originally tubular or cylindrical form.

We establish *Luthiera alomari* n. gen. n. sp. (Tweedt and Janussen, systematic paleontology in Appendix II), specimens of which represent the disarticulated fabrics and incomplete bodies of subconical to cylindrical sponges, with parallel monaxon sets forming body walls. The sponges primarily feature longitudinal spicule rods, with smaller spicule thatch potentially forming bands both longitudinally and around the sponge circumference. Although the majority of *Luthiera alomari* specimens consist of fragmented tissues, specimens with distinct rectangular spicule tracts (e.g. Figure 4.5) imply that these sponges were originally cylindrical or tubular forms ~2-4 cm in diameter, and may have reached lengths of 30+ cm.

Table 4.1. Spicule diameter ranges (in mm) of select Cambrian sponges. (*) indicates longitudinal monaxon-based skeleton.

	Large		Fine		Other	
	Diameter	Type	Diameter	Type	Diameter	Type
Choia striata Xiao et al.[1]	1.0-2.5	coronal oxeas	0.07-0.1	fine monaxons	—	—
Choia utahensis Walcott[1]	0.3-2.0	coronal oxeas	0.1	fine monaxons	—	—
Gabelia sp. Rigby & Murphy[1]	—	—	—	—	0.16	hexacts
**Hyalosinica archaica* Mehl & Reitner[1]	0.1-0.25	coarse monaxons	—	—	0.3-0.5	triaxons
Ischnospongia dendritica Wu et al.[2]	0.1-0.15	'long monaxons'	0.015-0.025	'plume-like'	—	—
Lantianospongia palifera Xiao et al.[1]	0.8-1.5	'basal monacts'	0.15	diacts	0.2-0.25	stauracts
**Leptomitus conicus* Garcia-Bellido et al.[3]	0.015-0.075	oxeas	—	—	—	—
**Leptomitus lineatus* Walcott[3]	0.05-0.1	coarse oxeas	0.02-0.025	fine oxeas	—	—
**Leptomitus teretiusculus* Chen et al.[3]	0.04-0.1	coarse oxeas	0.02-0.05	fine oxeas	—	—
**Leptomitus undulatus* Rigby & Collins[3]	0.06	coarse oxeas	0.015-0.075	fine oxeas		
Protospongia gracilis Xiao et al.[1]	—	—	—	—	0.03-0.05	stauracts
Ptilispongia maotianshanensis Wu et al.[2]	0.13-0.2	'large oxeas'	0.09	'small spicules'	—	—
Sanshadictya microreticulata Mehl & Reitner[4]	0.1-0.2	mon-, diacts	—	—	—	—
Sanshapentella dapingi Mehl & Erdtmann[1]	0.4	'dermal pentacts'	—	—	0.1-0.15	stauracts
Solactiniella plumata Mehl & Reitner[1]	0.1-0.2	diacts	0.05-0.1	'finer diacts'	—	—

Note: spicule measurements from references:

[1]Xiao et al. 2005; [2]Wu et al. 2014

[3]Garcia-Bellido et al. 2007

[4]Steiner et al. 1993

A number of Cambrian sponges have parallel longitudinal spicule arrays (Order Protomonaxonida, Finks and Rigby 2004) similar to those observed in *Luthiera alomari*. Based on cladistic analysis of skeletal structure, Botting et al. (2013) hypothesized that some of these 'protomonaxonids' represent hexactinellid precursors, and ancestrally featured only large longitudinal monaxons. However, longitudinal spicules in protomonaxonids are generally smaller in diameter (Table 4.1), and none display discrete regular spacing at the scale observed here. Interestingly, *Luthiera* spicule arrays resemble longitudinal spicules in the skeletal lattice of the living hexactinellid *Euplectella.* Spicule tracts in *Euplectella* are constructed by bundling and cementation of long monaxons into thick cylindrical struts ~0.2-0.3 mm in diameter and evenly spaced ~1.5-2.0 mm apart (Tabachnick 2002). The presence of rooting tufts combined with a longitudinal monaxon arrangement comparable to stem and crown group Hexactinellida leads us to tentatively consider *Luthiera alomari* a stem group hexactinellid.

Conclusion

These fossils provide the first evidence of spicule-producing sponges in the precambrian, making *Luthiera alomari* the oldest known definitive sponge. Unlike sponge fossils of the early Cambrian, *Luthiera* is preserved as cast impressions in fine sandstones similarly to representatives of the soft-bodied Ediacara biota, implying a robust spiculate framework and suggesting that a microbially-mediated taphonomic window was integral to the preservation of spicule shapes at fine resolution (Gehling et al. 1999). The recognition of biofabric impressions broadens the search image for both spicules and earlist poriferan life.

Luthiera alomari demonstrates the stratigraphic, and possibly ecological, overlap between sponges, Ediacaran soft-bodied enigmatica, and tube-building vermiform organisms at the close of the Neoproterozoic. These sponges reached relatively large size, with incomplete lengths of ~20-30 cm demonstrating that high sponge epifaunal tiering was attained prior to the Cambrian (cf. Yuan et al. 2002; Xiao et al. 2005). Sponges are significant ecosystem engineers, providing substantial ventilation of the water column, coupling pelagic-benthic ecosystem processes, and efficiently removing and packaging dissolved organic material (DOM) through filter feeding (Erwin and Tweedt 2012). The large number of *Luthiera* specimens and their presence on two paleocontinents suggests that by the latest Ediacaran, sponges were ecologically prominent enough to affect ecosystem change. As many of the enigmatic soft-bodied Ediacaran taxa are hypothesized to be osmotrophs reliant upon DOM, ecological co-occurrence of sponges may have significantly impacted osmotrophic Ediacaran communities (Laflamme et al. 2013). Thus, the mixed ecological assemblages of the late Ediacaran included animals not only capable of ecosystem structuring, but likely integral to shaping the oceans for the Cambrian explosion of bilaterian diversity (Lenton et al. 2014).

Acknowledgements

We thank Helke Mocke of the Namibian Geological Survey for her assistance with collections. Charles Hoffmann, Roger Swart and Gabbi Schneider of the Namibian Geological Survey provided logistical help. Marc Laflamme provided critical field resources and support. Lyle Nelson, Lidya Tarhan, Paul Myrow, Erik Sperling, Alex Morgan, Sara Mason, Thomas Boag, and Rachel Racicot contributed field assistance and discussion. Mr. Lothar Gessert provided access to Farm Swartpunt. We gratefully

acknowledge Prof. Carlos Alomar for granting permission to use his surname for our species designation. This work was funded by the NASA Astrobiology Institute Foundations of Complex Life MIT/Harvard research node.

Appendices

Appendix I: Character coding changes to the LP dataset

Characters 1 and 2: “Trunk annuli” and “Tegumental annulations”

These characters were adjusted to reflect the mutual inapplicability of annuli in arthropods with annulations in lobopods and onychophorans. Arthropod annuli reflect divisions of the exoskeleton that do not correspond to sites of muscle attachment as do ‘true segments’ (Boxshall 2004). Onychophoran, and presumably lobopod, annulations are developed in the epidermis and may reflect a fundamentally different form of epidermal specialization / cuticle development.

Characters 5 and 6: “Isolated sclerites/nodes” and “More than two plates or nodes on each trunk segment”

As indicated in the main text, these characters were subsumed as a single multistate character (5) with states [0] absent; [1] present, isolated; and [2] present, more than two per segment.

Character 19: “Distinct head”

This character was removed from the analysis. The presence or absence of a “distinct” head lacks enough specificity to provide useful information, and is repeated in characters that distinguish anterior differentiation. This character is a remnant of previous uncertainty in the location of the anterior region in some lobopods (Ramsköld and Chen 1998). Additionally, it may be argued that every lobopod, based on anterior appendages and / or the location of the mouth, has a ‘distinct head’. There is a possibility that

inflation or change in shape of the anteriormost body region in relation to the trunk may be preservational, and should not comprise a "distinct head" character (Murdock et al. 2014).

Character 204: "Grasping limbs"

The coding of some lobopods as possessing anterior 'grasping limbs' is fundamentally misleading and is adjusted to a [0] state. Although four large taxa have robust frontal appendages, these are annulated and do not possess the joints that would enable grasping in the same fashion as in arthropods. Indeed, Budd (1999) notes that the frontal appendages of *Kerygmachela* do not appear to show any flexibility.

Character 472: "Multi-faceted eyes"

The observation of dark spots in the head region of some lobopods is tenuous at best, and particularly given the relatively rapid loss of eyes during the decay process (Murdock et al. 2014). This character is adjusted to [0] for lobopods, with the exception of *Hallucigenia*, as more recent evidence may indicate potential dorsally-situated eye spots (Smith and Caron, 2015).

Character 473: "Rhabdomeric lateral eyes with new elements formed at a proliferation zone at side of developing eye field"

As noted in the main text, this character indicates compound eyes, but is coded as ambiguous for *Kerygmachela*, which definitively lacks evidence for compound eyes (or

any eyes). This character was re-coded as [0] for lobopods and [?] for those taxa lacking preserved anterior regions.

Character 531: “Proboscis”

The original coding of this character may have reflected a view that this is an organ unique to lobopods. Only *Diania* and *Onychodictyon* are coded as [1], and all arthropods are coded as inapplicable. *Opabinia* was indicated as lacking a proboscis, perhaps because the frontal appendage of this animal is commonly described as being derived from fused frontal appendages. Coding for *Opabinia* was adjusted to [1] to reflect the non-segmented and flexible nature of this appendage. Further character assessment may require that this character apply to arthropods, as pycnogonids possess proboscises.

Character 532: “Radially arranged circumoral structures (papillae, plates, or lamellae)”

This character was updated to reflect the new discovery of pharyngeal teeth in *Hallucigenia* (Smith and Caron 2015). Additionally, the ecdysozoan sister group *Priapulus* was originally coded as [0], even though circumoral / pharyngeal teeth are present in priapulid worms and may also be a plesiomorphic ecdysozoan characteristic. The *Priapulus* coding was adjusted, but the applicability of this character within onychophorans was not changed.

Character 533: “Circumoral structures as a circlet of overlapping plates with teeth on their inner margins”

This character was changed to inapplicable for all taxa lacking a “peytoia”-like mouth apparatus of circumoral plates, as the homology of these characters to other panarthropod mouth apparatuses is unclear.

Character 534: “Oral papillae”

Only onychophorans and lobopods possess rounded epidermal papillae. This character was adjusted to inapplicable for stem euarthropod taxa.

Character 565/6: “Gut caecae” and “Serially repeated midgut glands”

Lobopods and stem euarthropod taxa possessing “serial midgut glands” also were coded as possessing “gut caecae”, but these characters effectively double the signal derived from the presence of these glands. Characters 565 and 566 were combined.

Character 619: “Dorsal bands of blade-like gills”

This character only applies to lateral-lobe stem euarthropod taxa, and was adjusted to be inapplicable in all others.

Appendix II: Systematic paleontology

Systematic Paleontology

Sarah M. Tweedt and Dorte Janussen

Phylum Porifera Grant, 1836

Class Hexactinellida Schmidt, 1870

Order and Family undet.

Genus *Luthiera* gen. nov.

Type species.— *Luthiera alomari* gen. et sp. nov.

Diagnosis.— Elongate, subconical to tubular or cylindrical sponge, presence of osculum unknown. Skeleton composed of monaxon spicules of two to three size orders. Body walls with large, rod-like, parallel longitudinal monaxons 0.1-0.7 mm in diameter and regularly spaced 0.1-2.0 mm apart. Transverse monaxons of similar scale and spacing not observed. Thatch of small, <0.1 mm monaxons forms bands lying transverse and/or parallel to primary longitudinal monaxon rod arrays. Curved bundles of monaxons forming thicker, sub-cylindrical veins probably disarticulated rooting tufts.

Etymology.— From *luthier*, a maker of stringed musical instruments. In reference to the long, parallel arrays of spicule rods resembling strings along an instrument neck. Fossil specimens were also informally referred to as “guitar strings” in the field and throughout the course of study.

Occurrence.— Terminal Ediacaran of Farm Swartpunt, Urusis Fm, southern Namibia and Mt. Dunfee, Nevada, Deep Spring Fm, southwest United States.

Luthiera alomari n. gen., n. sp.

Figures 4.4-4.6

Diagnosis.— As for genus.

Etymology.— Named in honor of guitarist, producer and composer Carlos Alomar.

Description.— Most specimens are of fragmented preservation and show overlapping sponge wall fabrics. Fabrics consist of long, rod-like, sub-cylindrical monaxons in either parallel longitudinal sets or slightly radiating groups. Longitudinal arrays include 2-18+ monaxons regularly spaced 0.1-2.0 mm apart; monaxons may be paired, forming double-parallel sets. Arrays span 3.5-188 mm in length (incomplete) and 0.6-40 mm in width. Primary longitudinal monaxons are 0.1-0.7 mm in diameter. Smallest scale monaxons average 0.075 mm in diameter and occur in isolation or tightly packed as thatched / striated bands parallel, oblique, or transverse to longitudinal arrays. Larger, rectilinear to sub-cylindrical vein-like ridges 0.3-7.5 mm-wide co-occur with monaxon sets. Veins bound parallel arrays or lie obliquely over or under smaller-scale structure, and may show curvature or deformation. Array-bounding veins frequently delineate triangular to rectangular tracts 2-4 cm-wide and up to 28 cm-long. Some veins are striated or terminate in parallel monaxons, indicating that they are constructed of monaxone bundles or comprise stacked spicular tissue.

The discrete rectangular tracts or widest spicule arrays are consistently 20-40 mm-wide and usually bounded by 1-3 mm-wide veins; together these indicate flattened tubular or cylindrical sponge bodies, with veins representing compacted edges. All are incomplete, with no osculum or basal anchoring region preserved, and longest tracts (28

cm) indicate that the sponges may have reached heights exceeding 30 cm. Individual, curved sub-cylindrical veins likely sponge rooting tufts comprising bundled spicules.

Holotype F1460 and paratype F1241 are hyporelief impressions on sandstone-carbonate slab bases. The holotype has eight distinct arrays of 2-7 monaxons 0.17-0.31 mm-wide and spaced 0.55-2.0 mm apart. Arrays reach a maximum incomplete length of 172 mm and presumed incomplete width of 13.6 mm. More than five thicker veins bound or cross arrays, and finer striated texture occurs across most of the fossil surface (Figure 4.6). Sponge fabrics of F1241 are visible through "windows" where the uppermost (lowermost *in situ*) layer of sand has broken away to reveal fossil impressions below. Rectilinear veins with discrete edges in these windows may continue underneath the top sand lamina, becoming obscured by the additional sediment. The most distinct monaxon array (Figure 4.4A) comprises seven spicule rods 0.36 mm-wide and spaced 1.63 mm apart. Crossed veins adjacent to this array are ~0.8 mm-wide, and tightly packed sub-mm spicule thatch lies oblique to the larger structures.

Paratype F1237 features numerous curved sub-cylindrical veins 2.0-7.5 mm-wide, one of which terminates in a monxaon bundle (Figure 4.4D). The specimen has one of the longest longitudinal spicule arrays. The entire array measures 188 mm in length, with 5-6 spicule rods averaging 0.5 mm in diameter, 1.36 mm in spacing, and 8.2 mm in combined width.

Paratypes F1407 (Figure 4.5B) and F1411 (Figure 4.5D) show potential body impressions. A poorly preserved sub-triangular to rectangular impression in F1407 is delimited by indistinct veins. A large parallel monaxon array ~40 mm wide and 12.5 cm long on the same specimen is comprised of more than 12 monaxons averaging 0.2 mm in

diameter and spaced ~1 mm apart. Paratype F1411 preserves the most distinctive vein-bounded monaxon tract. The tract is 37 mm wide and 106 mm long. ~2 mm-wide veins bound more than 18 monaxons averaging 0.5 mm in diameter.

Discussion.— *Luthiera alomari* monaxons superficially resemble the late Ediacaran pseudofossil *Arumberia banksi* (Glaessner and Walter 1975) based on systematic diagnostic criteria, which describes sub-mm ridges separated by 0.5-3.0 mm furrows, as well as the restriction of *Arumberia* to late E-C strata (Bland 1984). *Arumberia* ridges, however, often radiate from curved apices and/or show bifurcations or convergence, and specimens co-occur with tool marks or other indications of an energetic depositional regime (Glaessner and Walter 1975). As *Arumberia* resembles experimentally-produced flute marks with skin-friction ridges, the taxon is considered a pseudofossil created by turbulent flow over microbially-bound sediment (McIlroy and Walter 1997). Flat tracts of *Arumberia* described by Bland (1984) may be distinct, but the specimens described herein are not considered equivalent.

Luthiera alomari is also reminiscent of *Swartpuntia* and *Pteridinium* negative impressions, insofar as these Ediacaran taxa include repeated structural units. When *Swartpuntia* and *Pteridinium* are preserved in negative relief, sutures between tubular elements are expressed as thin subparallel ridges (Narbonne et al. 1997). However, *Swartpuntia* and *Pteridinium* ridges are much larger, the furrows are concave rather than flat, and the ridges gently curve and gradually narrow toward a distinct distal margin (Narbonne et al. 1997). Parallel spicules in the sponge biofabrics do not represent impressions of these Ediacaran taxa.

The Paleozoic demosponge order Protomonaxonida (Finks and Rigby 2004) includes sponges with skeletons constructed of monaxons exclusively and includes numerous Cambrian sponge taxa, such as *Leptomitus* Walcott (García-Bellido et al. 2007; Botting et al. 2013), *Wapkia* Walcott (Botting et al. 2013), and *Hyalosinica* Mehl and Reitner (Steiner et al. 1993; Botting et al. 2013). Botting et al. (2013) viewed this skeleton type as more closely resembling the basal hexactinellid condition, and grouped these and other genera informally as 'protomonaxonid' hexactinellid precursors. Unlike *Luthiera*, however, longitudinal spicules in these Cambrian protomonaxonids achieve maximum diameters of ~0.2 mm, and none display discrete regular spacing at the scale observed here.

Luthiera architecture does resemble the longitudinal spicule components of the skeletal lattice in the living hexactinellid genus *Euplectella* ("Venus' flower basket"). *Euplectella* skeletal rods are constructed by the bundling and cementation of long monaxons into thicker cylindrical struts (Tabachnick 2002; Aizenberg et al. 2005). Fused longitudinal struts achieve larger diameters of 0.2-0.3 mm and are evenly spaced ~1.5-2.0 mm apart (Tabachnick 2002), comparable to *Luthiera* monaxon sizes. Notably, the degree of spicule cementation and fusion increases gradually during the ontogeny of *Euplectella* species, e.g. *E. oweni*, making all but the ontogenetically oldest and most mature body parts of the sponges susceptible to fragmentation (Saito et al. 2002). Ontogenetic change in spicule fusion may therefore provide a reason for frequent fragmentation as well as a mechanism for variation in strut diameter.

The presence of rooting tuft bundles combined with a longitudinal parallel arrangement of long monaxons is comparable to stem and crown group Hexactinellida, so

although the presence of triaxonal hexactine spicules is unknown, these features support a tentative assignment to the stem group of the Hexactinellida.

Material.— Holotype: F1460 (Figure 4.6); paratypes: F1237 (Figure 4.4D), F1241 (Figure 4.4A), F1407 (Figure 4.5B), F1411 (Figure 4.5D); other material: F1238 (Figure 4.4C), F1239, F1243, F1249, F1251, F1253, F1404, F1409, F1410 (Figure 4.4E), F1412, F1422, F1426 (Figure 4.4G), F1437, F1450, F1455, F1456, F1459, F1556 (Figure 4.4F).

Bibliography

Adamska, M., Degnan, S.M., Green, K.M., Adamski, M., Craigie, A., Larroux, C., and Degnan, B.M. (2007) Wnt and TGF-beta expression in the sponge *Amphimedon queenslandica* and the origin of metazoan embryonic patterning. *PLoS ONE* 2: e1031.

Adamska, M., Degnan, B.M., Green, K., and Zwafink, C. (2011) What sponges can tell us about the evolution of developmental processes. *Zoology* 114: 1–10.

Adamska, M., Larroux, C., Adamski, M., Green, K., Lovas, E., Koop, D., Richards, G.S., Zwafink, C., and Degnan, B.M. (2010) Structure and expression of conserved Wnt pathway components in the demosponge *Amphimedon queenslandica*. *Evolution & Development* 12: 494–518.

Aguinaldo, A.M.A., Turbeville, J.M., Linford, L.S., Rivera, M.C., Garey, J.R., Raff, R.A., and Lake, J.A. (1997) Evidence for a clade of nematodes, arthropods and other moulting animals. *Nature* 387:489–493.

Aizenberg, J., Weaver, J.C., Thanawala, M.S., Sundar, V.C., Morse, D.E., Fratzl, P., (2005) Skeleton of *Euplectella sp.*: Structural hierarchy from the nanoscale to the macroscale. *Science* 309: 275–278.

Akam, M. (2000) Arthropods: Developmental diversity within a (super) phylum. *Proceedings of the National Academy of Sciences, USA* 97: 4438–4441.

Allen, J.R.L. (1969) Erosional current marks of weakly cohesive mud beds. *Journal of Sedimentary Petrology* 39: 607–623.

Amthor, J.E., Grotzinger, J.P., Schröder, S., Bowring, S.A., Ramezani, J., Martin, M.W., and Matter, A. (2003) Extinction of *Cloudina* and *Namacalathus* at the Precambrian-Cambrian boundary in Oman. *Geology* 31: 431–434.

Antcliffe, J.B., Callow, R.H.T., and Brasier, M.D. (2014) Giving the early fossil record of sponges a squeeze. *Biological Reviews* 89: 972–1004.

Arendt, D. (2008) The evolution of cell types in animals: emerging principles from molecular studies. *Nature Reviews Genetics* 9: 868–883.

Arendt, D., Nubler-Jung, K. (1994) Inversion of dorso-ventral axis. *Nature* 371: 26.

Arendt, D., Wittbrodt, J. (2001) Reconstructing the eyes of Urbilateria. *Proceedings of the Royal Society London, Series B* 356: 1545–1563.

Arthur, W., Jowett, T., and Panchen, A. (1999) Segments, limbs, homology, and co-option. *Evolution & Development* 1: 74–76.

Backfisch, B., Rajan, V.B.V., Fischer, R.M., Lohs, C., Arboleda, E., Tessmar-Raible, K., and Raible, F. (2013) Stable transgenesis in the marine annelid *Platynereis dumerilii* sheds new light on photoreceptor evolution. *Proceedings of the National Academy of Sciences, USA* 110: 193–198.

Baele, G., Lemey, P., Bedford, T., Rambaut, A., Suchard, M.A., and Alekseyenko, A.V. (2012) Improving the accuracy of demographic and molecular clock model comparison while accommodating phylogenetic uncertainty. *Molecular Biology and Evolution* 29: 2157–2167.

Baguñà, J., Ruiz-Trillo, I., Paps, J., Loukota, M., Ribera, C., Jondelius, U., and Riutort, M. (2001) The first bilaterian organisms: simple or complex? New molecular evidence. *International Journal of Developmental Biology* 45: S133–S134.

Baguñà, J., Martinez, P., Paps, J., and Riutort, M. (2008) Back in time: A new systematic proposal for the Bilateria. *Philosophical Transactions of the Royal Society of London, B Biological Sciences* 363: 1481–1491.

Bengtson, S. (1991) Oddballs from the Cambrian start to get even. *Nature* 351: 184.

Benton, M.J., Donoghue, P.C.J., and Asher, R.J. (2009) Calibrating and constraining molecular clocks. *In:* Hedges, S.B., and Kumar, S. (eds.) *The Timetree of Life.* Oxford University Press: Oxford, UK.

Bergsten, J., Nilsson, A.N., and Ronquist, F. (2013) Bayesian tests of topology hypotheses with an example from diving beetles. *Systematic Biology* 62: 660–673.

Bergström, J., and Hou, X.-G. (2001) Cambrian Onychophora or Xenusians. *Zoologischer Anzeiger* 240: 237–245.

Bland, B.H. (1984) *Arumberia* Glaessner & Walter, A review of its potential for correlation in the region of the Precambrian-Cambrian boundary. *Geological Magazine* 121: 625–633.

Botting, J.P., Muir, L.A., Xiao, S., Li, X., and Lin, J.-P. (2012) Evidence for spicule homology in calcareous and siliceous sponges: biminerallic spicules in *Lenica* sp. from the Early Cambrian of South China. *Lethaia* 45: 463–475.

Botting, J.P., Muir, L.A., and Lin, J.-P. (2013) Relationships of the Cambrian Protomonaxonida (Porifera). *Palaeontological Electronica* 16: 23.

Bowring, S.A., Grotzinger, J.P., Condon, D.J., Ramezani, J., Newall, M.J., and Allen, P.A. (2007) Geochronologic constraints on the chronostratigraphic framework of the Neoproterozoic Huqf Supergroup, Sultanate of Oman. *American Journal of Science* 307: 1097–1145.

Boxshall, G.A. (2004) The evolution of arthropod limbs. *Biological Reviews* 79: 253-300.

Brasier, M.D., Green, O.R., and Shields, G. (1997) Ediacaran sponge spicule clusters from south-western Mongolia and the origins of the Cambrian fauna. *Geology* 25: 303–306.

Britten, R.J., and Davidson, E.H. (1969) Gene regulation for higher cells: A theory. *Science* 165: 349–357.

Britten, R.J. and Davidson, E.H. (1971) Repetitive and non-repetitive DNA sequences and a speculation on the origins of evolutionary novelty. *The Quarterly Review of Biology* 46: 111–138.

Broun, M., Gee, L., Reinhardt, B., and Bode, H.R. (2005) Formation of the head organizer in hydra involves the canonical Wnt pathway. *Development* 132: 2907–2916.

Buatois, L.A. and Mángano, M.G. (2016) Ediacaran ecosystems and the dawn of animals. *In:* Mángano, M.G. and Buatois, L.A. (eds.) *The Trace-Fossil Record of Major Evolutionary Events*, *Volume 1: Precambrian and Paleozoic.* Springer: Netherlands.

Budd, G.E. (1993) A Cambrian gilled lobopod from Greenland. *Nature* 364: 709–711.

Budd, G.E. (1996) The morphology of *Opabina regalis* and the reconstruction of the arthropod stem-group. *Lethaia* 29: 1–14.

Budd, G.E. (1997) Stem group arthropods from the Lower Cambrian Sirius Passet fauna of North Greenland. *In:* Forty, R.A., and Thomas, R.H. (eds.) *Arthropod relationships*. Chapman and Hall: London, p. 125–138.

Budd, G.E. (1999) The morphology and phylogenetic significance of *Kerygmachela kierkegaardi* Budd. *Transactions of Royal Society Edinburgh, Earth Science* 89: 249–290.

Budd, G.E. (2002) A palaeontological solution to the arthropod head problem. *Nature* 417: 271–275.

Budd, G.E., and Daley, A.C. (2012) The lobes and lobopods of *Opabinia regalis* from the middle Cambrian Burgess Shale. *Lethaia* 45: 83–95.

Budd, G.E. and Jensen, S. (2015) The origin of the animals and a 'Savannah' hypothesis for early bilaterian evolution. *Biological Reviews.* doi:10.1111/brv.12239.

Burkhardt, P., Stegmann, C.M., Cooper, B., Kloepper, T.H., Imig, C., Varoqueaux, F., Wahl, M.C., and Fasshauer, D. (2011) Primordial neurosecretory apparatus identified in the choanoflagellate *Monosiga brevicollis*. *Proceedings of the National Academy of Sciences, USA* 108: 15264–15269.

Callaerts, P., Halder, G., and Gehring, W.J. (1997) Pax-6 in development and evolution. *Annual Review Neuroscience* 20: 483–532.

Campbell, L.I., Rota-Stabelli, O., Edgecombe, G.D., Marchioro, T., Longhorn, S.J., Telford, M.J., Philippe, H., Rebecchi, L., Peterson, K.J., and Pisani, D. (2011) MicroRNAs and phylogenomics resolve the relationships of Tardigrada and suggest that velvet worms are the sister group of Arthropoda. *Proceedings of the National Academy of Sciences, USA* 108: 15920–15924.

Cañestro, C., Bassham, S., and Postlethwait, J. (2005) Development of the central nervous system in the larvacean *Oikopleura dioica* and the evolution of the chordate brain. *Developmental Biology* 285: 298–315.

Carroll, S.B., Grenier, J.K., and Weatherbee, S.D. (2001) From DNA to Diversity. Blackwell Science: Malden, MA.

Carroll, S.B. (2008) Evo-devo and an expanding evolutionary synthesis: A genetic theory of morphological evolution. *Cell* 134: 25–36.

Chapman, J.A., Kirkness, E.F., Simakov, O., Hampson, S.E., Mitros, T., Weinmaier, T., Rattei, T., Balasubramanian, P.G., Borman, J., Busam, D., Disbennett, K., Pfannkock, C., Sumin, N., Sutton, G.G., Devi Viswanathan, L., Walenz, B., Goodstein, D.M., Hellsten, U., Kawashima, T., Prochnik, S.E., Putnam, N.H., Shu, S., Blumberg, B., Dana, C.E., Gee, L., Kibler, D.F., Law, L., Lindgens, D., Martinez, D.E., Peng, J., Wigge, P.A., Bertulat, B., Guder, C., Nakamura, Y., Ozbek, S., Watanabe, H., Khalturin, K., Hemmrich, G., Franke, A., Augustin, R., Fraune, S., Hayakawa, E., Hayakawa, S., Hirose, M., Hwang, J. S., Ikeo, K., Nishimiya-Fujisawa, C., Ogura, A., Takahashi, T., Steinmetz, P.R.H., Zhang, X., Aufschnaiter, R., Eder, M.-F., Gorny, A.-K., Salvenmoser, W., Heimberg, A.M., Wheeler, B.M., Peterson, K.J., Böttger, A., Tishler, P., Wolf, A., Gojobori, T., Remington, K.A., Strausberg, R.L., Venter, J.C., Technau, U., Hobmayer, B., Bosch, T.C.G., Holstein, T.W., Fujisawa, T., Bode, H.R., David, C.N., Rokhsar, D.S., and Steele, R.E. (2010) The dynamic genome of Hydra. *Nature* 464: 592–597.

Chiori, R., Jager, M., Denker, E., Wincker, P., Da Silva, C., Le Guyader, H., Manuel, M., and Quéinnec, E. (2009) Are Hox genes ancestrally involved in axial patterning? Evidence from the Hydrozoan *Clytia hemisphaerica* (Cnidaria). *PLoS ONE* 4: e4231.

Chipman, A. (2010) Parallel evolution of segmentation by co-option of ancestral gene regulatory networks. *BioEssays* 32: 60–70.

Clarke, J.A. and Middleton, K.M. (2008) Mosaicism, modules, and the evolution of birds: Results from a Bayesian approach to the study of morphological evolution using discrete character data. *Systematic Biology* 57: 185–201.

Conway Morris, S. (1986) The community structure of the Middle Cambrian phyllopod bed (Burgess Shale). *Palaeontology* 29: 423–467.

Corsetti, F.A., and Hagadorn, J.W. (2003) The Precambrian-Cambrian transition in the southern Great Basin, USA. *The Sedimentary Record* 1: 4–8.

Cummings, M.P., Handley, S.A., Myers, D.S., Reed, D.L., Rokas, A., and Winka, K. (2003) Comparing bootstrap and posterior probability values in the four-taxon case. *Systematic Biology* 52: 477–487.

Darroch, S.A.F., Sperling, E.A., Boag, T.H., Racicot, R.A., Mason, S.J., Morgan, A.S., Tweedt, S., Myrow, P., Johnston, D.T., Erwin, D.H., and Laflamme, M. (2015) Biotic replacement and mass extinction of the Ediacara biota. *Proceedings of the Royal Society B: Biological Sciences* 282: 1–10.

Davidson, E.H. and Erwin, D.H. (2010) An integrated view of Precambrian eumetazoan evolution. *Cold Spring Harbor Symposium on Quantitative Biology* 79: 65–80.

Delle Cave, L. and Simonetta, A.M. (1975) Notes on the morphology and taxonomic position of *Aysheaia* (Onychophora?) and of *Skania* (undetermined phylum). *Monitore Zoologico Italiano* (N.S.) 9: 67–81.

De Robertis, E.M. (2008) Evo-Devo: Variations on ancestral patterning in bilateria. *Nature* 380: 37–40.

De Robertis, E.M., and Kuroda, H. (2004) Dorsal-ventral patterning and neural induction in *Xenopus* embryos. *Annual Review of Cell and Developmental Biology* 20: 285–308.

De Robertis, E.M., and Sasai, Y. (1996) A common plan for dorsoventral patterning in bilateria. *Nature* 380: 37–40.

dos Reis, M., Thawornwattana, Y., Angelis, K., Telford, M.J., Donoghue, P.C.J., and Yang, Z. (2015) Uncertainty in the timing of origin of animals and the limits of precision in molecular timescales. *Current Biology* 25: 2939–2950.

Dray, N., Tessmar-Raible, K., Le Gouar, M., Vibert, L., Christodoulou, F., Schipany, K., Guillou, A., Zantke, J., Snyman, H., and Béhague, J. (2010) Hedgehog signaling regulates segment formation in the annelid *Platynereis*. *Science* 329: 339–342.

Duboule, D., and Dollé, P. (1989) The structural and functional organization of the murine HOX gene family resembles that of *Drosophila* homeotic genes. *Journal of the European Molecular Biology Organization* 8: 1497–1505.

Dunn, C.W., Hejnol, A., Matus, D.Q., Pang, K., Browne, W.E., Smith, S.A., Seaver, E., Rouse, G.W., Obst, M., Edgecombe, G.D., Sørensen, M.V., Haddock, S.H.D., Schmidt-Rhaesa, A., Okusu, A., Møbjerg Kristensen, R., Wheeler, W.C., Martindale, M.Q., and Giribet, G. (2008) Broad phylogenomic sampling improves resolution of the animal tree of life. *Nature* 425: 745–749.

Dzik, J., and Krumbiegel, G. (1989) The oldest 'onychophoran' Xenusion: a link connecting phyla? *Lethaia* 22: 169–181.

Edgecombe, G.D. (2009) Palaeontological and molecular evidence linking arthropods, onychophorans, and other Ecdysozoa. *Evolution: Education and Outreach* 2: 178–190.

Edgecombe, G.D. (2010) Arthropod phylogeny: An overview from the perspective of morphology, molecular data and the fossil record. *Arthropod Structure & Development* 39: 74–87.

Edgecombe, G.D., Giribet, G., Dunn, C.W., Hejnol, A., Kristensen, R.M., Neves, R.C., Rouse, G.W., Worsaae, K., and Sørensen, M.V. (2011) Higher-level metazoan relationships: recent progress and remaining questions. *Organisms, Diversity & Evolution* 11: 151–172.

Eriksson, J., Tait, N.N., Budd, G.E., and Akam, M. (2009) The involvement of *engrailed* and *wingless* during segmentation in the onychophoran *Euperipatoides kanangrensis* (Peripatopsidae: Onychophora) (Reid 1996). *Development, Genes and Evolution* 219: 249–264.

Eriksson, J., Tait, N.N., Budd, G.E., Janussen, R., and Akam, M. (2010) Head patterning and Hox gene expression in an onychophoran and its implications for the arthropod head problem. *Development, Genes and Evolution* 220: 117–122.

Erwin, D.H. (2007) Disparity: morphological pattern and developmental context. *Palaeontology* 50: 57–73.

Erwin, D.H. (2008) Macroevolution of ecosystem engineering, niche construction, and diversity. *Trends in Ecology and Evolution* 23: 304–310.

Erwin, D.H. (2009) Early origin of the bilaterian developmental toolkit. *Philosophical Transactions of the Royal Society of London B: Biological Sciences* 364: 2253–2261.

Erwin, D.H. and Davidson, E.H. (2002) The last common bilaterian ancestor. *Development* 129: 3021–3032.

Erwin, D.H., and Davidson, E.H. (2006) Gene regulatory networks and the evolution of animal body plans. *Science* 311: 796–800.

Erwin, D.H. and Davidson, E.H. (2009) The evolution of hierarchical gene regulatory networks. *Nature Reviews Genetics* 10: 141–148.

Erwin, D.H., Laflamme, M., Tweedt, S.M., Sperling, E.A., Pisani, D., and Peterson, K.J. (2011) The Cambrian conundrum: Early divergence and later ecological success in the early history of animals. *Science* 334: 1091–1097.

Erwin, D.H., and Tweedt, S.M. (2012) Ecological drivers of the Ediacaran-Cambrian diversification of Metazoa. *Evolutionary Ecology* 26: 417–433.

Erwin, D.H. and Valentine, J.W. (2013) *The Cambrian Explosion: The Construction of Animal Biodiversity.* Roberts & Co.: Greenwood, CO.

Fahey, B., and Degnan, B.M. (2010) Origin of animal epithelia: Insights from the sponge genome. *Evolution & Development* 12: 601–617.

Fahey, B., Larroux, C., Woodcroft, B.J., and Degnan, B.M. (2008) Does the high gene density in the sponge NK homeobox gene cluster reflect limited regulatory capacity? *Biology Bulletin* 214: 205–217.

Fairclough, S.R., Chen, Z., Kramer, E., Zeng, Q., Young, S., Robertson, H.M., Begovic, E., Richter, D.J., Russ, C., Westbrook, M.J., Manning, G., Lang, B.F., Haas, B., Nusbaum, C., and King, N. (2013) Premetazoan genome evolution and the regulation of cell differentiation in the choanoflagellate *Salpingoeca rosetta*. *Genome Biology* 14: R15.

Fan Y., Wu, R., Chen, M.H., Kuo L., and Lewis P.O. (2011) Choosing among partition models in Bayesian phylogenetics. *Molecular Biology and Evolution* 28: 523–532.

Finks, R.M., and Rigby, J.K. (2004) Palaeozoic Demosponges, *In:* Finks, R.M., Reid, R.E.H., Rigby, J.K. (eds.) *Treatise on Invertebrate Paleontology, Part E, Porifera, Revised, Volume 3*: Boulder, CO, Lawrence, KS, Geological Society of America, University of Kansas Press, p. 9–171.

Finnerty, J.R., Pang, K., Burton, P., Paulson, D., and Martindale, M.Q. (2004) Origins of bilateral symmetry: *Hox* and *Dpp* expression in a sea anemone. *Science* 304: 1335–1337.

Forêt, S., Knack, B., Houliston, E., Momose, T., Manuel, M., Quéinnec, E., Hayward, D.C., Ball, E., and Miller, D.J. (2010) New tricks with old genes: the genetic basis of novel cnidarian traits. *Trends in Genetics* 26: 154–158.

Fortunato, S., Adamski, M., Bergum, B., Guder, C., Jordal, S., Leininger, S., Zwafink, C., Rapp, H.T., and Adamska, M. (2012) Genome-wide analysis of the sox family in the calcareous sponge *Sycon ciliatum*: Multiple genes with unique expression patterns. *EvoDevo* 3: 14.

Fritz, A.E., Ikmi, A., Seidel, C., Paulson, A., and Gibson, M.C. (2013) Mechanisms of tentacle morphogenesis in the sea anemone *Nematostella vectensis*. *Development* 140: 2212–2223.

Foote, M. 1990. Nearest-neighbor analysis of trilobite morphospace. *Systematic Zoology* 39: 371–382.

Foote, M. F. 1992. Paleozoic record of morphological diversity in blastozoan echinoderms. *Proceedings of the National Academy of Sciences, USA* 89: 7325–7329.

García-Bellido, D.C., Gozalo, R., Chirivella Martorell, J.B., and Liñán, E. (2007) The demosponge genus *Leptomitus* and a new species from the Middle Cambrian of Spain. *Palaeontology* 50: 467–478.

Garey, J.R., Krotec, M., Nelson, D.R., and Brooks, J. (1996) Molecular analysis supports a tardigrade-arthropod association. *Invertebrate Biology* 115: 79–88.

Gehling, J.G., and Rigby, J.K. (1996) Long expected sponges from the Neoproterozoic Ediacara Fauna of South Australia. *Journal of Paleontology* 70: 185–195.

Gehling, J.G. (1999) Microbial mats in terminal Proterozoic siliciclastics: Ediacaran death masks. *PALAIOS* 14: 40–57.

Gerber, S. (2014) Not all roads can be taken: development induces anisotropic accessibility in morphospace. *Evolution & Development* 16: 373–381.

Giribet, G., Edgecombe, G.D., and Wheeler, W.C. (2001) Arthropod phylogeny based on eight molecular loci and morphology. *Nature* 413: 157–161.

Glaessner, M.F. and Walter, M.R. (1975) New Precambrian fossils from the Arumberia Sandstone, Northern Territory, Australia. *Alcheringa* 1: 59–69.

Gould, S.J. (1977) *Ontogeny and Phylogeny*. Harvard University Press: Cambridge, MA.

Gould, S.J. (1991) The disparity of the Burgess Shale arthropod fauna and the limits of cladistic analysis: why we must strive to quantify morphospace. *Paleobiology* 17: 411–423.

Grotzinger, J.P., Bowring, S.A., Saylor, B.Z., and Kaufman, A.J. (1995) Biostratigraphic and geochronologic constraints on early animal evolution. *Science* 270: 598–604.

Halder, G., Callaerts, P., and Gehring, W.J. (1995) Induction of ectopic eyes by targeted expression of the *eyeless* gene in *Drosophila*. *Science* 267: 1788.

Hall, B.K. (2002) Palaeontology and evolutionary developmental biology: A science of the nineteenth and twenty-first centuries. *Palaeontology* 45: 647–669.

Harcet, M., Roller, M., Cetkovic, H., Peina, D., Wiens, M., Muller, W.E., and Vlahovicek, K. (2010) Demosponge EST sequencing reveals a complex genetic toolkit of the simplest metazoans. *Molecular Biology and Evolution* 27: 2747–2756.

Harrison, L.B., and Larsson, H.C. (2015) Among-character rate variation distributions in phylogenetic analysis of discrete morphological characters. *Systematic Biology* 64: 307–324.

Haug, J.T., Waloszek, D., Maas, A., Liu, Y., and Haug, C. (2012) Functional morphology, ontogeny and evolution of mantis shrimp-like predators in the Cambrian. *Palaeontology* 55: 369–399.

Hejnol, A., and Martindale, M.Q. (2009) Coordinated spatial and temporal expression of *Hox* genes during embryogenesis in the acoel *Convolutriloba longifissura*. *BMC Biology* 7: 65.

Holder, M.T., Sukumaran, J., and Lewis, P.O. (2008) A justification for reporting the majority-rule consensus tree in Bayesian phylogenetics. *Systematic Biology* 57: 814–821.

Holland, P.W.H. (2013) Evolution of homeobox genes. *WIREs Dev Biol* 2: 31–45.

Hou, X.-G., and Bergström, J. (1991) The arthropods of the Lower Cambrian Chengjiang fauna, with relationships and evolutionary significance. *In:* Simonetta, A.M., Conway Morris, S. (eds.) *The Early Evolution of Metazoa and the Significance of Problematic Taxa*. Cambridge University Press: Cambridge, UK.

Hughes, N.C. (1991) Morphological plasticity and genetic flexibility in a Cambrian trilobite. *Geology* 19: 913–916.

Hughes, N.C., Chapman, R.E., and Adrain, J.M. (1999) The stability of thoracic segmentation in trilobites: a case study in developmental and ecological constraints. *Evolution & Developmen* 1: 24–35.

Hui, J.H.L., Raible, F., Korchagina, N., Dray, N., Samain, S., Magdelenat, G., Jubin, C., Segurens, B., Balavoine, G., Arendt, D., and Ferrier, D.E.K. (2009) Features of the ancestral bilaterian inferred from *Platynereis dumerilii* ParaHox genes. *BMC Biology* 7: 43.

Hutchinson, G.E. (1930) Restudy of some Burgess Shale fossils. *U.S. National Museum Proceedings* 78: 1–24.

Hutchinson, G.E. (1969) *Aysheaia* and the general morphology of the Onychophora. *American Journal of Science* 267: 1062–1066.

Ikuta, T. (2011) Evolution of invertebrate deuterostomes and Hox/ParaHox genes. *Genomics Proteomics Bioinformatics* 9: 77–96.

Ingham, P., Nakano, Y., and Seger, C. (2011) Mechanisms and functions of Hedgehog signaling across the metazoa. *Nature Reviews Genetics* 12: 393–406.

Jablonski, D., and Bottjer, D.J. (1990) The origin and diversification of major groups: environmental patterns and macroevolutionary lags. *In:* Taylor, P.D., Larwood, G.P. (eds.) *Major Evolutionary Radiations*. Systematics Association Special Volume 42. Clarendon Press: Oxford, pp. 17–57.

Jacob, F. and Monod, J. (1961) Gene regulatory mechanisms in the synthesis of proteins. *Journal of Molecular Biology* 3: 318–356.

Jakob, W., Sagasser, S., Dellaporta, S., Holland, P., Kuhn, K., and Schierwater, B. (2004) The *Trox-2* Hox/ParaHox gene of *Trichoplax* (Placozoa) marks an epithelial boundary. *Development Genes and Evolution* 214: 170–175.

Jenner, R.A. (2002) Boolean logic and character state identity: pitfalls of character coding in metazoan cladistics. *Contributions to Zoology* 71: 67–91.

Jensen, S., and Runnegar, B.N. (2005) A complex trace fossil from the Spitskopf Member (terminal Ediacaran-? Lower Cambrian) of Southern Namibia. *Geological Magazine* 142: 561–569.

Kass R.E., and Raftery A.E. (1995) Bayes factors. *Journal of the American Statistical Association* 90: 773–795.

King, N., Westbrook, M.J., Young, S.L., Kuo, A., Abedin, M., Chapman, J., Fairclough, S., Hellsten, U., Isogai, Y., Letunic, I., Marr, M., Pincus, D., Putnam, N., Rokas, A., Wright, K.J., Zuzow, R., Dirks, W., Good, M., Goodstein, D., Lemons, D., Li, W., Lyons, J.B., Morris, A., Nichols, S., Richter, D.J., Salamov, A., JGI Sequencing, Bork, P., Lim, W.A., Manning, G., Miller, W.T., McGinnis, W., Shapiro, H., Tjian, R., Grigoriev, I.V., and Rokhsar, D. (2008) The genome of the choanoflagellate *Monosiga brevicollis* and the origin of metazoans. *Nature* 451: 783–788.

Knoll, A.H. (2011) The multiple origins of complex multicellularity. *Annual Reivew of Earth and Planetary Science* 39: 217–239.

Knoll, A.H., Carroll, S.B. (1999) Early animal evolution: Emerging views from comparative biology and geology. *Science* 284: 2129–2137.

Kraus, Y., Fritzenwanker, J.H. Genikhovich, G., and Technau, U. (2007) The blastoporal organiser of a sea anemone. *Current Biology* 17: R874–876.

Kuo, D.-H., and Weisblat, D.A. (2011) A new molecular logic for BMP-mediated dorsoventral patterning in the leech *Helobdella*. *Current Biology* 21: 1281–1288.

Laflamme, M; Darroch, S.A.F., Tweedt, S.M., Peterson, K.J., and Erwin, D.H. (2013) The end of the Ediacara biota: Extinction, biotic replacement, or Cheshire Cat?: *Gondwana Research* 23: 558–573.

Larroux, C., Luke, G.N., Koopman, P., Rohksar, D., Shimeld, S.M., and Degnan, B.M. (2008) Genesis and expansion of metazoan transcription factor gene classes. *Molecular Biology and Evolution* 25: 980–996.

Lee, P.N., Kumburegama, S., Marlow, H.Q., Martindale, M.Q., and Wikramanayake, A.H. (2007) Asymmetric developmental potential along the animal-vegetal axis in the anthozoan cnidarian, *Nematostella vectensis*, is mediated by Dishevelled. *Developmental Biology* 310: 169–186.

Legg, D.A., Ma, X., Wolfe, J.M., Ortega-Hernández, J., Edgecombe, G.D., and Sutton, M.D. (2011) Lobopodian phylogeny reanalysed. *Nature* 476: E2.

Legg, D.A., Sutton, M.D., and Edgecombe, G.D. (2013) Arthropod fossil data increase congruence of morphological and molecular phylogenies. *Nature Communications* 4: 2485.

Lenton, T.M., Boyle, R.A., Poulton S.W., Shields-Zhou, G.A., and Butterfield, N.J. (2014) Co-evolution of eukaryotes and ocean oxygenation in the Neoproterozoic era. *Nature Geoscience* 7: 257–265.

Lewis, E.B. (1978) A gene complex controlling segmentation in *Drosophila*. *Nature* 276: 565–570.

Lewis, P.O. (2001) A likelihood approach to estimating phylogeny from morphological character data. *Systematic Biology* 50: 913–925.

Leys, S.P., Cronin, T.W., Degnan, B.M., and Marshall, J.N. (2002) Spectral sensitivity in a sponge larva. *Journal of Comparative Physiology A* 188: 199–202.

Leys, S.P., and Riesgo, A. (2012) Epithelia, an evolutionary novelty of metazoans. *Journal of Experimental Zoology Part B: Molecular and Developmental Evolution* 318: 438–447.

Liu, J., and Dunlop, J.A. (2014) Cambrian lobopodians: A review of recent progress in our understanding of their morphology and evolution. *Palaeogeography, Palaeoclimatology, Palaeoecology* 398: 4–15.

Liu, J., Shu, D., Han, J., Zhang, Z., and Zhang, X.-G. (2006) A large xenusiid lobopod with complex appendages from the Lower Cambrian Chengjiang Lagerstätte. *Acta Palaeontologica Polonica* 51: 215–222.

Liu, J., Shu, D., Han, J. Zhang, Z., and Zhang, X.-G. (2008) Origin, diversification, and relationships of Cambrian lobopods. *Gondwana Research* 14: 277–283.

Liu, J., Steiner, M., Dunlop, J.A., Keupp, H., Shu, D., Ou, Q., Han, J., Zhang, Z., and Zhang, X.-G. (2011) An armoured Cambrian lobopodian from China with arthropod-like appendages. *Nature* 470: 526–530.

Love, G.D., Grosjean, E., Stalvies, C., Fike, D.A., Grotzinger, J.P., Bradley, A.S., Kelly, A.E., Bhatia, M., Meredith, W., Snape, C.E., Bowring, S.A., Condon, D.J., and Summons, R.E. (2009) Fossil steroids record the appearance of Demospongia during the Cryogenian period. Nature 457:718–721.

Lowe, C.J., Terasaki, M., Wu, M., Freeman Jr., R.M., Runft, L., Kwan, K., Haijo, S., Aronowicz, J., Lander, E. Gruber, C., Smith, M., Kirschner, M., and Gerhart, J. (2006) Dorsoventral patterning in hemichordates: Insights into early chordate evolution. *PLoS Biology* 4: e291.

Ma, X., Edgecombe, G.D., Legg, D.A., Hou, X.-G. (2014) The morphology and phylogenetic position of the Cambrian lobopod *Diania cactiformis*. *Journal of Systematic Paleontology* 12: 445–457.

Ma, X., Hou, X., Edgecombe, G.D., Strausfeld, N.J. (2012) Complex brain and optic lobes in an early Cambrian arthropod. *Nature* 490:258–263.

Magie, C.R., Pang, K., Martindale, M.Q. (2005) Genomic inventory and expression of *Sox* and *Fox* genes in the cnidarian *Nematostella vectensis*. *Development Genes and Evolution* 215: 618–630.

Mallatt, J.M., Garey, J.R., and Shultz, J.W. (2004) Ecdysozoan phylogeny and Bayesian inference: first use of nearly complete 28S and 18S rRNA gene sequences to classify the arthropods and their kin. *Molecular Phylogenetics and Evolution* 31: 178–191.

Mallatt, J.M., and Giribet, G. (2006) Further use of nearly complete 28S and 18S rRNA genes to classify Ecdysozoa: 37 more arthropods and a kinorhynch. *Molecular Phylogenetics and Evolution* 40: 772–794.

Maloof, A.C., Rose, C.V., Calmet, C.C., Beach, R., Samuels, B.M., Erwin, D.H., Poirier, G.R., Yao, N., and Simons, F.J. (2010) Probable animal body-fossils from pre Marinoan limestones, South Australia. *Nature Geosciences* 3: 653–659.

Martin, C., and Mayer, G. (2014) Neuronal tracing of oral nerves in a velvet worm-implications for the evolution of the ecdysozoan brain. *Frontiers in Neuroanatomy* 8: 7.

Martinelli, C., and Spring, J. (2008) Distinct expression patterns of the two T-box homologues *Brachyury* and *Tbx2/3* in the placozoan *Trichoplax adhaerens*. *Development Genes and Evolution* 213: 492–499.

Maxwell, E.K., Ryan, J.F., Schnitzler, C.E., Browne, W.E., and Baxevanis, A.D. (2012) MicroRNAs and essential components of the microRNA processing machinery are not encoded in the genome of the ctenophore *Mnemiopsis leidyi*. *BMC Genomics* 13: 714.

Mayr, E. (1960) The emergence of novelty. *In:* Tax, S. (ed.) *The Evolution of Life*. University of Chicago Press, Chicago, pp. 349-380.

McIlroy, D. and Walter, M.R. (1997) A reconsideration of the biogenicity of *Arumberia banksi* Glaessner & Walter. *Alcheringa* 21: 79–80.

Mehl-Janussen, D. (1999) Die frühe Evolution der Porifera. *Münchner Geowissenschaftliche Abhandlungen Reihe A* 37: 1-72.

Miller, D.J., and Ball, E.E. (2009) The gene complement of the ancestral bilaterian – was Urbilateria a monster? *Journal of Biology* 8: 89.

Miller, M.A., Pfeiffer, W., and Schwartz, T. (2010) Creating the CIPRES Science Gateway for inference of large phylogenetic trees. *In:* Proceedings of the Gateway Computing Environments Workshop (GCE), 14 Nov. 2010, New Orleans, LA.

Momose, T., and Houliston, E. (2007) Two oppositely localized frizzled RNAs as axis determinants in a cnidarian embryo. *PLoS Biology* 5: e70.

Momose, T., Derelle, R., and Houliston, E. (2008) A maternally localized Wnt ligand required for axial patterning in the cnidarian *Clytia hemisphaerica*. *Development* 135: 2105–2113.

Momose, T., Kraus, Y., and Houliston, E. (2012) A conserved function for Strabismus in establishing planar cell polarity in the ciliated ectoderm during cnidarian larval development. *Development* 139: 4375–4382.

Mounce, R.C.P., and Wills, M.A. (2011) Phylogenetic position of *Diania* challenged. *Nature* 476: E1.

Murdock, D.J.E., Gabbott, S.E., Mayer, G. and Purnell, M.A. (2014) Decay of velvet worms (Onychophora), and bias in the fossil record of lobopodians. *BMC Evolutionary Biology* 14: 222.

Narbonne, G.M., Saylor, B.Z., and Grotzinger, J.P. (1997) The youngest Ediacaran fossils from Southern Africa. *Journal of Paleontology* 71: 953–967.

Narbonne, G.M. (2005) The Ediacara Biota: Neoproterozoic origin of animals and their Ecosystems. *Annual Review of Earth and Planetary Sciences* 33: 421–442.

Nichols, S.A., Dirks, W., Pearse, J.S., and King, N. (2006) Early evolution of animal cell signaling and adhesion genes. *Proceedings of the National Academy of Sciences, USA* 103: 12451–12456.

Nichols, S.A., Roberts, B.W., Richter, D.J., Fairclough, S.R., and King, N. (2012) Origin of metazoan cadherin diversity and the antiquity of the classical cadherin/beta catenin complex. *Proceedings of the National Academy of Sciences, USA* 109: 13046–13051.

Nielsen, C. (1995) *Animal Evolution: Interrelationships of the Living Phyla*. Oxford University Press: Oxford, England.

Nosenko, T., Schreiber, F., Adamska, M., Adamski, M., Eitel, M., Hammel, J., Maldonado, M., Muller, W.E.G., Nickel, M., Schierwater, B., Vacelet, J., Wiens, M., and Wörheide, G. (2013) Deep metazoan phylogeny: When different genes tell different stories. *Molecular Phylogenetics and Evolution* 67: 223–233.

Nylander, J.A.A., Ronquist, R., Huelsenbeck, J.P., and Nieves-Aldrey, J.L. (2004) Bayesian phylogenetic analysis of combined data. *Systematic Biology* 53: 47–67.

Panganiban, G., et al. (1997) The origin and evolution of animal appendages. *Proceedings of the National Academy of Sciences, USA* 94: 5162–5166.

Pani, A.M., Mullarkey, E.E., Aronowicz, J., Assimacopoulos, S., Grove, E.A., and Lowe, C.J. (2012) Ancient deuterostome origins of vertebrate brain signaling centres. *Nature* 483: 289–296.

Pang, K., Ryan, J.F., Baxevanis, A.D., and Martindale, M.Q. (2011) Evolution of the TGF-beta signaling pathway and its potential role in the ctenophore, *Mnemiopsis leidyi*. *PLoS ONE* 6: e24152.

Paradis E., Claude J., and Strimmer K. (2004) APE: analyses of phylogenetics and evolution in R language. *Bioinformatics* 20: 289–290.

Parfrey, L.M. and Lahr, D.J.G. (2013) Multicellularity arose several times in the evolution of eukaryotes. *BioEssays* 35: 339–347.

Petersen, C.P., and Reddien, P.W. (2009) Wnt signaling and the polarity of the primary body axis. *Cell* 139: 1056–1068.

Peterson, K.J. and Eernisse, D.J. (2001) Animal phylogeny and the ancestry of bilaterians: inferences from morphology and 18S rDNA gene sequences. *Evolution & Development* 3: 170–205.

Philippe, H., Lartillot, N., and Brinkmann, H. (2005) Multigene analyses of bilaterian animals corroborate the monophyly of Ecdysozoa, Lophotrochozoa, and Protostomia. *Molecular Biology and Evolution* 22: 1246–1253.

Philippe, H., Brinkmann, H., Copley, R.R., Moroz, L.L., Nakano, H., Poustka, A.J., Wallberg, A., Peterson, K.J., and Telford, M.J. (2011a) Acoelomorph flatworms are deuterostomes related to *Xenoturbella*. *Nature* 470: 255–258.

Philippe, H., Brinkmann, H., Lavrov, D.V., Littlewood, D.T.J., Manuel, M., Wörheide, G., and Baurain, D. (2011b) Resolving difficult phylogenetic questions: Why more sequences are not enough. *PLoS Biology* 9: e1000602.

Pisani, D., Pett, W., Dohrmann, M., Feuda, R., Rota-Stabelli, O., Philippe, H., Lartillot, N., and Wörheide, G. (2015) Genomic data do not support comb jellies as the sister group to all other animals. *Proceedings of the National Academy of Sciences, USA* 112: 15402–15407.

Putnam, N.H., Srivastava, M., Hellsten, U., Dirks, B., Chapman, J., Salamov, A., Terry, A., Shapiro, H., Lindquist, E., Kapitonov, V.V., Jurka, J., Genikhovich, G., Grigoriev, I.V., Lucas, S.M., Steele, R.E., Finnerty, J.R., Technau, U., Martindale, M.Q., and Rokhsar, D.S. (2007) Sea anemone genome reveals ancestral eumetazoan gene repertoire and genomic organization. *Science* 317: 86–96.

Ogura, A., Ikeo, K., and Gojobori, T. (2005) Estimation of ancestral gene set of bilaterian animals and its implication to dynamic change of gene content in bilaterian evolution. *Gene* 345: 65–71.

Rambaut A, Suchard M.A., Xie, D. and Drummond, A.J. (2014) Tracer v1.6, Available from http://beast.bio.ed.ac.uk/Tracer.

Ramos, O.M., Barker, D., and Ferrier, D.E.K. (2012) Ghost loci imply Hox and ParaHox existence in the last common ancestor of animals. *Current Biology* 22: 1951–1956.

Ramsköld, L., and Chen, J.-Y. (1998) Cambrian Lobopodians: Morphology and Phylogeny. *In:* Edgecombe, G.D. (ed.) *Arthropod Fossils and Phylogeny*. Columbia University Press: New York.

Ramsköld, L. and Hou, X.-G. (1991) New early Cambrian animal and onychophoran affinities of enigmatic metazoans. *Nature* 251: 225–228.

Raup, D.M. (1996) Geometric analysis of shell coiling: general problems. *Journal of Paleontology* 40: 1178–1190.

R Core Team. (2015) R: A language and environment for statistical computing. R Foundation for Statistical Computing, Vienna, Austria. URL https://www.R project.org/.

Richards, G.S., and Degnan, B.M. (2012) The expression of Delta ligands in the sponge *Amphimedon queenslandica* suggest an ancient role for Notch signaling in metazoan development. *EvoDevo* 3: 1–15.

Ringrose, J.H., van den Toorn, H.W.P., Eitel, M., Post, H., Neerincx, P., Schierwater, B., Altelaar, A.F.M., and Heck, A.J.R. (2013) Deep proteome profiling of *Trichoplax adhaerens* reveals remarkable features at the origin of metazoan multicellularity. *Nature Communications* 4: 1–7.

Rivera, A.S., Ozturk, N., Fahey, B., Plachetzki, D.C., Degnan, B.M., Sancar, A., and Oakley, T.H. (2012) Blue-light-receptive cryptochrome is expressed in a sponge eye lacking neurons and opsin. *Journal of Experimental Biology* 215: 1278–1286.

Rivera, A., Winters, I., Rued, A., Ding, S., Posfai, D., Cieniewicz, B., Cameron, K., Gentile, L., and Hill, A. (2013) The evolution and function of the Pax/Six regulatory network in sponges. *Evolution & Development* 15: 186–196.

Robinson, J.M., Sperling, E.A., Bergum, B., Adamski, M., Nichols, S.A., Adamska, M., and Peterson, K.J. (2013) The identification of microRNAs in Calcisponges: Independent eolution of microRNAs in basal metazoans. *Joural of Experimental Zoology Part B: Molecular and Developmental Evolution* 320: 84–93.

Robison, R.A. (1985) Affinities of *Aysheaia* (Onychophora), with description of a new Cambrian species. *Journal of Paleontology* 59: 226–235.

Rokas, A. (2008) The origins of multicellularity and the early history of the genetic toolkit for animal development. *Annual Review of Genetics* 42: 235–251.

Ronquist, F., Klopfstein, S., Vilhelmsen, L., Schulmeister, S., Murray, D.L., and Rasnitsyn, A.P. (2012) A total-evidence approach to dating with fossils, applied to the early radiation of the Hymenoptera. *Systematic Biology* 61: 973–999.

Ronquist, F., Teslenko, M., van der Mark, P., Ayres, D.L., Darling, A., Höhna, S., Larget, B., Liu, L., Suchard, M.A., and Huelsenbeck, J.P. (2012b) MrBayes 3.2: efficient Bayesian phylogenetic inference and model choice across a large model space. *Systematic Biology* 61: 539–542.

Rota-Stabelli, O., and Telford, M.J. (2008) A multi criterion approach for the selection of optimal outgroups in phylogeny: Recovering some support for Mandibulata over Myriochelata using mitogenomics. *Molecular Phylogenetics and Evolution* 48: 103–111.

Rota-Stabelli, O., Daley, A.C., and Pisani, D. (2013) Molecular timetrees reveal a Cambrian colonization of land and a new scenario for Ecdysozoan evolution. *Current Biology* 23: 392-398.

Röttinger, E., Dahlin, P., and Martindale, M.Q. (2012) A framework for the establishment of a cnidarian gene regulatory network for "endomesoderm" specification: The inputs of β-catenin/TCF signaling. *PLoS Genetics* 8: e1003164.

Rowland, S.J. (2001) Archaeocyaths – a history of phylogenetic interpretation. *Journal of Paleontology* 75: 1065–1078.

Ryan, J.F., Pang, K., Mullikin, J.C., Martindale, M.Q., Baxevanis, A.D., and Progra, N.C.S. (2010) The homeodomain complement of the ctenophore *Mnemiopsis leidyi* suggests that Ctenophora and Porifera diverged prior to the ParaHoxozoa. EvoDevo 1: 9.

Ryan, J.F., Pang, K., Schnitzler, C.E., Nguyen, A.D., Moreland, R.T., Simmons, D.K., Koch, B.J., Francis, W.R., Havlak, P., NISC Comparative Sequencing Program, Smith, S.A., Putnam, N.H., Haddock, S.H.D., Dunn, C.W., Wolfsberg, T.G., Mullikin, J.C., Martindale, M.Q., and Baxevanis, A.D. (2013) The genome of the ctenophore *Mnemiopsis leidyi* and its implications for cell type evolution. *Science* 342: 124592.

Saina, M., Genikhovich, G., Renfer, E., and Technau, U. (2009) BMPs and Chordin regulate patterning of the directive axis in a sea anemone. *Proceedings of the National Academy of Sciences, USA* 106: 18592–18597.

Saito, T., Uchida, I., and Takeda, M. (2002) Skeletal growth of the deep-sea hexactinellid sponge *Euplectella oweni*, and host selection by the symbiotic shrimp *Spongicola japonica* (Crustacea: Decapoda: Spongicolidae). *Journal of Zoology* 258: 521–529.

Sansom, R.S., Gabbott, S.E., and Purnell, M.A. (2010) Non-random decay of chordate characters causes bias in fossil interpretation. *Nature* 463: 797–800.

Saylor, B.Z., and Grotzinger, J.P. (1996) Reconstruction of important Proterozoic Cambrian boundary exposures through the recognition of thrust deformation in the Nama Group of southern Namibia. *Communications of the Geological Survey of Namibia* 11: 1–12.

Schierwater, B., Eitel, M., Osigus, H.J., von der Chevallerie, K., Bergmann, T., Hadrys, H., Cramm, M., Heck, L., Jakob, W., Lang, M.R., and DeSalle, R. (2011) *Trichoplax* and Placozoa: One of the crucial keys to understanding metazoan evolution. *In:* DeSalle, R., Schierwater, B. (eds.) *Key Transitions in Animal Evolution*. Science Publishers: Enfield, NH, pp. 289–326.

Schierwater, B., and Kamm, K. (2010) The early evolution of Hox genes: A battle of believe? *In:* Deutsch, J. (ed.) Hox Genes' Studies from the 20th to the 21st Century, *Advances in Experimental Medicine and Biology* 689. Landes Bioscience: New York, pp. 81–90.

Schmidt-Rhaesa, A., Bartolomaeus, T., Lemburg, C., Ehlers, U., and Garey, J.R. (1998) The position of the Arthropoda in the phylogenetic system. *Journal of Morphology* 238: 263–285.

Schmitz, M.D. (2012) Radiometric ages used in GTS2012, *In:* Gradstein, F., Ogg, J., Ogg, G., eds., *The Geologic Time Scale.* Elsevier: Boston, MA p. 427–449.

Schneider, C.A., Rasband, W.S., and Eliceiri, K.W. (2012) NIH Image to ImageJ: 25 years of image analysis. *Nature Methods* 9: 671–675.

Scholtz, G., and Edgecombe, G.D. (2006) The evolution of arthropod heads: reconciling morphological, developmental and palaeontological evidence. *Development, Genes and Evolution* 216: 395–415.

Sebé-Pedrós, A., Ruiz-Trillo, I., de Mendoza, A., Lang, B.F., and Degnan, B.M. (2011) Unexpected repertoire of metazoan transcription factors in the unicellular holozoan *Capsaspora owczarzaki*. *Molecular Biology and Evolution* 28: 1241–1254.

Sebé-Pedrós, A., Ariza-Cosano, A., Weirauch, M.T., Leininger, S., Yang, A., Torruella, G., Adamski, M., Adamska, M., Hughes, T.R., Gómez-Skarmeta, J.L., and Ruiz-Trillo, I. (2013) Early evolution of the T-box transcription factor family. *Proceedings of the National Academy of Sciences, USA* 110: 16050–16055.

Shenk, M.A., and Steel, M.A. (1994) A molecular snapshot of the metazoan 'Eve'. *Trends in Biochemical Science* 18: 459–463.

Shubin, N., Tabin, C., and Carroll, S. (1997) Fossils, genes and the evolution of animal limbs. *Nature* 388: 639–648.

Shubin, N., Tabin, C., and Carroll, S. (2009) Deep homology and the origins of evolutionary novelty. *Nature* 457: 818–823.

Simakov, O., Marletaz, F., Cho, S.-J., Edsinger-Gonzales, E., Havlak, P., Hellsten, U., Kuo, D.-H., Larsson, T., Lv, J., Arendt, D., Savage, R., Osoegawa, K., de Jong, P., Grimwood, J., Chapman, J.A., Shapiro, H., Aerts, A., Otillar, R.P., Terry, A.Y., Boore, J.L., Grigoriev, I.V., Lindberg, D.R., Seaver, E.C., Weisblat, D.A., Putnam, N.H., and Rokhsar, D.S. (2013) Insights into bilaterian evolution from three spiralian genomes. *Nature* 493: 526–532.

Sinigaglia, C., Busengdal, H., Leclère, L., Technau, U., and Rentzsch, F. (2013) The bilaterian head patterning gene *six3/6* controls aboral domain development in a cnidarian. *PLoS Biology* 11: e1001488.

Smith, A.B. (1994) Rooting molecular trees: problems and strategies. *Biological Journal of the Linnean Society* 51: 279–292.

Smith, E.F., Macdonald, F.A., Petach, T.A., Bold, U., and Schrag, D.P. (2016a) Integrated stratigraphic, geochemical, and paleontological late Ediacaran to early Cambrian records from southwestern Mongolia. *Geological Society of America Bulletin* 128: 442–468.

Smith, E.F., Nelson, L.L., Strange, M.A., Eyster, A.E., Rowland, S.M., Schrag, D.P., and Macdonald, F.A. (2016b) The last of the Ediacara Biota: Two exceptionally preserved body fossil assemblages from Mt. Dunfee, Nevada. *Geology* 44: 911–914.

Smith, M.R., and Caron, J.-B. (2015) *Hallucigenia*'s head and the pharyngeal armature of early ecdysozoans. *Nature* 523: 75–79.

Smith, M.R., and Ortega-Hernández, J. (2014) *Hallucigenia*'s onychophoran-like claws and the case for Tactopoda. *Nature* 514: 363–366.

Snodgrass, R.E. (1938) Evolution of the Annelida, Onychophora, and Arthropoda. *Smithsonian Miscellaneous Collections* 97: 50.

Spencer, M.R., and Wilberg, E.W. (2013) Efficacy or convenience? Model-based approaches to phylogeny estimation using morphological data. *Cladistics* 29: 663–671.

Sperling, E.A., Peterson, K.J., and Pisani, D. (2009) Phylogenetic-signal dissection of nuclear housekeeping genes supports the paraphyly of sponges and the monophyly of eumetazoa. *Molecular Biology and Evolution* 26: 2261–2274.

Sperling, E.A., Pisani, D., and Peterson, K.J. (2007) Poriferan paraphyly and its implications for Precambrian palaeobiology. *In:* Vickers-Rich, P., Komarower, P. (eds.) *The Rise and Fall of the Ediacaran Biota*. London, Geological Society Special Publication 286: 355–368.

Sperling, E.A., Vinther, J. (2010) A placozoan affinity for *Dickinsonia* and the evolution of late Proterozoic metazoan feeding modes. *Evolution & Development* 12: 201–209.

Sperling, E.A., Robinson, J.M., Pisani, D., and Peterson, K.J. (2010) Where's the glass? Biomarkers, molecular clocks, and microRNAs suggest a 200-Myr missing Precambrian fossil record of siliceous sponge spicules. *Geobiology* 8: 24–36.

Sperling, E.A., Peterson, K.J., and Laflamme, M. (2011) Rangeomorphs, *Thectardis* (Porifera?) and dissolved organic carbon in the Ediacaran oceans. *Geobiology* 9: 24–33.

Srivastava, M., Begovic, E., Chapman, J., Putnam, N.H., Hellsten, U., Kawashima, T., Kuo, A., Mitros, T., Salamov, A., Carpenter, M.L., Signorovitch, A.Y., Moreno, M.A., Kamm, K., Grimwood, J., Schmutz, J., Shapiro, H., Grigoriev, I.V., Buss, L.W., Schierwater, B., Dellaporta, S.L., and Rokhsar, D.S. (2008) The *Trichoplax* genome and the nature of placozoans. *Nature* 454: 955–960.

Srivastava, M., Larroux, C., Lu, D.R., Mohanty, K., Chapman, J., Degnan, B.M., and Rokhsar, D.S. (2010a) Early evolution of the LIM homeobox gene family. *BMC Biology* 8: 1–13.

Srivastava, M., Simakov, O., Chapman, J., Fahey, B., Gauthier, M.E.A., Mitros, T., Richards, G.S., Conaco, C., Dacre, M., Hellsten, U., Larroux, C., Putnam, N.H., Stanke, M., Adamska, M., Darling, A., Degnan, S.M., Oakley, T.H., Plachetzki, D.C., Zhai, Y.F., Adamski, M., Calcino, A., Cummins, S.F., Goodstein, D.M., Harris, C., Jackson, D.J., Leys, S.P., Shu, S.Q., Woodcroft, B.J., Vervoort, M., Kosik, K.S., Manning, G., Degnan, B.M., and Rokhsar, D.S. (2010b) The *Amphimedon queenslandica* genome and the evolution of animal complexity. *Nature* 466: 720–U723.

Steinmetz, P.R.H., Kraus, J.E.M, Larroux, C., Hammel, J.U., Amon-Hassenzahl, A., Houliston, E., Wörheide, G., Nickel, M., Degnan, B.M., and Technau, U. (2012) Independent evolution of striated muscles in cnidarians and bilaterians. *Nature* 487: 231–234.

Steele, R.E., David, C.N., and Technau, U. (2011) A genomic view of 500 million years of cnidarian evolution. *Trends in Genetics* 27: 7–13.

Steiner, M., Mehl, D., Reitner, J., and Erdtmann, B.-D. (1993) Oldest entirely preserved sponges and other fossils from the Lowermost Cambrian and a new facies reconstruction of the Yangtze platform (China). *Berliner Geowissenschaftliche Abhandlungen (E)* 9: 293–329.

Stromberg, C.A.E. (2005) Decoupled taxonomic radiation and ecological expansion of open-habitat grasses in the Cenozoic of North America. *Proceedings of the National Academy of Sciences, USA* 102: 11980–11984.

Sullivan, J.C., Kalaitzidis, D., Gilmore, T.D., and Finnerty, J.R. (2006) Rel homology domain-containing transcription factors in the cnidarian *Nematostella vectensis*. *Development Genes and Evolution* 217: 63–72.

Swofford D. (2002) PAUP*: phylogenetic analysis using parsimony (* and other methods). Version 4.0b10. Sinauer Associates: Sunderland, MA.

Tabachnik, K.R. (2002) Euplectellidae Gray, 1867, *in*: Hooper, J.N.A., Van Soest, R.W.M., eds., *System Porifera: A Guide to the Classification of Sponges* Kluwer Academic / Plenum Publishers: New York, p. 1388–1434.

Telford, M.J., Bourlat, S.J., Economou, A., Papillon, D., and Rota-Stabelli, O. (2008) The evolution of the Ecdysozoa. *Philosophical Transactions of the Royal Society B* 363: 1529–1537.

True, J. R. and Carroll, S. B. (2000) Gene co-option in physiological and morphological evolution. *Annual Review of Cell and Developmental Biology* 18: 53–80.

Tweedt, S.M., and Erwin, D.H. (2015) Origin of metazoan developmental toolkits and their expression in the fossil record. *In:* Nedelcu, A.M., Ruiz-Trillo, I., eds., *Evolutionary Transitions to Multicellular Life*. Springer: Berlin, Germany, p. 47–77.

Valentine, J.W., Jablonski, D., and Erwin, D.H. (1999) Fossils, molecules and embryos: new perspectives on the Cambrian explosion. *Development* 126: 851–859.

Vij, S., Rink, J.C., Ho, H.K., Babu, D., Eitel, M., Narasimhan, V., Tiku, V., Westbrook, J., Schierwater, B., and Roy, S. (2012) Evolutionarily ancient association of the FoxJ1 transcription factor with the motile ciliogenic program. *PLoS Genetics* 8: e1003019.

Waddington, C.H. (1957) *The strategy of the genes. A discussion of some aspects of theoretical biology.* George Allen & Unwin: London.

Waggoner, B.M. (1996) Phylogenetic hypotheses of the relationships of arthropods to precambrian and Cambrian problematic fossil taxa. *Systematic Biology* 45: 190–222.

Wagner, G.P., and Altenberg, L. (1996) Complex adaptations and the evolution of evolvability. *Evolution* 50: 967–976.

Wagner, G.P. (2014) *Homology, Genes and Evolutionary Innovation*. Princeton University Press: Princeton, NJ.

Wagner, P.J. (2012) Modelling rate distributions using character compatibility: implications for morphological evolution among fossil invertebrates. *Biology Letters* 8: 143–146.

Walcott, C.D. (1911) Middle Cambrian annelids. Cambrian geology and paleontology, II. *Smithsonian Miscellaneous Collections* 57: 110–144.

Walcott, C.D. (1912) Middle Cambrian Branchiopoda, Malacostraca, Trilobita, and Merostomata. Cambrian geology and paleontology, II. *Smithsonian Miscellaneous Collections* 57: 146–228.

Walcott, C.D. (1931) Addenda to descriptions of Burgess Shale fossils, with explanatory notes by C.E. Resser. *Smithsonian Miscellaneous Collections* 85: 8.

Wallace, M.W., Hood, A.v.S., Woon, E.M.S., Hoffmann, K.-H., and Reed, C.P. (2014) Enigmatic chambered structures in Cryogenian reefs: The oldest sponge-grade organisms? *Precambrian Research* 255: 109–123.

Whiteaves, J.F. (1892) Description of a new genus and species of phyllocarid crustacean from the Middle Cambrian of Mount Stephen, British Columbia. *Canadian Record of Science* 5: 205–208.

Whittington, H.B. (1978) The lobopod animal *Aysheaia pedunculata* Walcott, Middle Cambrian, Burgess Shale, British Columbia. *Philosophical Transactions of the Royal Society of London, B, Biological Sciences* 284: 165–197.

Wickham, H. (2007) Reshaping Data with the reshape Package. *Journal of Statistical Software* 21: 1–20. URL http://www.jstatsoft.org/v21/i12/.

Winchell, C.J., Valencia, J.E., and Jacobs, D.K. (2010) Expression of *Distal-less*, *dachshund*, and *optomotor blind* in *Neanthes arenaceodentata* (Annedlida, Nereididae) does not support homology of appendage-forming mechanisms across the Bilateria. *Development Genes & Evolution* 220: 275–295.

Winchell, C.J., and Jacobs, D.K. (2013) Expression of the Lhx genes *apterous* and *lim1* in an errant polychaete: implications for bilaterian appendage evolution, neural development, and muscle diversification. *EvoDevo* 4: 4.

Windsor, P.J., and Leys, S.P. (2010) Wnt signaling and induction in the sponge aquiferous system: evidence for an ancient origin of the organizer. *Evolution & Development* 12: 484–493.

Wright, A.M. and Hillis, D.M. (2014) Bayesian analysis using a simple likelihood model outperforms parsimony for estimation of phylogeny from discrete morphological data. *PLoS ONE* 9: 1-6.

Wu, W., Zhu, M., and Steiner, M. (2014) Composition and tiering of the Cambrian sponge communities. *Palaeogeography, Palaeoclimatology, Palaeoecology* 398: 86–99.

Wyder, S., Kriventseva, E.V., Schröder, R., Kadowaki, T., and Zdobnov, E.M. (2007) Quantification of ortholog losses in insects and vertebrates. *Genome Biology* 8: R242.

Xavier-Neto, J., Castro, R.A., Sampaio, A.C., Azambuja, A.P., Castillo, H.A., Cravo, R.M., and Simões-Costa, M.S. (2007) Parallel avenues in the evolution of hearts and pumping organs. *Cell and Molecular Life Sciences* 64: 719–734.

Xiao, S., Hu, J., Yuan, X., Parsley, R.L., and Cao, R. (2005) Articulated sponges from the Lower Cambiran Hetang Formation in southern Anhui, China: their age and implications for the early evolution of sponges. *Palaeogeography, Palaeoclimatology, Palaeoecology* 220: 89–117.

Xie, W., Lewis, P.O., Fan, Y., Kuo, L., and Chen, M.-H. (2011) Improving marginal likelihood estimation for Bayesian phylogenetic model selection. *Systematic Biology* 60: 150–160.

Xu, X., and Pol, D. (2014) *Archaeopteryx*, paravian phylogenetic analysis, and the use of probability-based methods for paleontological datasets. *Journal of Systematic Paleontology* 12: 323–334.

Yin, Z., Zhu, M., Davidson, E.H., Bottjer, D.J., Zhao, F., and Tafforeau, P. (2015) Sponge grade body fossil with cellular resolution dating 60 Myr before the Cambrian. *Proceedings of the National Academy of Sciences, USA* 112: E1453–1460.

Yuan, X., Xiao, S., Parsley, R.L., Zhou, C., Chen, Z., and Hu, J. (2002) Towering sponges in an Early Cambrian Lagerstätte: Disparity between nonbilaterian and bilaterian epifaunal tierers at the Neoproterozoic-Cambrian transition. *Geology* 30: 363–366.

Zhang, X.-G. and Briggs, D.E.G. (2007) The nature and significance of the appendages of *Opabinia* from the Middle Cambrian Burgess Shale. *Lethaia* 40: 161–173.

Zhou, C.M., and Xiao, S.H. (2007) Ediacaran $\delta^{13}C$ chemostratigraphy of South China. *Chemical Geology* 237: 89–108.

Zhu, M., Babcock, L.E., and Peng, S. (2006) Advances in Cambrian stratigraphy and paleontology: Integrating correlation techniques, paleobiology, taphonomy and paleoenvironmental reconstruction. *Palaeoworld* 15: 217–222.

UNIVERSITY OF MARYLAND
DEPARTMENT OF CELL BIOLOGY AND MOLECULAR GENETICS

Biosciences Research Building
College Park, Maryland 20742-4407
301.405.1084 TEL 301.314.1248 FAX

1/23/17

Alexander Chen, Ph.D.
Associate Dean of the Graduate School
University of Maryland

Dear Dr. Chen,

This letter is written to signify that the dissertation committee has approved the use of previously published co-authored work in the final dissertation of Sarah Tweedt, Biological Sciences Graduate Program, UID 111421152. In accordance with the Graduate School's policy the dissertation committee has determined that the following chapter is a substantial and accepted contribution to the included work.

The citation for Chapter 2 (previously published in its entirety) is:
Tweedt, S.M. and Erwin, D.H. (2015) Origin of metazoan developmental toolkits and their expression in the fossil record. *In*: Ruiz-Trillo, I., Nedelcu, A. (eds.) *Evolutionary Transitions to Multicellular Life*. Springer: New York. p 47-77. doi: 10.1007/978-94-017-9642-2_3.

Sarah Tweedt was lead author and researcher on this synthesis chapter, and produced all data / meta-analysis, summaries and conclusions of the comparative molecular information. D. Erwin contributed guidance on chapter structure and contributed the section of historical context. Both authors worked together to review and edit the final paper.

Per Graduate School policy this letter identifies the scope and nature of the student's contribution to the previously published co-authored work included in the dissertation and a copy of this letter will be included in the dissertation submission.

Sincerely,

Dr. Charles F. Delwiche, Dissertation Committee Chair

Sarah Tweedt, Graduate Student, Biological Sciences